NOVEL STRATEGIES FOR CHARACTERIZING T CELL RESPONSES IN SIV-INFECTED RHESUS MONKEYS

by

Amy Shi

B.S. Chemical Engineering (2004)

M.S. Materials Science and Engineering (2007)

Massachusetts Institute of Technology

SUBMITTED TO THE HARVARD-MIT DIVISION OF HEALTH SCIENCES AND TECHNOLOGY IN PARTIAL FULFILLMENT OF THE REQUIREMENTS FOR THE DEGREE OF

MASTER OF SCIENCE IN HEALTH SCIENCES AND TECHNOLOGY

AT THE

MASSACHUSETTS INSTITUTE OF TECHNOLOGY

SEPTEMBER, 2009

Signature of Author: _____
Harvard-MIT Division of Health Sciences and Technology
August 7, 2009

Certified by: _____
Norman L. Letvin, M.D.
Professor of Medicine
Thesis Supervisor

Accepted by: _____
Ram Sasisekharan, Ph.D.
Director, Harvard-MIT Division of Health Sciences and Technology
Edward Hood Taplin Professor of Health Sciences and Technology

NOVEL STRATEGIES FOR CHARACTERIZING T CELL RESPONSES IN SIV-INFECTED RHESUS MONKEYS

By

Amy Shi

Submitted to the Harvard-MIT Division of Health Sciences and Technology
On August 7, 2009 in Partial Fulfillment of the
Requirements for the Degree of Master of Science in
Health Sciences and Technology

ABSTRACT

Human Immunodeficiency Virus (HIV) is the cause of Acquired Immune Deficiency Syndrome (AIDS) and has killed over 25 million people since the disease was first recognized in 1981. As of 2007, 33 million people globally are infected with HIV and this number is growing.[1] HIV infects and depletes CD4+ helper T cells, affecting the ability of the immune system to defend the host against common infections. While anti-retroviral therapy has decreased morbidity and mortality, these drugs are not curative. In addition, they are beyond the financial reach of many HIV infected patients. Thus, the development of strategies to control HIV spread is a high priority. The most relevant animal model for studying HIV is the Simian Immunodeficiency Virus (SIV) – infected rhesus monkey.

While HIV research has focused on studying peripheral blood specimens, mucosal sites have recently been identified as a focal point for HIV replication and tissue destruction. They are usually the sites of primary infection in the setting of sexual transmission and they are also important sites of immune depletion. If methods for controlling the replication of the virus early after infection in mucosal sites are available, it may be possible to eliminate the virus prior to systemic spread.

While strategies for generating strong neutralizing antibody responses have not yet been developed, emerging data suggest that CD8+ cytotoxic T cells can contribute substantially to early virus control. It is important to study CD8+ T cells in the setting of SIV infection in rhesus monkeys, particularly in mucosal sites, using functional as well as transcriptional assays. One of the challenges in studying mucosal cellular immunity is the limited number of cells available in biopsies, making traditional assay systems such as flow cytometry very difficult to employ. Here, technologies for isolating rare cell populations and extracting RNA from these cells for gene expression analysis were developed. These technologies were then applied to peripheral blood specimens, looking at gene expression differences between virus-specific CD8+ T cells in Mamu-A*01+ and Mamu-A*02+ monkeys. The ultimate goal of these studies is to gain a better understanding of SIV immunopathogenesis (as a model for HIV immunopathogenesis) and to find a way to control or eliminate the virus.

Thesis Supervisor: Norman L. Letvin
Title: Professor of Medicine

TABLE OF CONTENTS

ABSTRACT **2**

TABLE OF CONTENTS **3**

LIST OF TABLES **4**

LIST OF FIGURES **5**

ACKNOWLEDGEMENTS **7**

CHAPTER 1: INTRODUCTION **8**

HIV BACKGROUND 9
IMMUNE RESPONSES TO HIV 10
HIV AS A MUCOSAL PATHOGEN 13
TECHNOLOGIES USED TO STUDY CELLULAR IMMUNE RESPONSES 13
CHALLENGES OF STUDYING MUCOSAL T CELL IMMUNITY 14
GENE EXPRESSION PROFILING AS A NEW TOOL TO STUDY CELL BIOLOGY 15

CHAPTER 2: CELL CAPTURE AND RELEASE OF EPITOPE-SPECIFIC CD8+ T LYMPHOCYTES **19**

INTRODUCTION 19
MATERIALS AND METHODS 25
RESULTS 32
DISCUSSION 43

CHAPTER 3: DEVELOPMENT OF TECHNIQUES FOR RNA EXTRACTION, AMPLIFICATION, AND GENE EXPRESSION ANALYSIS USING LIMITED NUMBERS OF CELLS **46**

INTRODUCTION 46
MATERIALS AND METHODS 51
RESULTS 58
DISCUSSION 71

CHAPTER 4: GENE EXPRESSION PROFILE OF PERIPHERAL BLOOD SIV GAG EPITOPE-SPECIFIC CD8+ T LYMPHOCYTES DURING PRIMARY SIV INFECTION IN MAMU-A*01+ AND MAMU-A*02+ RHESUS MONKEYS **73**

INTRODUCTION 73
MATERIALS AND METHODS 78
RESULTS 82
DISCUSSION 96

CHAPTER 5: DISCUSSION **99**

REFERENCES **103**

List of Tables

TABLE 3.1. NUMBERS OF GENES DETECTED AND R SQUARED VALUES FOR LIMITING DILUTIONS OF TOTAL RNA ON ILLUMINA HUMAN BEADCHIP. 59
TABLE 3.2. ARNA YIELDS FROM AMBION MESSAGE AMP II ARNA AMPLIFICATION KIT (WITH 2 ROUNDS) AND EPICENTRE 2 ROUND AMPLIFICATION KIT. 62
TABLE 3.3. COMPARISON OF ARNA YIELD FROM PURIFIED RNA AND CELL LYSATE FROM MUCOSAL AND BLOOD P11C+ CD8+ T LYMPHOCYTES. 69
TABLE 4.1 AMPLIFIED BIOTIN-ARNA FROM TOTAL CD8+ T CELLS FROM MM107-2006 (A*01+) AND MM337-2008 (A*02+). 91

List of Figures

FIGURE 2.1. MURINE CD8+ T CELL ISOLATION WITH DYNABEADS. 33
FIGURE 2.2. POSITIVE SELECTION OF MURINE EPITOPE-SPECIFIC CD8+ T LYMPHOCYTES (P18+) WITH MILTENYI MICROBEADS USING A TWO-STEP PURIFICATION PROTOCOL. 34
FIGURE 2.3. POSITIVE SELECTION OF RHESUS MONKEY EPITOPE-SPECIFIC CD8+ T LYMPHOCYTES (P11C+) WITH MILTENYI MICROBEADS USING A TWO-STEP PURIFICATION PROTOCOL. 34
FIGURE 2.4. ISOLATION OF EPITOPE-SPECIFIC CD8+ T LYMPHOCYTES USING MILTENYI MULTIMACS WITH MICROBEADS 35
FIGURE 2.5. DIFFERENCE IN PURITY OF CD8+ T CELLS AND EPITOPE-SPECIFIC CD8+ T CELLS WITH AND WITHOUT LYSIS OF RED BLOOD CELLS (RBCS). 36
FIGURE 2.6. DIFFERENCE IN PURITY OF EPITOPE-SPECIFIC CD8+ T CELLS WITH DECREASED AMOUNTS OF MILTENYI ANTI-PHYCOERYTHRIN (ANTI-PE) MICROBEADS. 37
FIGURE 2.7. MASK AND SCHEMATIC OF DIAMOND-SHAPED MICROFLUIDIC CHAMBER WITH POLES 38
FIGURE 2.8. CAPTURE OF EPITOPE-SPECIFIC CD8+ T LYMPHOCYTES USING ANTI-PHYCOERYTHRIN (PE) ANTIBODIES AND PDMS-BASED MICROFLUIDIC SYSTEM. 39
FIGURE 2.9. RECTANGULAR MICROFLUIDIC CELL SORTER WITH BIOTIN-AVIDIN CHEMISTRY 40
FIGURE 2.10. BIOTINYLATED ANTI-PE COVERAGE OF MICROFLUIDIC CHAMBER SURFACE. 41
FIGURE 2.11. HELE-SHAW DEVICE. 42
FIGURE 3.1. QUANTITY AND RNA INTEGRITY OF TRIZOL EXTRACTED RNA FROM LIMITING DILUTIONS OF FACS SORTED P11C+ CD8+ T CELLS. 60
FIGURE 3.2. HISTOGRAM OF P-VALUES COMPARING AMBION VERSUS EPICENTRE AMPLIFIED ARNA. 63
FIGURE 3.3. SCATTERPLOTS AND CORRELATION COEFFICIENTS OF PAIRS OF ARNA SAMPLES AMPLIFIED WITH THE AMBION OR EPICENTRE METHODS AND STARTING FROM DIFFERENT RNA AMOUNTS. 64
FIGURE 3.4. NUMBER OF GENES EXPRESSED IN THE AMBION OR EPICENTRE AMPLIFIED ARNA. 65
FIGURE 3.5. NANODROP READING FOR AMPLIFIED ARNA FROM HELA CONTROL AND 1 UL OF LYSATE FROM 1,000 NORMAL MONKEY PERIPHERAL BLOOD MONONUCLEAR CELLS (PBMCS). 67
FIGURE 3.6. AGILENT BIOANALYZER READOUTS FOR AMPLIFIED ARNA FOR HELA CONTROL AND 1 UL OF CELL LYSATE FROM 1,000 MONKEY PBMCS. 67
FIGURE 3.7. SYBR GREEN QPCR OF GAPDH ON AMPLIFIED CELL LYSATE FROM MONKEY PBMCS AS WELL AS HELA AND CONTROL RNAS. 68
FIGURE 3.8. COMPARISON OF ARNA YIELD FROM PURIFIED RNA AND CELL LYSATE FROM MUCOSAL AND BLOOD P11C+ CD8+ T LYMPHOCYTES. 69
FIGURE 3.9. SCHEMATIC OF GENE EXPRESSION PROFILING ASSAY FOR EPITOPE-SPECIFIC CD8+ T LYMPHOCYTES. 70
FIGURE 4.1. EFFECT OF LONG-TERM INCUBATION OF TETRAMER-STAINED CELLS ON ICE ON PHOSPHORYLATION OF CD3Z. 83
FIGURE 4.2. STAINING WITH ANTI-PHOSPORYLATED CD3Z AND FIXING AT 37°C. 84
FIGURE 4.3. STAINING WITH ANTI-PHOSPORYLATED CD3Z AND FIXING ON ICE. 85
FIGURE 4.4. SCHEMATIC FOR SORTING TOTAL AND NAÏVE CD8+ T CELLS FOR BASELINE MEASUREMENTS. 86
FIGURE 4.5. RNA INTEGRITY AND QUANTITY FROM BASELINE TOTAL AND NAÏVE CD8+ T CELLS FOR MM107-20076 (A*01+) AND MM337-2008 (A*02+) PRE-CHALLENGE ON DAY 0. 87
FIGURE 4.6. TETRAMER CELL SORTING FOR MM107-2006 (A*01+) ON DAY 14 POST SIVMAC251 INTRA-RECTAL CHALLENGE. 88
FIGURE 4.7. TETRAMER CELL SORTING FOR MM337-2008 (A*02+) ON DAY 14 POST SIVMAC251 INTRA-RECTAL CHALLENGE. 89
FIGURE 4.8. RNA INTEGRITY AND QUANTITY FROM TETRAMER POSITIVE CELLS ON DAY 14 POST SIVMAC251 CHALLENGE FOR MM107-2006 (A*01+) AND MM337-2008 (A*02+). 90
FIGURE 4.9. AMPLIFIED BIOTIN-ARNA FROM TOTAL CD8+ T CELLS FROM MM107-2006 (A*01+) AND MM337-2008 (A*02+). 91
FIGURE 4.10. MAMU-A*01-RESTRICTED, SIV EPITOPE-SPECIFIC T LYMPHOCYTE RESPONSES IN SIVMAC251-INFECTED MAMU-A*01+ RHESUS MONKEYS 93
FIGURE 4.11. MAMU-A*02-RESTRICTED, SIV EPITOPE-SPECIFIC T LYMPHOCYTE RESPONSES IN SIVMAC251-INFECTED MAMU-A*02+ RHESUS MONKEYS 94

FIGURE 4.12. SIV VIRAL LOAD KINETICS AND MAGNITUDE FOR MAMU-A*01+ (A) AND MAMU-A*02+ (B) RHESUS MONKEYS. 95

Acknowledgements

Without the collaboration of my colleagues, none of this work would have been possible. I'd like to thank Ana, who has worked side by side with me for the last two years to develop the technologies described here. I'd like to thank Amy and Sindy, the microfluidic gurus, Kevin, the Illumina expert, and Marco Ramoni's group, the bioinformatics experts. Many thanks to Leila for antibody conjugation, to the entire Flow Cytometry lab (especially Lauren, Katie, and Michelle) for flow cytometry support, to Joern for setting up the Miltenyi collaboration, to Avi-Hai for teaching me how to work with mouse models, to Angela at the New England Primate Center (NEPRC) for taking care of our monkeys, to Christa for driving me to and from the NEPRC to inoculate monkeys, and to Piya for working with me to develop RNA technologies. My intellectual development as a budding immunologist is in great part due to the insights and knowledge imparted to me by the Letvin graduate students and post-docs. Thank you all. I'd like to thank all my financial sponsors, including NDSEG, NSF, CHAVI, and NIAID. And last but not least, my deepest gratitude does to my mentor and advisor, Norm Letvin, who is not only a brilliant scientist, but is also an amazing mentor who cares not only for my development as a scientist, but also as a professional and a human being. Thank you for taking me under your wings and for teaching me over the past two and half years. I consider myself greatly privileged to be your student.

I'd like to thank the Harvard-MIT Division of Health Sciences and Technology for giving me the opportunity to experience so much in the past several years, from research, to clinical medicine, to business. Special thanks to Cathy, who has been a great friend to me the past nine years – thank you for your unending support and your faith in me. Many thanks to the people in the HST office, especially Traci, Julie, Domingo, and Laurie, for making the administrative and financial aspects of graduate school a complete breeze.

I'd like to thank my friends from high school, undergrad, HST, biblestudy, church, lab, and SP, who have shared with me the joys and frustrations of graduate school. Thank you for always being there to listen, to laugh with, to cry with, and to pray with. Thank you for believing in me, for encouraging me to try new things, and for always giving me a reason to be joyful. Without you, graduate school would have been colorless and dull.

I'd like to thank my wonderful parents, Ying and Shixiang, for always believing in me even when I didn't believe in myself, for teaching me the importance of a balanced education both in and out of school, and for always putting my happiness first. I love you both very much. I'd also like to thank Jason, my boyfriend of 5 years and now my fiancé, who has patiently stood by me during my graduate career, always believing in my abilities. You have been a steady rock I could hold onto throughout the ups and downs of graduate school – thank you for always being there and for loving me.

My greatest thanks goes to God, who reminds me daily that He is in control and to be not "anxious about anything, but in everything, by prayer and petition, with thanksgiving, present your requests to God. And the peace of God, which transcends all understanding, will guard your hearts and your minds in Christ Jesus." (Phillipians 4:6-7) He who made the entire world has touched my life and has given me serenity, courage, love, and hope.

CHAPTER 1: Introduction

Human Immunodeficiency Virus (HIV) is the cause of Acquired Immune Deficiency Syndrome (AIDS) and has killed over 25 million people since the disease was first recognized in 1981. As of 2007, 33 million people globally are infected with HIV and this number is growing.[1] HIV infects and depletes CD4+ helper T cells, affecting the ability of the immune system to defend the host against common infections. While anti-retroviral therapy has decreased morbidity and mortality, these drugs are not curative. In addition, they are beyond the financial reach of many HIV patients. Thus, the development of strategies to control HIV spread is a high priority.

Understanding of the biology underlying HIV disease progression is essential for developing effective therapies and an effective vaccine. Part of the challenge in clarifying AIDS pathogenesis lies in the lack of adequate assay systems to probe the questions we need to answer. In the space of cellular immunity, one of the challenges lies in the limited amount of information that can be obtained by traditional assays such as ELISPOT and intracellular cytokine staining (ICS). In addition, cell number limitations in particular anatomical compartments such as mucosa, make it very difficult to employ traditional assay systems, which typically require millions of cells. Development of novel technologies for studying cellular immunity in limited numbers of cells in the setting of SIV infection can help us gain a better understanding of SIV immunopathogenesis (as a model for HIV immunopathogenesis) and to find a way to control or eliminate it.

HIV Background

HIV is a retrovirus and is a member of the lentivirus family. Due to its low-fidelity replication, viral mutants are rapidly created, causing a viral swarm or quasi-species inside the host.[2-4] This ability to mutate allows HIV to adapt to and evade host immune responses and also makes it extremely difficult to contain.[5,6]

Structure

HIV has two copies of single-stranded RNA, enclosed by a conical shell composed of the viral capsid protein. Each strand of RNA is tightly encapsulated by nucleocapsid proteins that protect the RNA from nucleases.[7,8] Reverse transcriptase and integrase are encoded by the RNA and are integral for development and replication of the virion.[9] Matrix proteins surround the viral capsid, ensuring the integrity of the virion. Virions are formed when capsid buds off from the host cells, taking along some of the membrane containing the viral envelope glycoproteins gp120 and gp41.

Genome

HIV contains major genes that are common to all retroviruses: *gag, env, and pol. Gag* is a structural gene that encodes for a number of proteins that are necessary for the infrastructure of the virus. *Env* encodes for the glycoproteins gp120 and gp41 which are embedded in viral envelope and are required for viral entry into host cells. *Pol* encodes for viral enzymes needed for replication, including reverse transcriptase, integrase, and protease. Other accessory genes such as *tat, vpr, rev, nef, vif, and vpu* enhance HIV replication and likely contribute to viral pathogenicity.

Primate SIV model

Simian Immunodeficiency Virus (SIV) has become the model of choice for studying the pathogenesis and transmission of HIV because the SIV infection of rhesus monkeys (*Macaca Mulatta*) shares many of the same pathogenic features of HIV-1 infection in humans.[10] The primate SIV model has enabled researchers to prospectively design vaccine and challenge experiments, something that is impossible in humans.

Immune responses to HIV

Both the innate and the adaptive immune responses will likely be important in the control of HIV replication and pathogenesis. The innate immune response is the earliest response and can kill infected cells through cytolytic mechanisms or can amplify the immune response through cytokines and chemokines. The adaptive immune response consists of the humoral arm and the cellular arm. The humoral immune response works by directing antibodies against viral Env to potentially inactivate or clear the virus. The cellular immune response targets HIV indirectly by killing cells that harbor the virus.

Innate immune response

The innate immune response can act rapidly because it uses extant cells and mediators.[11] Natural killer cells (NK), granulocytes, and possibly γδ-T cells provide the initial line of defense upon stimulation by chemical signals at the site of infection.[12-15] NK cells and γδ-T cells can kill infected cells through cytolytic mechanisms while neutrophils release antimicrobial defensins.[12-15] Host macrophages and dendritic cells also play a large role at an early stage after infection by presenting viral antigens and by secreting cytokines and chemokines to amplify the immune response. There is still much that is not known about the power of the innate immune system to

control HIV. However, with time, the innate immune response gives way to the adaptive immune response, which requires presentation of viral antigens on cell surface MHC molecules.

Humoral immune response

While many viruses are controlled by host antibodies, the natural antibody response to HIV is too late, too weak, and not protective. The humoral immune response takes several weeks after infection to develop, which is much too late to be effective in controlling HIV spread.[11] The importance of the humoral response, however, is evident in the number of ways HIV has evolved to evade host antibodies.[16] For example, the Env proteins gp120 and gp41, which are most accessible to antibody binding, are heavily glycosylated and can form trimeric complexes that prevent antibody access to vulnerable domains of the envelope.[16-18] The more vulnerable variable loops of gp120 should be prime targets for neutralizing antibodies but, unfortunately, the loops are too variable to be recognized by the highly focused neutralizing antibodies that develop following infection. Increasing the effectiveness of the humoral response to HIV will require tremendous innovation in immunogen design, a clear and logical method for evaluating immunogens, and thorough structural and molecular analyses of current neutralizing antibodies and Env proteins.[16,19] The current inability of the humoral immune response to neutralize HIV suggests that the burden of HIV control lies with the cellular arm of the immune system and that for a vaccine to be successful, a focus on improving the cellular immune response may be necessary.

Cellular immune response

The cellular arm of the immune system is active at an early stage (approximately one week post-infection) and plays a major role in fighting many viral infections. In HIV, studies have shown that CD8+ cytotoxic T lymphocytes (CTLs) play a large role in the control of HIV replication and spread.[20] Soon after the discovery of HIV, CD8+ T cells were found to inhibit viral replication in autologous CD4+ T lymphocytes.[21] CTL effector molecules include perforin, granzyme and Fas, as well as soluble factors such as beta-chemokines (RANTES, MIP-1α and MIP-1β) and other poorly defined factors.[11,22] The emergence of virus-specific CTL response correlates temporally with a decrease in viral loads and poor CTL response is associated with poor viral control.[23,24] Depletion of CD8+ lymphocytes in an SIV primate model results in high viral loads and development of lethal SIV infection.[25-27] However, clearance of HIV is always incomplete, even in the presence of a robust CD8+ T cell response. Some have attributed the failure for viral control to the ineffective response of virus-specific CD4+ T cells.[28,29] Others have suggested that the continuous state of immune activation fuels viral persistence, leading to CTL dysfunction or exhaustion.[30-32] New findings also suggest that viral escape, MHC polymorphisms, and the kinetics of cell killing are other factors contributing to failure in controlling HIV replication and pathogenesis.[33] While the cellular immune response to HIV is the most intensely studied part of the immune response to HIV, there is still much we do not understand about why the CTL response is not sufficient to control HIV replication. With the development of new technologies, such as gene expression profiling and bioinformatics, we have a chance to probe more intensely the underlying host-virus biology with the hope of finding ways to augment the cellular immune response. However, while the cellular immune response thus far provides the best control of HIV, CD8+ T cells probably do not account for all HIV

containment.[34] There may therefore be other mechanisms contributing to virus control. A vaccine that engages all aspects of the immune system will likely provide the best protection against HIV.

HIV as a mucosal pathogen

While most HIV researchers have focused on studying peripheral blood specimens, mucosal sites have recently been identified as focal points for HIV replication and tissue destruction. They are usually the sites of primary infection in the setting of sexual transmission and they are also sites of immune depletion.[35] In nonhuman primates, simian immunodeficiency virus (SIV) can be transmitted without epithelial damage. This may also be true of HIV in humans. There is a need to study HIV at the mucosal level because it is the site of first infection and also the site of most significant CD4+ T cell depletion.[36] For a vaccine to be effective, it may need to act at the mucosal level.[37-40] Antigen-specific CD8+ T lymphocytes are the predominant cellular defense against viral infections including HIV and SIV.[24,41] From these observations, it is evident that a study of antigen-specific CD8+ T lymphocytes in mucosal compartments in the setting of SIV infection will be essential for understanding the underlying biology of HIV infection. If methods for controlling the replication of the virus early after infection in mucosal sites are available, it may be possible to eliminate the virus prior to systemic spread.

Technologies used to study cellular immune responses

Standard methods for studying cellular immune responses include enzyme-linked immunosorbent spot (ELISPOT) and intracellular cytokine staining (ICS).

The ELISPOT assay is based on the ELISA immunoassay and can be used to identify and enumerate cytokine-producing cells. In HIV-infected individuals, the IFN-gamma ELISPOT

assay has been used to identify HIV-specific CD8+ T cells. ELISPOT is attractive as an assay because it is rapid, inexpensive, easy to use, and sensitive. However, there are several limitations, including a need for large cell numbers for each evaluated sample and the uncertainty of whether all HIV-specific CD8+ T cells can be identified based on their IFN-gamma production following peptide stimulation.[42]

ICS is an assay that can detect single cell expression of cytokines following stimulation with specific antigens.[43] ICS allows for simultaneous detection, quantification, and phenotypic characterization of each cell.[43] Cells are first permeabilized and then stained with cytokine antibodies. Flow cytometric analysis is used to determine the amount of cytokine produced or accumulated. The major advantage of ICS over the ELISPOT assay is the ability to measure multiple parameters in the same cell. However, there are limitations in this assay technology, including a need for large cell numbers per sample, and the difficulty in performing ICS on mucosal samples due to the chronic activation of the cells in these tissues.

Challenges of Studying Mucosal T Cell Immunity

One of the major challenges in the study of mucosal T lymphocyte immunity is the limitation in the number of antigen-specific T lymphocytes that can be extracted from mucosal biopsies. Traditional methods of studying lymphocytes, such as ICS and ELISPOT, require large cell samples (millions of cells), which are impossible to obtain from the small biopsy specimens that can be sampled from mucosal compartments. In addition, these assay systems only extract limited information from the cells (ie. presence of cell surface receptors and production of a handful of cytokines).

Therefore, it is important, both for research purposes and for clinical trial applications, to develop appropriate assay systems designed for working with small numbers of cells in an easy and reproducible fashion and that would allow for additional information to be gathered from the cells, including gene expression data.

Gene Expression profiling as a new tool to study cell biology

The identity and abundance of mRNA species within a cell dictate, to a large extent, the biological potential of that cell.[44] While post-transcriptional mechanisms modify protein expression in many ways, most cellular changes begin from changes in gene transcription. Recent advent of microarray technology has made it possible to assess the global mRNA profile of cells.

The use of miniaturized microarrays for gene expression profiling was first described in 1995 by Schena et al using a microtiter plate containing 48 cDNA probes.[45] Since then, this tool has been developed extensively and can now probe tens of thousands of genes in parallel and can process multiple samples at a time on a single chip. Microarrays consist of an arrayed series of thousands of microscopic spots of DNA oligonucleotides, containing picomoles of a specific DNA sequence. These oligonucleotides act as probes to hybridize a cDNA or aRNA sample (target). Probe-target hybridization is then detected and quantified by detection of fluorophore-, silver-, or chemiluminescence-labeled targets to determine relative abundance of nucleic acid sequences in the target. In standard microarrays, the probes are attached to a solid surface, which can be glass or silicon, via a covalent bond. Other microarray platforms (such as Illumina), use microscopic beads. DNA Microarrays can be used to measure changes in expression levels, to

detect single nucleotide polymorphisms (SNPs), in genotyping or in resequencing mutant genomes.

Over the past 15 years, microarrays have been used extensively to help scientists take a global view of biological systems. While unable to assess aspects of cellular regulation, such as translational control or intracellular compartmentalization, the evaluating of coding mRNA provides a direct representation of transcriptional and post-transcriptional regulation.[46] For immunologists, this technology has allowed a glimpse into the "immunological genome" defined as the inventory of genes expressed in different immune system cells and the ways in which those transcripts are connected in regulatory networks and vary during differentiation and immune responses.[46] Microarrays have been used to explore perturbations associated with specific immunological diseases in order to identify key cellular or molecular pathways active in the setting of those diseases.[47-50] Studies have attempted to identify gene 'signatures' associated with various hematopoietic cell subpopulations,[51] human leukocytes,[52] and an assortment of tissues representing the mouse immune system.[53] The Novartis Symatlas project analyzed over 60 organs in humans and mice, some of which corresponded to sorted cell populations.[54] The Genentech IRIS project analyzed the gene profile for a number of immune cell subpopulations including CD4 T cells, CD8 T cells, NK cells, DCs, and neutrophils.[55]

The first study in HIV using DNA microarrays was done by Geiss et al in 2000 and looked at host cell gene expression following infection of a CEM cell line with HIV.[56] Since then, microarray studies in human immune cells have helped to reveal novel potential mechanisms of HIV-mediated pathogenesis. Studies have addressed gene modulation associated with immune dysregulation, susceptibility to apoptosis, virus replication and viral persistence.[57]

Microarray studies on HIV-infected PBMCs in vitro have shown that viral envelope facilitate virus replication by upregulating proviral cytokines, chemokines, and transcription factors with long-terminal repeat (LTR) expression.[58,59] Greater activation of p38 MAPK pathway genes associated with R5 gp120 versus X4 gp120 indicated a potential mechanism for favoring R5 virus replication.[59-61] The HIV viral protein R (vpr) has been implicated in down-modulation of immune-response genes required for accessory cell function and cell cycle genes.[62-64] In vivo PBMC microarray studies have elucidated gene correlates of viremia such as low IL-7 receptor α expression and high perforin expression in viremic patient PBMCs and not in 12 aviremic, untreated patients.[65] Genes involved in immature T lymphocyte differentiation, apoptosis, HIV replication, and homeostasis have been shown in PBMCs to be correlated with clinical status and disease progression.[66] Microarray studies in CD4+ T cells have confirmed previously suggested pro-apoptotic mechanisms of CD4+ T-cell induced cell death as well as the role of Nef in enhancing virus replication in CD4+ T cells through a Nef-mediated cholesterol biosynthesis pathway.[57,67-71] In vivo CD4+ T cells studies have shown up-regulation of genes required for virus production, assembly, and release, including genes associated with transcriptional modulation, RNA processing, and protein modification/trafficking.[72]

Microarray studies looking at HIV-mediated latency have revealed several candidate mechanisms contributing to latency in vitro and may possibly act in vivo such as transcriptional quiescence, up-regulation of transcriptional repressors, inhibition of RNA metabolism and processing, down-regulation of surface receptors to evade immune recognition, and up-regulation of virus entry receptors and translation machinery.[56]

Microarray studies of HIV infection and replication in macrophages have confirmed the pro-inflammatory gene commitment thought to enhance virus replication and persistence. HIV-infected macrophages up-regulate IFN/NF-κB-responsive chemokines and cytokines thought to enhance virus dissemination by promoting recruitment of CD4+ T cells and other macrophages to the infection site.[58,73] Up-regulation of cytoskeletal reorganization genes has been identified to enhance virus fusion to host cell membranes.[58] Proviral transcription factors are also up-regulated when macrophages are stimulated with gp120, indicating a potential for envelope interactions to mediate activation independent of infection.[74]

Microarray studies have also uncovered a gene-to-function relationship between anti-apoptotic genes and greater cell survival.[75] Finally, microarrays have been used to obtain genetic correlates of immune modulation pre-and post-ART treatment or associated with vaccine trials.

While the use of microarrays in studying HIV infection seems to be ubiquitous, microarray studies using whole tissues from HIV-infected individuals have been limited.[57] Often, mixed populations of cells have to be assayed from PBMCs and mucosa due to cell number and technology limitation. Development of tools to allow for microarray studies to be conducted on small focused subpopulations of cells will be extremely useful.

CHAPTER 2: Cell capture and release of epitope-specific CD8+ T lymphocytes

Introduction

The study of virus-specific CD8+ T cells in the setting of HIV or SIV infection may potentially reveal important mechanisms in viral pathogenesis and lead to new strategies for viral containment. A challenge in studying these small populations of cells lies in the lack of appropriate assay systems for evaluating small cell numbers. Traditional methods of studying lymphocytes, such as ELISPOT and intracellular cytokine staining (ICS), require large cell samples (millions of cells), which are impossible to obtain from the small biopsy specimens that can be sampled from mucosal compartments. In addition, these assay systems are capable of extracting only a limited amount of information from the cells, namely a handful of cell surface receptors and the production of a few cytokines.

Gene expression analysis using microarray technology is a powerful tool for probing host immune responses and disease pathogenesis in the setting of HIV or SIV infection. With the development of appropriate assays for working with small cell numbers, virus-specific CD8+ T cell populations in human or primate models can be probed at the transcriptional level.

With gene expression analysis of virus-specific CD8+ T cells being the final goal, there are two challenges that must be addressed. The first challenge is to capture the virus-specific CD8+ T cells and separate them from the total lymphocyte population. The captured population needs to be >95% pure and the assay system should not result in substantial cell loss. The second

challenge is to extract high quality RNA from the isolated virus-specific CD8+ T cells and amplify the RNA if necessary. The first challenged will be addressed in this chapter and the second one will be addressed in the following chapter.

There are three different methods of cell capture that can potentially be used to isolate virus-specific CD8+ T cells. The first is immuno-magnetic separation using beads. The second is to develop a microfluidic system that will use an ELISA-like surface chemistry. The last is fluorescence-activated cell sorting (FACS).

Immuno-magnetic cell separation

Immuno-magnetic separation has been used for isolating cells for a number of biological applications.[76-80] This method relies on having monoclonal antibodies that can help distinguish between cell types to be separated. There are two basic methods for performing immuno-magnetic separation: the tube-based method and the column-based method. The tube-based method uses micron-sized beads that can be selected using a magnet and the column-based method uses nano-sized particles that must pass through a ferromagnetic spheres column to increase cell capture capacity.[80]

The two most commonly used magnetic beads systems are the MACS microbeads and the Dynal dynabeads. MACS microbeads are superparamagnetic particles 50 nm in diameter and composed of dextran and iron oxide.[80] These beads need to pass through a ferromagnetic spheres column to increase cell capture capacity and various columns are available through Miltenyi Biotec. In general, two types of Miltenyi columns, 'MS' and 'LS' columns are

optimized for positive selection and two others, 'LD' and 'CS' columns are optimized for depletion. Dynabeads are polystyrene spherical beads with a core of iron oxide.[80] They are 2.8 um in diameter and usually need to be removed from the cell surface before further analysis of isolated cell populations.

To isolate virus epitope-specific CD8+ T lymphocytes from a total lymphocyte population, these cells can be labeled via their T cell receptors with the appropriate MHC class I tetramer conjugated to phycoerythrin (PE) or other fluorescent dyes. There is a MACS anti-PE bead that can bind to the PE-labeled tetramer associated with the epitope-specific CD8+ T cells and facilitate isolation of this rare cell population. There is no anti-PE Dynabead and therefore, a secondary anti-PE antibody would have to be used in combination with the Dynal mouse IgG cleavable bead system to do this cell isolation. Both methods have their advantages and disadvantages. The MACS system has the advantage of using beads that are directly linked to the PE labeled tetramer positive cells and FACS can be employed on these labeled cells without need to remove the beads. This system, however, has the disadvantage of using smaller (50 nm) beads that may not have enough mass to successfully retain cells. In addition, a column separation can result in heavy cell loss. Dynabeads have the advantage of having a greater surface area for interacting with cells than the MACS beads and could potentially retain the bead-cell conjugates better. However, there are several disadvantages to the system. There are no anti-PE dynabeads and therefore attachment would have to occur through the use of a secondary antibody. Second, the anti-mouse IgG antibody on the bead can potentially bind to exposed Fc portions of cell surface receptors of mouse antigen presenting cells. One way to circumvent this problem is by blocking the beads with mouse anti-FcRY after incubation with

the secondary antibody. Lastly, dynabeads are too large for FACS and need to be removed before sorting via DNase treatment, adding another level of complexity and contributing to additional cell loss. It is unclear which system would work better and, therefore, both will be tried.

Integrated Microfluidic Devices

Because they employ small volumes and are amenable to automation, microfluidic devices provide a potentially important platform for studying small populations of cells in a high throughput fashion. Microfluidic devices offer other advantages, including reproducibility of data because of limited user manipulations, rapid processing time, ease of use, infrequent contamination, and ability to integrate multiple components. Microfluidic devices have been developed for a variety of biological applications, including cell capture,[81-84] PCR,[85-91] chemical cytometry,[92] and microarray analysis.[93-95] In addition, significant advances in polymers and substrates used to create these microfluidic devices have been made. [96-99]

However, most of the microfluidic systems developed to date do not meet the requirements of a device for purifying small numbers of specific cells and carrying out RNA analysis on large numbers of specimens. They either require complicated accessory equipment,[84] allow for specific cell capture but not release,[100-104] allow for cell capture and release but in an equipment intensive and non-high-throughput manner,[105] or perform cell concentrating but not specific cell sorting.[82,106] The development of a microfluidic system that is inexpensive, easy to use, and can both capture specific immune cell populations and release them for subsequent applications such as RNA analysis is needed to study virus-specific CD8+ T lymphocyte populations.

Poly dimethyl siloxane (PDMS) - based microfluidic systems, pioneered in George Whitesides' laboratory at Harvard University, can be high throughput, rapid, specific, amenable for use under sterile conditions and can be associated with less cell loss than traditional FACS because of their small size.[107] PDMS has advantages over other substrates such as glass and silicon because of its low cost and ease of processing.[108] Surface chemistry that enables specific binding of PE-labeled tetramer bound cells can be created. Depending on chamber shape and dimensions, a design that minimizes cell loss but maximizes sorting efficiency (as measured by sorting time and purity of sorted population) can be developed. The speed of introducing the cells into the chamber, washing conditions, collection conditions, tubing preparation, and magnet strength are all critical parameters to consider. The purity of the collected cells can be analyzed by flow cytometric analysis or fluorescent microscopy.

Fluorescent-activated cell sorting (FACS)

FACS is a vital tool in biological research and clinical diagnostics, and particularly in stem cell research.[109-115] A heterogeneous population of cells can be purified into fractions containing a single cell type based on a combination of user-defined parameters. Cells in suspension and labeled with fluorescent tags are pressurized into a narrow and directed fluid stream.[116] The cells file in a single line past an analysis point at which one or more laser beams are directed. Any fluorescent tags on the cells are excited by the laser and this signal is collected by an array of photo-detectors and optical filters. These signals indicate to the computer how to divert the droplets of cells that file past the analysis point.

FACS has become a powerful tool in biotechnology, facilitating research and development in areas such as drug screening, protein engineering, and cell signal profiling.[117] FACS has some disadvantages. Because particles are analyzed individually, the process of cell sorting is slow. Top high-speed flow cytometers perform at approximately $1x10^5$ drops per second.[116] In addition, cell loss is high. However, the factor that is most critical to gene expression analysis is high purity (>95%) of the assayed cell population and FACS provides this.

Materials and Methods

Mice and immunization

Six- to eight-week-old female BALB/c mice were purchased from Charles River Laboratories (Wilmington, MA) and maintained under specific-pathogen-free conditions. Research on mice was approved by the Beth Israel Deaconess Institutional Animal Care and Use Committee. Groups of mice were immunized either intraperitoneally with rVac-gp160 (2×10^7 PFU) or intramuscularly with rAd-gp140 (2×10^7 particles) or DNA-gp120 (50 μg of DNA in a 100 μl total injection volume; 50 μl was delivered into each quadriceps muscle). Ten weeks after the first immunization, mice were boosted with both homologous and heterologous combinations of immunogens using the previously mentioned vectors via the same route and with the same quantity as described for the priming immunization.[118]

Rhesus monkeys

Three Mamu-A*01+ Indian-origin rhesus monkeys (*Macaca mulatta*), chronically infected with SIVmac251, were used for experiments. These animals were maintained in accordance with the guidelines of the Committee on Animals for the Harvard Medical School and the Guide for the Careand Use of Laboratory Animals.

Antibodies, tetramers, and peptides

Tetrameric H-$2D^d$ complexes folded with gp120 p18 epitope peptide (RGPGRAFVTI) were prepared as previously described,[119] and conjugated to Streptavidin-PE (DAKO). The antibodies used in this study were directly coupled phycoerythrin (PE), and allophycocyanin (APC). The

following anti-mouse monoclonal antibodies were used: anti-CD8α (clone 53-6.7; eBiosciences), and rat anti-mouse Fc Block (clone 2.4G2; BD Pharmingen).

Immunomagnetic Separation

Spleens from BALB/c mice were harvested in RPMI 1640 medium containing 40 U of heparin per ml. Splenocytes or lymphocytes were isolated from individual mice and peripheral blood mononuclear cells were isolated using Lympholyte-M (Cedarlane). RBCs were lysed by using ACK buffer (0.15 M NH_4Cl, 1 mM $KHOC_3$, and 0.1 mM disodium EDTA) when indicated by the experiment. The cells were then washed with PBS/2%FBS and counted.

Dynal CELLection Pan Mouse IgG Kit selection of CD8+ T cells

Cleavable IgG dynabeads (Invitrogen) were added to mouse anti-PE (Biolegend; Clone PE001) at a concentration of 25 ul of beads to 1 ul of 0.5 mg/ml anti-PE. The beads were incubated with the anti-PE for 30 min at 4°C, rocking, and then washed twice and resuspended in 25 ul of PBS/0.5%BSA. Mouse PBMCs were isolated as described above and were blocked with 2 ul rat anti-mouse Fc Block (clone 2.4G2; BD Pharmingen) for every 10^6 PBMCs, and incubated for 15 min at 4°C. The cells were then stained with PE-conjugated anti-CD8 (clone 53-6.7; eBiosciences) and incubated for 15 min at RT and washed twice. The dynabeads coated with anti-PE were added to the cells at a concentration of 5 ul beads/anti-PE to 10^7 cells. In addition, 2 ul of rat anti-mouse Fc Block (clone 2.4G2; BD Pharmingen) was added and the mixture was rocked for 30 min at 4°C. The cell and bead mixture was then washed and resuspended in media according to manufacturer (Invitrogen) specifications. DNase I was added to the samples according to manufacturer (Invitrogen) instructions, cleaving off the dynabeads, leaving free

CD8+ T cells behind. The beads were separated from the cells using a magnet and the cells were spun down at 6,700 rpm for 5 min to remove free cleaved antibodies. The collected cell pellet was fixed with PBS-1% formaldehyde. Samples were collected on an LSR II instrument (BD Biosciences) and analyzed using the FlowJo software (TreeStar).

Dynal CELLection Pan Mouse IgG Kit selection of epitope-specific CD8+ T cells

Mouse PBMCs were isolated as described above. CD8+ T lymphocytes were purified with negative selection using the CD8a+ T cell isolation kit for mouse (Miltenyi Biotec). The cells were stained with PE-conjugated tetramer (H-2Dd/p18) and anti-PE coated dynabeads (as described above) were incubated with the cells, along with 2 ul of rat anti-mouse Fc Block (clone 2.4G2; BD Pharmingen). The cells/beads were washed and the dynabeads were cleaved off according to manufacturer specifications (Invitrogen). The cells were then stained with APC-conjugated anti-CD8 (clone 53-6.7; eBiosciences) and fixed with PBS-1% formaldehyde. Samples were collected on an LSR II instrument (BD Biosciences) and analyzed using the FlowJo software (TreeStar).

Miltenyi immuno-magnetic isolation of epitope-specific CD8+ T cells

Mouse PBMCs were isolated as described above. CD8+ T lymphocytes were purified with negative selection using the CD8a+ T cell isolation kit for mouse (Miltenyi Biotec) or CD8+ T cell isolation kit for non-human primates (Miltenyi Biotec). Epitope-specific CD8+ T cells were then isolated by staining the cells with PE-conjugated tetramer (H-2Dd/p18 for mice cells or Gag-p11c for monkey cells) for 15 min at 4°C, washing with PBS/2%FBS and incubating with 20 ul Anti-PE Microbeads (Miltenyi Biotec) per 10^7 cells for 15 min at 4°C, washing with PBS

pH 7.2, 0.5% BSA and 2 mM EDTA and applying the sample to the Miltenyi manual MS columns, Automacs, or Multimacs. The collected positive fraction was fixed with PBS-1% formaldehyde. Samples were collected on an LSR II instrument (BD Biosciences) and analyzed using the FlowJo software (TreeStar).

Design of microfluidic channels

Microfluidic channels were made by curing a prepolymer of polydimethylsiloxane (PDMS) upon a master, which was fabricated by standard photolithography.[107] In brief, negative photoresist was spun upon a silicon wafer to a specified height. A particular pattern of interest was designed and printed upon a transparency to mask off regions of the photoresist. The photoresist was exposed to ultraviolet light (UV), which crosslinked regions exposed to UV. Those regions masked by the patterned transparency remained uncrosslinked. The uncrosslinked photoresist was removed and the wafer was silanized.

A prepolymer of PDMS (1:10 curing agent : base) was poured upon the silanized wafer and the masters were baked for at least 4 hours at 70°C. To ease in the removal of PDMS, ethanol was added to the master as the PDMS was peeled away from the master. Holes were punched at the inlets and outlets of the PDMS mold with a syringe. With a plasma sealer, the glass and PDMS was exposed to 1 min of plasma and the two surfaces were immediately brought together, resulting in a permanent seal. The channels were placed upon a 120°C hotplate for at least 30 min to ensure a seal and sterilize the channels.

Patterning of the microfluidic channel with antibodies using the cross-linker GMBS

The glass was silanized within 15 min after plasma-sealing the PDMS to glass. The channel was rinsed with ethanol before injecting in 4% (v/v) 3-mercaptopropyltrimethoxysilane (in ethanol). The channels were incubated with silane for 1 hr at room temperature, then rinsed with ethanol to remove excess silane. To activate the silane, 0.28% v/v 4-Maleimidobutyric acid sulfo-N-succinimidyl ester (GMBS; in ethanol) was added for 15 min at room temperature. Again, the channel was rinsed thoroughly with ethanol to remove excess reagent. After drying the channels with a stream of nitrogen, phosphate-buffered saline (PBS) was added.

Functionalization of the surface of the microfluidic channels

Channels consisting of stamps of a clear polymer, polydimethylsiloxane (PDMS), enabled visualization of the cells within the channel. These stamps of PDMS were sealed to cleaned glass microscope slides to enable imaging with an inverted microscope. Prior to loading cells into the microfluidic channel, the surface of the channel was functionalized to bind tetramer-positive CD8+ T cells. In brief, the surface was coated with 3-mercaptopropyltrimethoxysilane for 1 h, and activated the silane with 0.28% v/v 4-Maleimidobutyric acid sulfo-N-succinimidyl ester (GMBS). In the case of direct binding of antibody to GMBS, anti-phycoerythrin (Anti-PE) antibody (Biolegend) was then added at a concentration of 0.15 mg/ml in PBS and bound to the GMBS. For the chemisty involving a neutravidin and biotin interaction, after the GMBS coverage and wash, neutravidin was then injected into the channel at a concentration of 10 ug/ml in PBS and incubated for 2 hours at 4°C, followed by a rinse with PBS. Anti-PE (Biolegend) was biotinylated in-house according to the protocol in the Molecular Probes

Handbook and was added to the channels at a concentration of 10ug/ml and incubated overnight at 4°C. The channels were then blocked with 1-10% bovine serum albumin (BSA) in phosphate-buffered saline (PBS) for one hour at room temperature to prevent non-specific binding of tetramer-negative cells to the functionalized surface of the microfluidic channel. This blocking was crucial to prevent significant background since the percentage of tetramer-positive T cells is low (~1%).

Loading of cells into channels

A purified population of CD8+ T cells was obtained using the CD8+ T cell isolation kit (mouse or monkey) as described above. Prior to loading the CD8+ T cells into the channels, the cells were stained with PE-conjugated H-2D$_d$/p18 tetramer for 15 min at 4°C then washed with PBS/2%BSA. The cells were then resuspended in PBS at a concentration of 8,300 cells/ul according to previous titrations. Using a syringe pump to obtain a slow and steady flow in the channel, a volume of cells equivalent to the volume of the channels was loaded. The cells were incubated in the channels for 5 min at room temperature to allow the cells to bind to the surface. The entire device was kept in the dark to prevent photobleaching of the PE-labeled tetramers. After 5 min, we used a syringe pump to rinse the channels with buffer (PBS/1%BSA) to remove any non-specific cells from the channel.

Testing antibody coverage of microfluidic channels containing biotin-avidin chemistry

Anti-PE (Biolegend) was biotinylated (Invitrogen) according to the protocol in the Molecular Probes Handbook. 50 ul of 10 ug/ml biotinylated anti-PE was incubated in the channels coated with neutravidin (described above) at 4°C for 18 hours. The channels were then washed twice

with filtered and degassed PBS/1%BSA/0.09%Azide (wash buffer) then blocked with 100 ul of PBS/5% BSA for 2 hours at room temperature. The channels were washed twice with 100 ul of wash buffer. Free phycoerythrin (PE) at a molar ratio of 2:1 to the biotinylated anti-PE was added and incubated in the dark for 20 min at room temperature. The channels were then washed twice with 100 ul of wash buffer and placed in 4°C until imaging.

Counting total cells bound

Microfluidic channels were sealed to the microscopy slides in order to mount the channels upon a standard-sized, microscope stage. After binding the tetramer-positive cells to the channel and removing the unbound cells, each region of the channel was imaged and the number of fluorescent PE-labeled tetramer positive cells was counted. By counting the total number of fluorescent cells and comparing it to the total number of cells injected into the channel, the percentage of tetramer positive CD8+ T cells bound was determined.

Results

A number of approaches for isolating epitope-specific CD8+ T lymphocytes were explored, including immuno-magnetic separation, microfluidic cell sorting, and fluorescence-activated cell sorting (FACS). Each method was optimized and the methods were compared for their ability to isolate pure cell populations.

Immuno-magnetic cell separation

Two immuno-magnetic cell separation systems were investigated: Dynal and Miltenyi. In both systems, experiments showed that a two-round purification procedure was necessary to obtain the highest purity of epitope-specific CD8+ T cells. A first round was done to select for CD8+ T cell and a second round of purification was used to select for epitope-specific CD8+ T cells.

Using the Dynal CELLection Pan Mouse IgG Kit with an anti-PE secondary antibody, CD8+ T cells were isolated with 96.4±0.9% purity (Fig. 2.1). However, the Dynal system was not able to purify epitope-specific CD8+ T cells, using tetramers, yielding purities of less than 20% (data not shown) and with substantial cell losses.

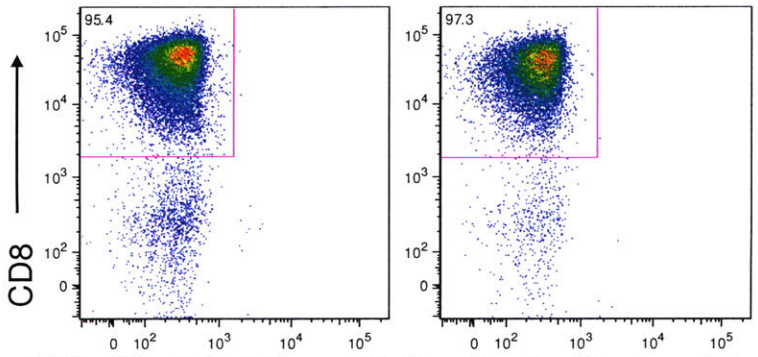

Figure 2.1. Murine CD8+ T cell isolation with Dynabeads. The two plots were generated in two separate experiments.

The Miltenyi system was explored as another option for a two-round purification of epitope-specific CD8+ T cells. One can perform a negative selection with the Miltenyi CD8+ T cell isolation kit followed by positive selection of the epitope-specific CD8+ T cells with Miltenyi anti-PE microbeads.

Using the Miltenyi CD8+ T cell isolation kit followed by positive selection of epitope-specific CD8+ T cells with Miltenyi anti-PE microbeads, a 36-fold enrichment of epitope-specific CD8+ T cells (initial 2.7% to final 96.8%) in the murine system (Fig. 2.2) and a 38-fold enrichment (initial 2.34% to final 89.5%) in the nonhuman primate system was achieved (Fig. 2.3). These experiments were performed with either the Miltenyi manual MS columns or the Miltenyi Automacs.

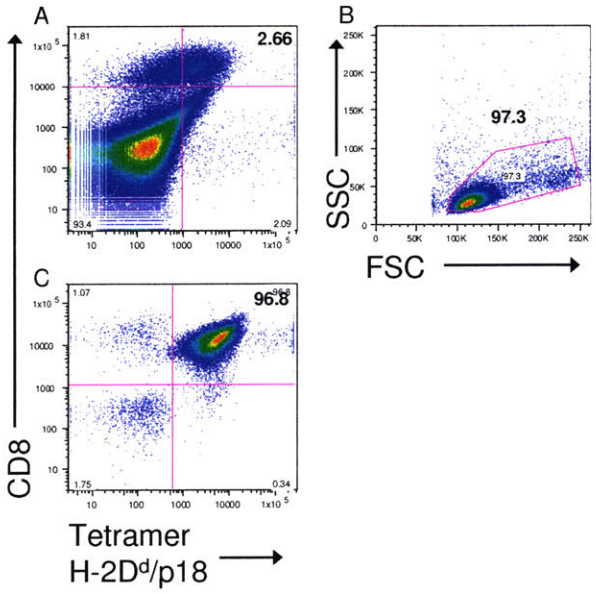

Figure 2.2. Positive selection of murine epitope-specific CD8+ T lymphocytes (p18+) with Miltenyi Microbeads using a two-step purification protocol. **(A)** Total cell population before two-step purification. **(B)** Gating strategy **(C)** Purified epitope-specific CD8+ T cell population.

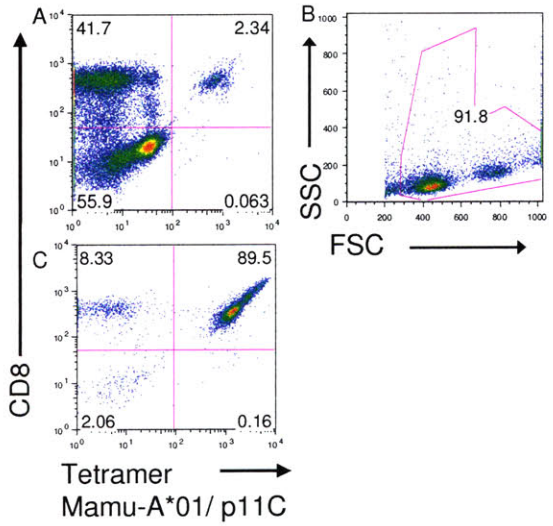

Figure 2.3. Positive selection of rhesus monkey epitope-specific CD8+ T lymphocytes (p11C+) with Miltenyi Microbeads using a two-step purification protocol. **(A)** Total cell population before two-step purification. **(B)** Gating strategy. **(C)** Purified epitope-specific CD8+ T cell population.

However, repeated experiments showed that neither the manual columns nor the Automacs consistently provided epitope-specific CD8+ T cell purities above 80%. For gene expression analysis, purities should be greater than 95%. The manual columns and Automacs are also not optimal because they are not high-throughput.

In collaboration with Miltenyi Biotec, we tested a Multi-Macs cell sorter under development in their R&D laboratories. This cell sorter was similar to the Miltenyi Automacs but could process 24 samples in parallel. Upon testing our application with this sorter, however, we found that cell purities were inconsistent in repeated experiments, varying between 10% and 80% purity using similar experimental conditions (Fig. 2.4).

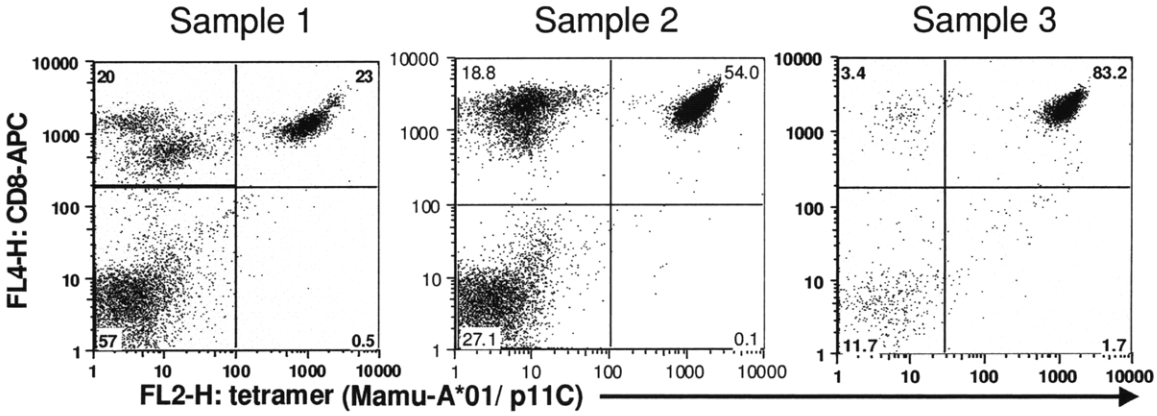

Figure 2.4. Isolation of epitope-specific CD8+ T lymphocytes using Miltenyi Multimacs with microbeads. All three samples were processed similarly.

We attempted to optimize the system by varying the amount of antibody-coated microbeads used and by lysing red blood cells to eliminate them from the final lymphocyte population. While lysing red blood cells improved CD8+ T cell purity, the final purity of epitope-specific CD8+

lymphocytes did not improve (Fig. 2.5). Decreasing amounts of microbeads that were used also did not improve the purity of the final cell populations (Fig. 2.6).

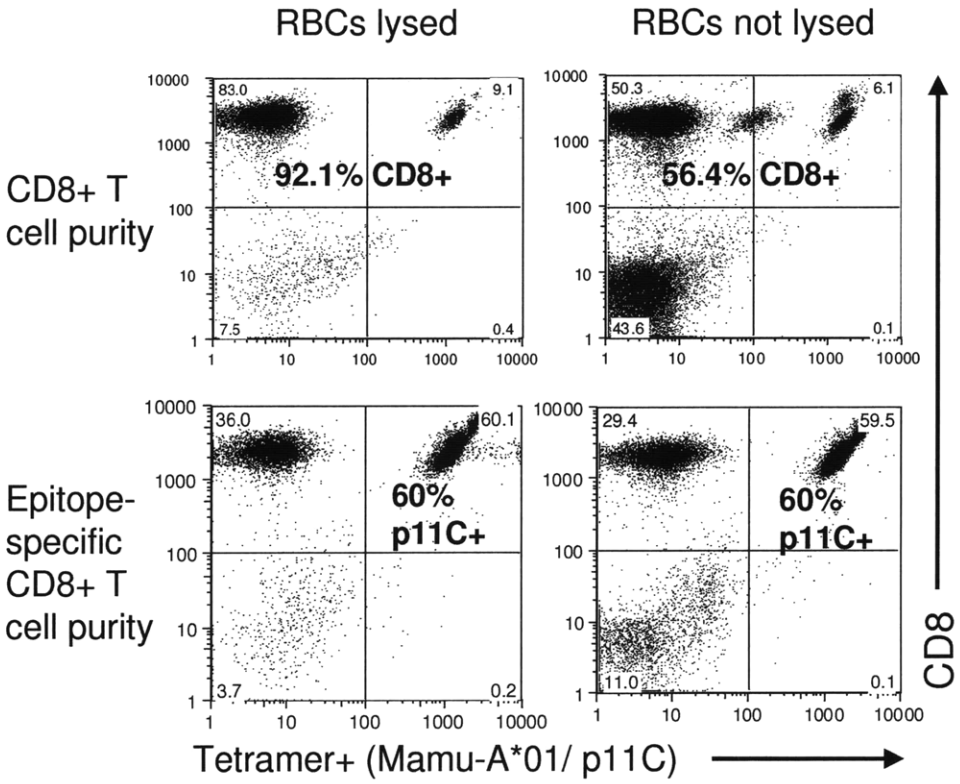

Figure 2.5. Difference in purity of CD8+ T cells and epitope-specific CD8+ T cells with and without lysis of red blood cells (RBCs).

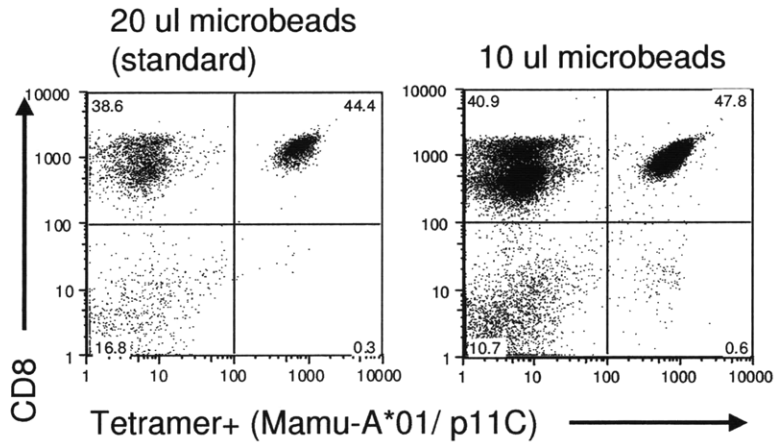

Figure 2.6. Difference in purity of epitope-specific CD8+ T cells with decreased amounts of Miltenyi anti-phycoerythrin (anti-PE) microbeads. The standard protocol according to the manufacturer (Miltenyi Biotec) indicates 20ul microbeads for every 10^7 cells.

Microfluidic cell sorter

A poly dimethyl siloxane (PDMS)-based microfluidic system for cell sorting was developed as described in the Materials and Methods section of this chapter. The system was first tested for isolation of epitope-specific CD8+ T cells using cleavable dynabeads (CELLection Pan Mouse IgG Kit) combined with an APC conjugated anti-phycoerythrin (PE) antibody adsorbed onto the PDMS surface. This method yielded very low epitope-specific CD8+ T cell purity (<10%) and was associated with high cell losses. In this system, the dynabeads had to be cleaved off before the cells could pass through the flow cytometer for analysis. These results suggested that this cleavage did not operate efficiently and, as a result, led to high cell losses as well as low cell purities.

The use of microbeads for this procedure was then explored. Miltenyi anti-PE Microbeads are small and do not need to be removed prior to flow cytometric analysis. Microfluidic channels were prepared as described in the Materials and Methods section of this chapter and the channels were incubated overnight with anti-PE, allowing the antibody to attach to the surface through the use of a cross-linker (GMBS). A number of different anti-PE antibodies (Biolegend, Sigma, and Stemsep) were tested. Different BSA concentrations in the blocking buffer were also tested. Channel design was also varied by adding posts to increase surface area for cell-antibody interaction (Fig. 2.7). In addition, other variables such as duration of incubation, flow rates and wash volumes were manipulated to select the optimal conditions for epitope-specific CD8+ T cell isolation.

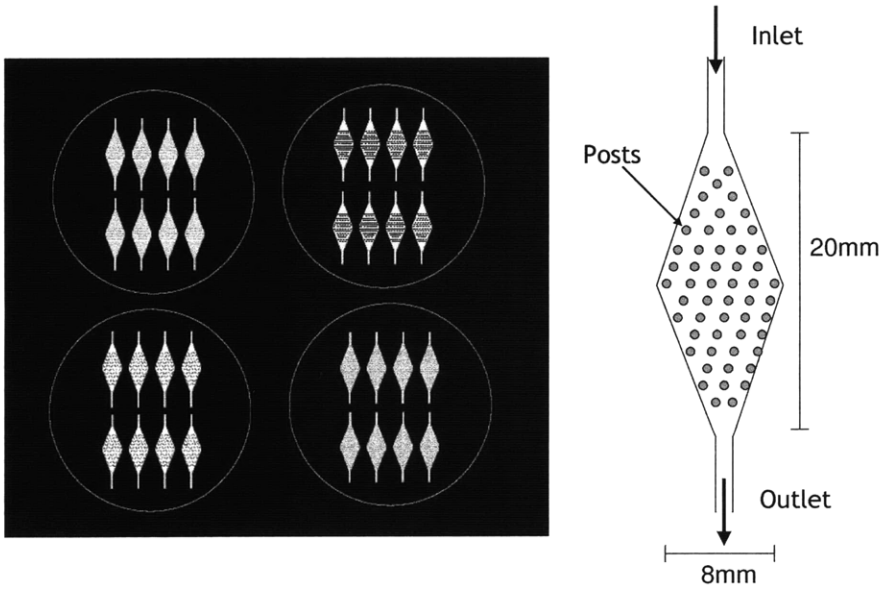

Figure 2.7. Mask and schematic of diamond-shaped microfluidic chamber with poles.

The highest purity of epitope-specific CD8+ T cells obtained was 63% (3632 tetramer-specific cells/ 5298 total cells in the whole field) (Fig. 2.8). Few T cells were captured in a control non-coated chamber (0 tetramer binding cells /111-131 total cells). This was achieved using the

Biolegend anti-PE antibody with 10% BSA block, incubation time of 20 min, and 80 ul of wash buffer at flow rates of 10-20 ul/min.

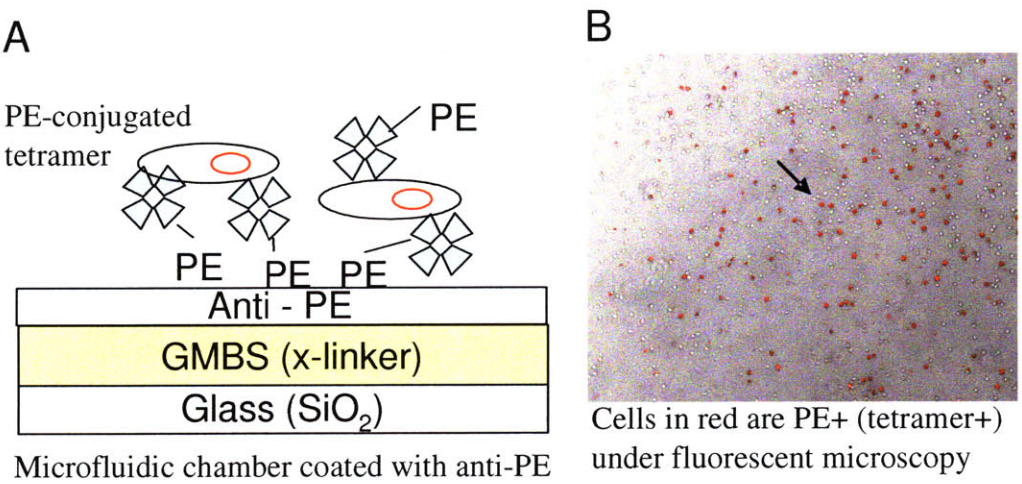

Figure 2.8. Capture of epitope-specific CD8+ T lymphocytes using anti-phycoerythrin (PE) antibodies and PDMS-based microfluidic system. **(A)** Microfluidic chambers are coated with anti-PE and total cells stained with PE-tetramer are flowed through the chambers. **(B)** Tetramer positive cells are visualized with red fluorescence (indicated by arrow). A purity of 63% was achieved.

It was not possible to obtain epitope-specific CD8+ cells with greater than 63% purity using this this particular chemistry. Therefore, other approaches were investigated.

In a different approach, the strong biotin-avidin interaction ($Kd=10^{-13}M$) was utilized to maintain the anti-PE antibody on the surface of the chamber. The Biolegend anti-PE was biotinylated as described in the Materials and Methods section of this chapter and we attached neutravidin to the silanized glass surface of the chambers by way of a cross-linker (GMBS). The channels were

then incubated with the biotinylated anti-PE. The shape of the channel was also changed to a rectangular one with rounded edges because diamond-shaped design trapped cells in its corners (Fig. 2.9).

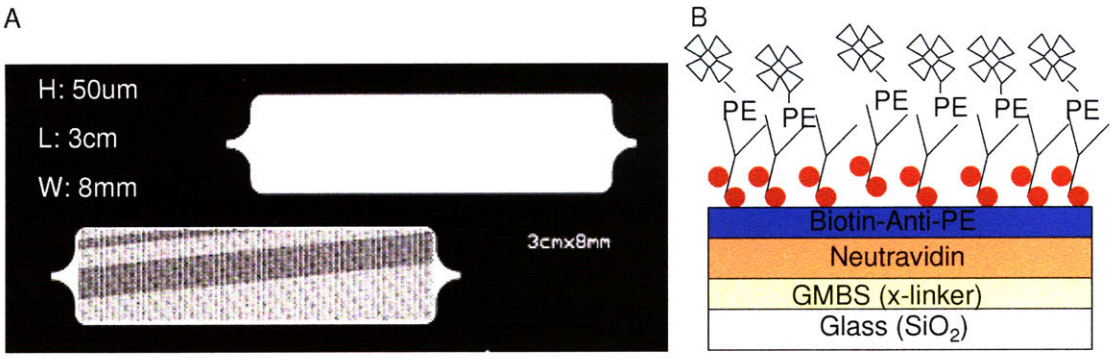

Figure 2.9. Rectangular microfluidic cell sorter with biotin-avidin chemistry. (A) Chambers are rectangular with rounded edges with and without posts. **(B)** Biotinylated anti-PE is linked to the surface through a neutravidin-biotin interaction.

Using this new microfluidic design, anti-PE coverage of the surface was evaluated by incubating the chambers with free phycoerythrin. Coverage was complete and uniform in the channels with the posts, showing no non-specific binding in the negative control (Fig. 2.10). The areas around the posts showed the greatest fluorescence because the posts allow for stacking of antibody all along its length and when visualized from above, exhibits high fluorescence intensity. In between the posts, the antibody is collected only in one layer and therefore in contrast, looks dark. The chambers without the post also showed uniform coverage of free phycoerythrin (data not shown). Since the posts provide greater surface area for cell-antibody interaction, they will likely be the best for cell sorting.

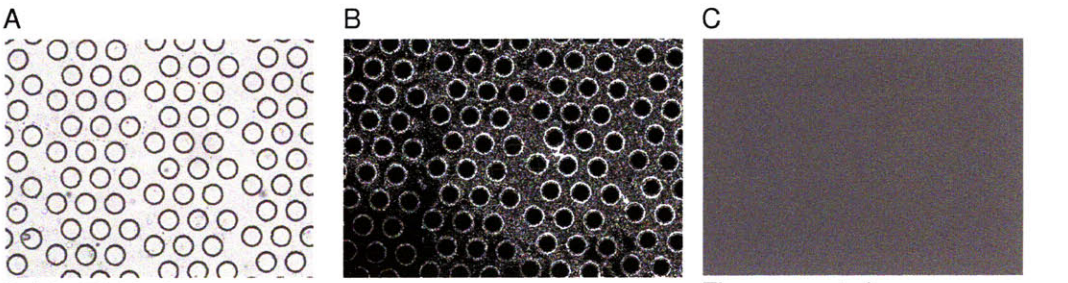

Figure 2.10. Biotinylated anti-PE coverage of microfluidic chamber surface. Chambers are incubated with free PE and visualized with a fluorescent microscope**. (A)** Bright field view shows snapshot of chamber with posts. **(B)** Fluorescent view shows biotin-anti-PE coating visualized as bright circles around the posts. **(C)** Negative control chamber

To understand dynamic cell attachment behavior at different shear rates, a Hele-Shaw device can be used (Fig. 2.11).[104] This device can be used to optimize flow rates so that the greatest number of epitope-specific CD8+ T cell are captured with the lowest amount of non-specific binding. These experimental results are pending.

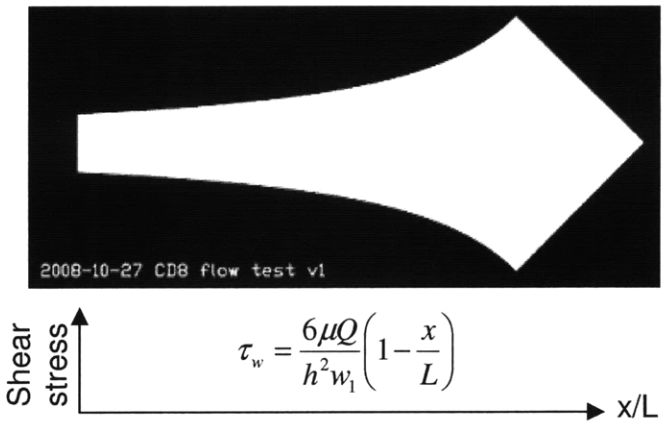

Figure 2.11. Hele-Shaw Device. Shear stress varies along the length of the device and by observing where antigen-specific CD8+ T cells attach, the optimal flow rate for greatest specific cell capture and smallest non-specific attachment can be determined.

Fluorescence-Activated Cell Sorting (FACS)

While a microfluidic cell sorter is being developed, a fluorescence-activated cell sorter (FACS) will be used for isolation of epitope-specific CD8+ T cells. FACS consistently provides greater than 99% pure populations of epitope-specific CD8+ T cells. While FACS is time-consuming and is associated with high cell loss (approximately 50%), the purity of the cells that are obtained is unsurpassed.

Discussion

Dynabeads facilitated the isolation of CD8+ T cells from total PBMCs to a high purity as shown in Figure 2.1. However, they were not capable of isolating virus epitope-specific CD8+ T cells. This suggests that these beads are more useful for sorting large populations but not rare cell populations such as epitope-specific CD8+ T cells, which can comprise only 1-2% of a total cell population. It is possible that the cleavage process, which involves rigorous pipetting and shaking, may disturb the tetramer binding to the cells, since this is not nearly as high affinity an interaction as the one between the CD8 molecule and an anti-CD8 antibody.

Miltenyi beads had an advantage over dynabeads in that they did not need to be removed before an analysis of the cells isolated using the beads. This quality may have contributed to the superiority of their capabilities in isolating virus epitope-specific CD8+ T cells. In addition, the Miltenyi system does not require a secondary antibody and is therefore simpler. Instead, the anti-PE was linked directly to the microbeads and was added to PE labeled tetramer positive cells without an intermediate linker. However, results from our studies suggest that even this system is not able to consistently isolate highly purified populations of virus epitope-specific CD8+ T cells. Immuno-magnetic separation using the Multimacs, the manual MS columns, or the Automacs did not yield cells of high enough purity for our needs. Virus epitope-specific cells can represent a very small percentage of total mononuclear cells, especially in the setting of chronic infection. While immuno-magnetic separation is practical for isolation of large subpopulations of cells, it is neither strong enough nor specific enough to isolate subpopulations

that represent only 1-2% of a cell population. A more stringent system is therefore needed to capture and separate these rare cell populations.

Microfluidic channels represent a potentially useful alternative to immuno-magnetic separation because it involves limited user manipulations, rapid processing time, ease of use, reduction in contamination, and can integrate multiple components. However, this technology will take more time to reach maturity. Upon successful capture and release of virus epitope-specific cells from a larger total cell population, one can imagine integrating a module for downstream RNA extraction that can be used for gene expression analysis. A chamber with multiple inlets would allow the introduction of lysis buffer and other reagents into a compartment with the cells. The RNA could be collected on silicon coated columns built into the chamber or on beads packed in the chamber. Initially, the collected RNA could be release through an outlet into an eppendorf for macroscale RNA processing. Based on work by other laboratories,[120] it is feasible to design an addition process for cDNA amplification via solid phase reaction on beads or columns. A heating element would need to be attached to the device as well as inlets for reaction buffers and dNTPs. For each of the inlets, microvalves and micropumps could be engineered,[120,121] and the timing could be controlled by a computer-run system. The ultimate result would be an integrated device capable of sorting virus epitope-specific CD8+ T cells from a total lymphocyte population and could perform downstream RNA extraction and cDNA amplification for gene expression analysis.

Since these technologies do not yet exist, fluorescence-activated cell sorter (FACS) is the best available technology to use to isolate virus epitope-specific CD8+ T cells. FACS provides a very

high purity of isolated cell subpopulations. For gene expression analysis, purity of the cell population to be studied is of utmost importance so that one can be certain that the expression levels seen on an array originate from the cells being studied. However, FACS does have disadvantages, namely high cell loss (30-50%) and long processing time. The processing of cells from PBMC extraction to cell isolation using FACS may induce changes in the biology of the cells that are distinct from the changes associated with the biologic events being studied. However, since cells are processed the same way, comparison of gene expression profiles should reveal differences associated with biologic events and not sample processing.

CHAPTER 3: Development of techniques for RNA extraction, amplification, and gene expression analysis using limited numbers of cells

Introduction

The validity of gene expression data is dependent on using good quality RNA. While adequate amounts of high integrity RNA can be obtained from millions of cells, it is difficult to obtain high integrity RNA from limited numbers of cells. However, often, as is in the case of studying virus epitope-specific CD8+ T cells, the cell population of interest is small. Therefore, the development of techniques for extraction of high yield and high quality RNA and subsequent amplification and gene expression analysis is of tremendous importance.

RNA Integrity

RNA can be rapidly digested by nearly ubiquitous RNase enzymes, compromising its analysis. RNA integrity has been evaluated using agarose gel electrophoresis stained with ethidium bromide, producing two bands comprising the 28S and 18S ribosomal RNA species.[122] RNA is considered to be of high quality if the ratio of 28S:18S bands is about 2.0 or higher. However, this method is highly subjective, requiring human interpretation of gel images. A newer and more automated method for evaluating the quality of extracted RNA uses the concept of the RNA Integrity Number (RIN) calculated by the Agilent Bioanalyzer using a Bayesian approach.[122,123] The RIN is calculated using a combination of a number of different features to allow for robust measurement. These features include the total RNA ratio (fraction of area in 18S and 28S regions compared to total area under the curve), the height of the 28S peak, the fast

area ratio, and the marker height.[122] RNA with a RIN of 7 or greater is adequate for downstream applications such as RT-PCR, amplification, and gene expression analysis.

RNA Isolation

There are two characteristics to consider in RNA isolation: quality and quantity. When working with limited number of cells, very few RNA isolation methods are capable of yielding measurable quantities of high integrity RNA. Individual eukaryotic cells contain on the order of 1-10 pg of total RNA, varying based on organism, species, tissue type, and viability of the cells.[115] While several studies have been published comparing RNA yield and quality from different extraction methods, varying results are suggested by different scientists and often results contradict each other.[124-129] RNA extraction is a very sensitive procedure and can yield different results in different hands. For example, for one group, the Trizol method provided poor quality RNA and low yields,[124] while for another group, it proved to be superior to any other methods.[128] In many instances, the type of tissue or cell in question as well as the nature of downstream applications is pertinent to the choice of RNA extraction method.

There are three basic types of methods for extraction of RNA: a tube-based phase separation extraction method (ie. Trizol),[130,131] a silica-gel membrane-based spin-column method (ie. RNeasy Micro-Kit or Arcturus PicoPure Kit), and a paramagnetic oligo(d)T-bead method (ie. μMACS). Column methods often have the advantage of very high purity, since the sample is passed through a mesh filter, but have the disadvantage of high RNA loss. Tube-based phase separation methods can result in high yields because there is no column, but there is the potential of contaminants in the final RNA sample.

RNA Amplification

Microarray analysis require a minimum of 25 ng of unamplified aRNA or 1.5 ug of amplified poly(A)+ RNA for the Illumina platform, and 2-5 ug of unamplified poly(A)+ RNA for the Affymetrix platform. It is often not possible to obtain this much RNA from sorted cell populations from mucosal biopsies and peripheral blood. Therefore, amplification techniques are essential for studies involving microarray analysis of cellular subpopulations. Most amplification techniques are based on the work of Eberwine, which uses in vitro transcription of RNA to achieve linear increases of RNA concentration.[132] The first strand cDNA is synthesized by an RNA-dependent reverse transcriptase, and is primed by a phage promoter (T7, T3, or SP6) linked oligo-dT primer that binds to the poly(A)+ tail of mRNA.[133] The second strand cDNA is then synthesized with a DNA polymerase I followed by aRNA synthesis from the cDNA template using an RNA polymerase corresponding with the promoter sequence (T7, T3, or SP6).[115] The second round of amplification is similar to the first except first strand cDNA synthesis is primed using random primers and a T7, T3, or SP6 promoter-linked oligo-dT primer is used for second strand synthesis.[115] aRNA products are biased toward the 3' end of the transcript because of the initial priming at the poly(A)+ tail.[134] However, this bias exists for all amplified aRNA products and relative levels of gene expression can be compared.[134] The optimized Eberwine RNA amplification method can amplify mRNA up to 10^3-fold after one round and up to 10^5-fold after two rounds of amplification.[135-137] Therefore, approximately 10 ng of input total RNA is necessary for successful microarray hybridization.[138] The number of cycles of amplification can be increased to raise yield and it has been reported that a linear relationship between transcript abundances is maintained after five cycles of RNA amplification.[139] Recently,

however, optimized methods based on the Eberwine method have been developed by a number of different companies that have allowed for starting RNA amount in the picogram range.[140-145]

Another method of amplifying RNA uses the polymerase chain reaction (PCR). This has potential for high yield and simpler experimental procedures.[115] A number of different groups have tried to amplify RNA this way.[134,146-153] However, PCR-based amplification methods can skew the original quantitative relationships between genes from an initial population.[134] Some groups have attempted to combine PCR and IVT to increase fidelity because only a limited number of PCR cycles are used.[154] The suitability of PCR RNA amplification for microarry analysis depends on a number of factors, including: 1) degree of fidelity 2) degree of coverage by microarrays and 3) polarity of probes.[115]

While most RNA amplification methods require purified total input RNA, it has been shown that cell lysates can be directly amplified successfully.[155] The use of cell lysates has the advantage of not risking the loss of RNA during purification and, therefore, is amenable to amplifying RNA from very limited numbers of cells.

Gene expression analysis

Two microarray platforms are available for studying virus epitope-specific CD8+ T cells from rhesus monkeys. The first is the Illumina Beadchip platform, which consists of microscopic beads with hundreds of thousands copies of 50-mer probes. The human BeadChips target more than 25,000 annotated genes with more than 48,000 probes covering the RefSeq (Build 36.2, Rel 22) and the UniGene (Build 99) databases. Anywhere from 6 to 12 arrays can be run

simultaneously on the same BeadChip and starting unamplified RNA requirements are between 50 ng and 100 ng. The second platform is the Affymetrix GeneChip platform, which consists of 1.3 million oligonucleotides synthesized using photolithography on a glass substrate. Affymetrix recently developed a Rhesus Macaque Genome Array with 52,024 probes sets of 25-mer probes that query 47,000 rhesus monkey transcripts. Microgram amounts of starting RNA are required for the Affymetrix arrays.

Materials and Methods

Animals

All animals used in this study were Indian-origin rhesus monkeys (*Macaca mulatta*). The monkeys were all chronically infected with SIVmac251 for over ten years. These animals were maintained in accordance with the guidelines of the Committee on Animals for the Harvard Medical School and the Guide for the Care and Use of Laboratory Animals.

Antibodies, tetramers, and peptides

Mamu-A*01/p11C,C-M/B2m (SIVmac Gag) tetramer complexes were prepared as previously described.[156,157] Streptavidin-PE (ProZyme) was mixed stepwise with biotinylated Mamu-A*01/peptide at a molar ratio of 1:4 to produce the tetrameric complexes. Conjugated antibodies used in this study included anti-human anti-CD3 APC (Clone SP34.2; BD-Pharmingen). The anti-human anti-CD8 (clone SK1; BD-Pharmingen) monoclonal antibody was directly coupled to fluorescein isothiocyanate (FITC). A live/dead fixable blue amine dye (UV excitation; Invitrogen) was used to differentiate between live and dead cells on the flow cytometer.

Peripheral blood mononuclear cell (PBMC) preparation

Peripheral blood was collected from rhesus monkeys, and PBMCs were recovered by standard Ficoll density-gradient centrifugation. The recovered cells were then washed twice with PBS containing 2% FBS. Cells were stained with Mamu-A*01/p11C,C-M/B2m tetramer for 15 min at 4°C in the dark. Cells were then stained with a mixture of anti-CD3 and anti-CD8 Abs for 10 min at 4°C in the dark. The cells were washed with PBS/2%FBS and resuspended in 1 ml of

cold PBS for every 10^7 cells. The p11C+ CD8+ T cells were sorted using the FACS-Vantage Flow Cytometer/Cell Sorter (Becton-Dickinson) and collected in RNAprotect (Qiagen).

Cell extraction from Gastrointestinal Tract biopsies

Pinch biopsies (8-10 pieces) were taken from the duodenum and distal colon of anesthetized monkeys at the New England Primate Center. The biopsies were shipped on ice in 40 ml RPMI containing 10% FBS and were processed the same day. The biopsies were pelleted at 1,500 rpm for 7 min. The supernatant was discarded and the biopsies were dissected further into smaller sections before being resuspended in 40 ml warm RPMI/10%FBS containing 300 U/ml Collagenase II and 30 U/ml DNAse I. The mixture was shaken well and placed in a shaking 37°C water bath for exactly 45 min, with manual shaking every 15 min. The digested biopsies were then spun down at 1,500 rpm for 7 min, the supernatant was discarded, and 5ml of cold RPMI/10%FBS was added to the sample. The tissue was disrupted through an 18G animal feeding needle (Fisher Scientific) several times to release the cells and transferred through a 70 μm cell strainer into a clean 50 ml conical. The cell strainer was washed with an additional 45 ml of RPMI/10%FBS. The cells were spun down at 2,000 rpm for 5 min, the supernatant was discarded, and the cells were resuspended in 10 ml RPMI/10%FBS. The cell mixture was layered gently over a percoll gradient consisting of 2 ml of 35% isotonic Percoll underlaid with 2 ml of 60% isotonic Percoll (Sigma). Isotonic Percoll was made by adding 50 ml 10X PBS to 450 ml Percoll. The cells were centrifuged for 25 min at 1,800 rpm and the lymphocytes were collected from the layer between the 35% and 60% Percoll layers and transferred to a fresh tube. The collected lymphocytes were washed twice in cold PBS2%FBS at 2,000 rpm for 5 min and counted. The cells were stained with a live/dead fixable blue amine dye (Invitrogen), incubated

for 15 min at 4°C in the dark. After washing with PBS/2%/FBS, the cells were then stained with Mamu-A*01/p11C,C-M/B2m tetramer for 15 min at 4°C in the dark. They were washed once with PBS2%FBS and then stained with a mixture of anti-CD3 and anti-CD8 Abs for 10 min at 4°C in the dark. The cells were washed with PBS/2%FBS and resuspended in 1 ml of cold PBS for every 10^7 cells. The p11C+ CD8+ T cells were sorted using the FACS-Vantage Flow Cytometer/Cell Sorter (Becton-Dickinson) and collected in RNAprotect (Qiagen) if the RNA was to be extracted immediately. For cells that would be frozen immediately for freeze/thaw lysis direct into RNA amplification, the cells were collected in 100 ul PBS in 96 well plates and transferred to eppendorf tubes to be frozen at -80°C.

Cell extraction from bronchoalveolar lavage (BAL)

Bronchoalveolar lavage on rhesus monkeys was performed under anesthesia at the New England Primate center. The samples were shipped on ice and processed the same day. PBMCs were recovered by standard Ficoll density-gradient centrifugation. The recovered cells were then washed twice with PBS containing 2% FBS and counted. The cells were stained with a live/dead fixable blue amine dye (Invitrogen), and incubated for 15 min at 4°C in the dark. After washing with PBS/2%/FBS, the cells were stained with Mamu-A*01/p11C,C-M/B2m tetramer for 15 min at 4°C in the dark. They were washed once with PBS2%FBS and then stained with a mixture of anti-CD3 and anti-CD8 Abs for 10 min at 4°C in the dark. The cells were washed with PBS/2%FBS and resuspended in 1 ml of cold PBS for every 10^7 cells. The p11C+ CD8+ T cells were sorted using the FACS-Vantage Flow Cytometer/Cell Sorter (Becton-Dickinson) and collected in RNAprotect (Qiagen) if the RNA was to be extracted immediately. For cells that

would be frozen immediately for freeze/thaw lysis direct into RNA amplification, the cells were collected in 100 ul PBS in 96 well plates and transferred to eppendorf tubes to be frozen at -80°C.

RNA Extraction

Cells collected in RNAprotect (Qiagen) were spun down at 800 g for 10 min, discarding the supernatant. Cells collected in PBS were spun down 1,500 rpm for 7 min, discarding the supernatant. The appropriate lysis buffer was immediately added. RNA was extracted from the cells according to manufacturer instructions for the Arcturus PicoPure Kit (MDS Analytical Technologies), the RNeasy Micro Kit (Qiagen), or Trizol (Invitrogen).

Briefly, using the Arcturus PicoPure Kit, 100 ul of Extraction Buffer was added to the cells and incubated at 42°C for 30 min. The cells were spun down and the supernatant was transferred to a new tube. Equal volume of 70% ethanol was added and the mixture was transferred to a purification column. Two wash buffers were used to wash through the column, along with a 15 min Dnase treatment step at room temperature. The RNA was then eluted with 11 ul of Elution Buffer and stored at -80°C.

Using the RNeasy Micro Kit, 350 ul RLT Buffer containing 10 ul/ml of B-Mercaptoethanol was added to the cells. The lysate was spun through a Qiashredder and then mixed with 70% ethanol and placed in an RNeasy MinElute spin column. The column was washed with Buffer RW1, followed by a Dnase I treatment for 15 min at room temperature. The column was washed with buffer RW1, Buffer RPE, and 80% ethanol before the RNA was eluted in 14 ul of RNase-free water. The RNA was stored at -80°C.

Using the Trizol procedure, 1 ml of Trizol was added to the cell pellet and incubated for 5 min at room temperature. Two hundred microliters of chloroform was added and shaken vigorously by hand for 15 seconds, and incubated at room temperature for 2-3 min. The samples were then centrifuged at 13,000 rpm for 15 min at 4°C. The colorless upper aqueous phase was carefully transferred to a new tube, and 2 ul of linear acrylamide was added and mixed in. An equal volume of isopropyl alcohol was then added and mixed. The mixture was incubated at room temperature for 10 min and centrifuged at 13,000 rpm for 10 min at 4°C. The supernatant was removed and the RNA was washed with 1 ml of 70% ethanol and centrifuged at 10,500 rpm for 5 min at 4°C. The supernatant was completely removed and the RNA pellet was allowed to airdry. The RNA was then resuspended in RNase-free water and stored at -80°C.

RNA Amplification

RNA was amplified from purified total RNA or cell lysates using the TargetAmp 2-Round Biotin-aRNA Amplification Kit 3.0 (Epicentre Biotechnologies) or the MessageAmp II aRNA Amplification Kit (Ambion). For cell lysates, the frozen cells post-FACS sort were thawed rapidly and then a portion of the lysate was input into the amplification procedure. Briefly, both methods go through two rounds of cDNA synthesis and in vitro transcription (IVT). Both prime the first strand cDNA synthesis with a T7-Oligo(dT) primer. For the Epicentre method, the first strand cDNA synthesis is catalyzed by either Superscript II or III Reverse Transcriptase (Invitrogen). The double stranded cDNA is synthesized by a DNA polymerase and the IVT is catalyzed by a T7 polymerase. The first round IVT runs for 4 hours and the 2nd round IVT rounds for 9 hours, with biotin-UTP added in the 2nd IVT. RNA purification is performed using

the Zymo RNA Clean and Concentrator (Zymo Research) between the first and second rounds of amplification and the RNeasy MinElute Cleanup Kit (Qiagen) after the second round of amplification. For the Ambion MessageAmp Kit, the first strand cDNA synthesis is catalyzed by ArrayScript (Ambion). Both IVT reactions last for 14 hours, with the biotin-NTPs added in the 2nd round IVT. In addition to the RNA purifications between rounds and after the final IVT, there are also two cDNA purification steps after 2nd strand cDNA synthesis for each round.

Microarray processing

Amplified aRNA was hybridized to the Illumina HumanWG-6 v3.0, HumanRef-8 v3.0, or HumanHT-12 Expression BeadChips according to the manufacturer's instructions (Illumina, San Diego, CA, USA). The HumanWG-6 v3.0 BeadChip assays 48,000 transcripts and profiles six samples simultaneously. The HumanRef-8 BeadChip targets approximately 24,500 well-annotated RefSeq transcripts profiles eight samples in parallel. The HumanHT-12 BeadChip has the same panel of probes as the HumanWG-6 v3.0 BeadChip but can process 12 samples in parallel. The Beadchips contain content derived from the National Center for Biotechnology Information Reference Sequence (NCBI RefSeq) database (Build 36.2, Release 22). Arrays were scanned with an Illumina bead array reader confocal scanner, according to the manufacturer's instructions. Array data processing was performed using Illumina BeadStudio software.

Bioinformatic analysis comparing amplification protocols

The goal of this study was to compare the effects of these methods on the variability of the results. Human Brain RNA (Ambion) in different starting amounts was amplified using either

TargetAmp 2-Round Biotin-aRNA Amplfication Kit 3.0 (Epicentre Biotechnologies) or the MessageAmp II aRNA Amplification Kit (Ambion). Triplicates of each sample were provided and the aRNA was hybridized to the Illumina HumanHT-12 BeadChip. The total number of probes is large (nearly 50,000) and there is the danger of having the noise overwhelm the signal if all the probes are compared at the same time. Therefore, a subset of probes (30 at a time) was sampled to identify differences in the variability of the methods. To compare the variability, a regression model was constructed. This model broke down the gene expression into two components: the average contribution from each gene, and the average contribution from each method. If the two amplification methods are quite different, the difference between their contributions can be expected to be large. The p value is determined using a t-test. This sampling is repeated and the procedure is tested 1,000 times, giving 1,000 p-values. From these p-values, the overall p-value for the difference can be estimated. To assess the overall p-value, the median p-value is taken to get a robust summary measure. To test the difference in amplifications, arrays 402, 403, and 461 were used to represent the Ambion amplification, and arrays 407, 408, 412, and 413 were used to represent the Epicentre amplification (Fig. 3.3). These arrays all used aRNA amplified from 100 pg of starting RNA.

Results

Selection of gene expression platform

Two gene expression platforms were investigated: the Affymetrix GeneChip Rhesus Macaque Genome Array and the Illumina Human Beadchip. The two platforms were tested for sensitivity and reproducibility for assessing gene expression levels in rhesus monkey lymphocytes. Using RNA samples derived from peripheral blood mononuclear cells of 2 normal rhesus monkeys, the Illumina Human BeadChip had better reproducibility than the Affymetrix GeneChip. The reproducibility between the two samples was 46% for the Affymetrix GeneChip and 98% for the Illumina Human BeadChip. Illumina Human BeadChips also required less starting RNA, needing only 50 ng according to manufacturer specifications. Affymetrix technology requires microgram levels of starting RNA.

The divergence of the human and rhesus genomes did not present a problem in the use of the Illumina technology for this application. There is significant homology between the human and rhesus genome, so differences at the protein or exonic DNA level should be small. In fact, a pilot experiment hybridizing human samples on the Illumina Human BeadChip resulted in the detection of 10,000-11,000 expressed genes while a rhesus monkey sample on the Illumina Human BeadChip resulted in the detection of 7-8,000 expressed genes. The same rhesus monkey sample placed on the Affymetrix Rhesus GeneChip also resulted in the detection of 7,000 expressed genes. For the reasons of superior reproducibility, less required starting RNA, and adequate homology, the Illumina Human BeadChip was chosen as the gene expression platform for future studies.

RNA requirement for Illumina platform

To determine the minimum amount of unamplified total RNA required for the Illumina Beadchip to generate clear and reproducible data, limiting dilutions of total RNA were tested on the Illumina Beadchip (all done on Human-8 v2 Beadchip except for the 100ng sample which was run on the Human-6 v2 chip). R squared values as well as numbers of genes present are shown for different starting quantities of RNA (Table 3.1).

Table 3.1. Numbers of genes detected and R squared values for limiting dilutions of total RNA on Illumina Human BeadChip. All samples were hybridized to Illumina Human-8 v2 Beadchips except for the 100 ng sample which was hybridized to the Human-6 v2 chip.

RNA Amount (ng)	Genes Detected	R Squared
100	8000	*0.998*
50	6000	0.995
25	6000	0.995
10	4900	0.99
5	4300	0.97

The results show that as low as 25 ng of starting unamplified RNA can be used on the Illumina Human BeadChip without a significant decline in R squared values.

RNA Extraction from limited cell numbers

With 25 ng of total RNA as a target, methods for extracting high yield and high integrity RNA from epitope-specific CD8+ T lymphocytes were investigated. A number of protocols were tested, including the Qiagen RNeasy Micro Kit, the Arcturus PicoPure Kit, and the traditional phenol/chloroform Trizol procedure. Our results showed that the Trizol method consistently provided the highest RNA yield and the RNeasy Micro Kit provided the highest RNA integrity. While high integrity RNA is of paramount importance for down-stream chip analysis, we have

never been able to extract detectable RNA from fewer than 10,000 epitope-specific CD8+ T cells using RNeasy Micro Kit. From mucosal samples, 100 to 600 epitope-specific CD8+ T lymphocytes are typically isolated, well below the limit for the Rneasy Micro kit. Therefore, it was decided that the Trizol method was the best available option. The Trizol procedure was therefore optimized further to obtain detectable and high integrity RNA.

Extraction of RNA from small numbers of cells was successfully achieved using the Trizol method. From blood-derived epitope-specific (p11C+) CD8+ T lymphocytes, RNA with a high RNA integrity number (RIN>7) as measured by Agilent Bioanalyzer was obtained from 10,000, 1,000, 800 and 600 FACS-sorted p11C+ CD8+ T lymphocytes (Fig. 3.1).

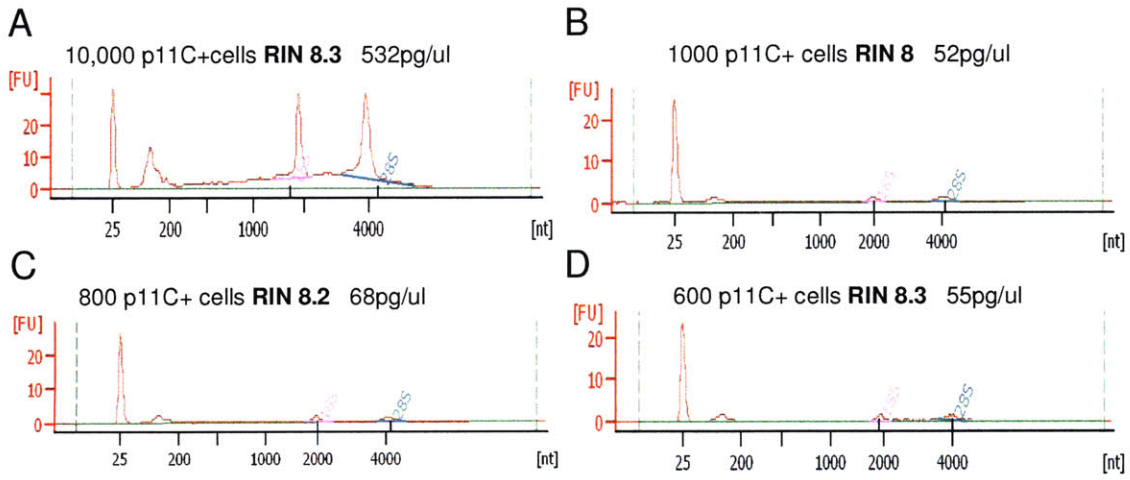

Figure 3.1. Quantity and RNA integrity of Trizol extracted RNA from limiting dilutions of FACS sorted p11C+ CD8+ T cells. All cells were resuspended in 10 ul RNase-free water. **(A)** 10,000 p11C+ cells **(B)** 1,000 p11C+ cells **(C)** 800 p11C+ cells **(D)** 600 p11C+ cells.

However, regardless of extraction method, 25 ng of purified RNA is more than can be obtained from fewer than 500 epitope-specific CD8+ T lymphocytes. Therefore, RNA amplification is necessary to obtain sufficient amounts of RNA for Illumina Beadchip analysis.

Selection of RNA amplification method

In order to be compatible with the Illumina platform, total RNA must be amplified and transformed to aRNA (antisense RNA). There are two commercially available kits that provide two rounds of RNA amplification with a transformation to biotin-aRNA during the second amplification. They are the Epicentre TargetAmp 2-Round Biotin-aRNA Amplification Kit 3.0 and the Ambion MessageAmp II aRNA Amplification Kit.

The Epicentre Kit can amplify from a minimum of 10 pg of starting RNA to a maximum of 500 pg of starting RNA. The reaction is primed from a T7-Oligo(dT) primer and goes through two separate rounds of cDNA synthesis and in vitro transcription. The Ambion MessageAmp Kit works with a minimum of 100 pg and a maximum of 100 ng starting RNA for the 2-round amplification. Like the Epicentre Kit, the RNA is also primed from a T7-Oligo(dT) primer and goes through two rounds of cDNA synthesis and *in vitro* transcription. Some of the enzymes and reagents are different between the two kits as well as some of the manipulations.

The Epicentre and Ambion kits were first compared for aRNA yield and quality. Yield was determined using the Nanodrop ND1000 and RNA quality was determined with both the Agilent Bioanalyzer and Illumina Human Beadchip analysis, looking at the RNA Integrity Number (RIN) in the former and the number of expressed genes and hybridization controls in the latter.

Both methods yielded similar amounts of aRNA from 100 pg of starting RNA (Table 3.2). Both amplification protocols also produced aRNA of appropriate and similar lengths (250-5000 nt in length; data not shown).

Table 3.2. aRNA yields from Ambion Message Amp II aRNA Amplification Kit (with 2 rounds) and Epicentre 2 Round Amplification Kit. Ambion human brain control RNA was used.

Starting RNA amount (nanogram)	aRNA Yields	
	Ambion Kit	Epicentre Kit
100	548ug	N/A
0.5	N/A	31ug
0.1	6.5ug	8.8ug
No RNA control	648 ng	617ng

To investigate the hybridization quality and gene expression signal of aRNA products amplified by the two different methods, triplicates of amplified aRNA were processed from each starting RNA amount. For the Ambion MessageAmp Kit, we used the recommended amount of starting RNA (100 ng) as well as the minimum amount of starting RNA (100 pg). For the Epicentre kit, we used the maximum allowed amount of starting RNA (500 pg) as well as 100 pg starting RNA to match the set amplified by the Ambion Kit. All the samples, as well as negative controls (containing no starting RNA), were hybridized to Illumina Human-12 BeadChips and analyzed as described in the methods section.

Comparing the 100 pg triplicates amplified using the Ambion or Epicentre methods, there was no statistically significant difference between the two methods, giving a p value of 0.37 (Fig. 3.2).

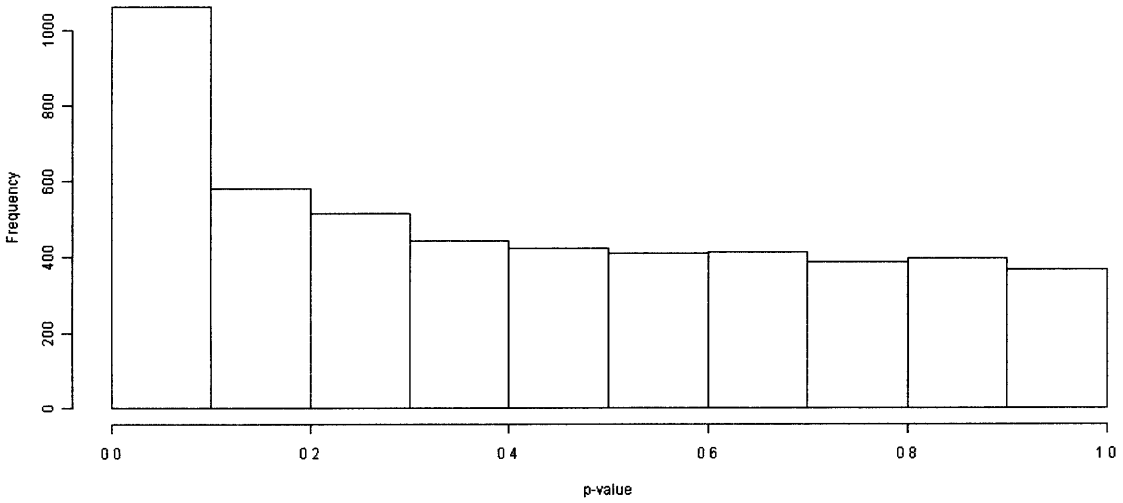

Figure 3.2. Histogram of p-values comparing Ambion versus Epicentre amplified aRNA. P value is 0.37.

The values for the samples were highly correlated (Fig. 3.3). The identification numbers along the diagonal in Fig. 3.3 are described by the key to the left of the figure: 398, 455, and 458 are all Ambion amplified samples from a starting RNA amount of 100 ng, and so on. Correlation within platforms for final RNA quantities starting with the same RNA amounts was consistently above 0.9, with the exception of sample 461. This outlier value possibly represents an error during processing. The correlations among arrays 398, 455, and 458 (all Ambion amplified from 100ng starting RNA) were nearly perfect (0.99 to 1). This suggests that as the starting RNA amount increases, the reproducibility of gene expression profiles across samples should increase. Comparing across amplification methods, but with the same starting RNA amount (100 pg), the correlation is still fairly strong with values between 0.86 and 0.88 (with the exception of sample 461). Lastly, comparing within the same amplification method but between different starting RNA amounts, the correlation is also fairly robust, with values greater than 0.9 for most pairs.

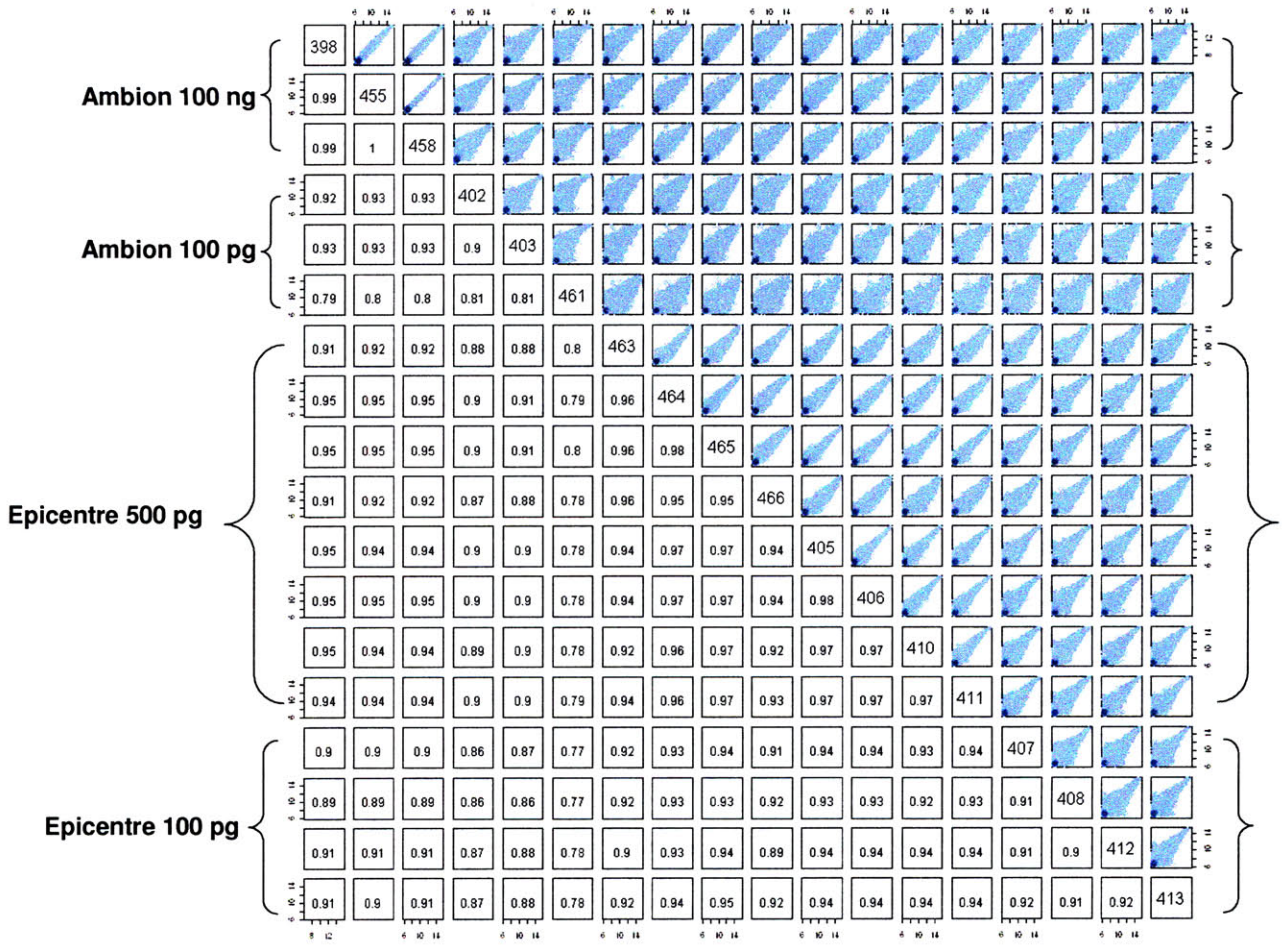

Figure 3.3. Scatterplots and correlation coefficients of pairs of aRNA samples amplified with the Ambion or Epicentre methods and starting from different RNA amounts. Sample identification numbers lie on the diagonal and are described by the key to the left of the figure.

These results are further corroborated by the profile of the number of genes expressed in each sample (Fig. 3.4). Sample 461 is again an outlier with many fewer expressed genes than the other samples. The number of expressed genes also decreases modestly as the starting RNA amount decreases.

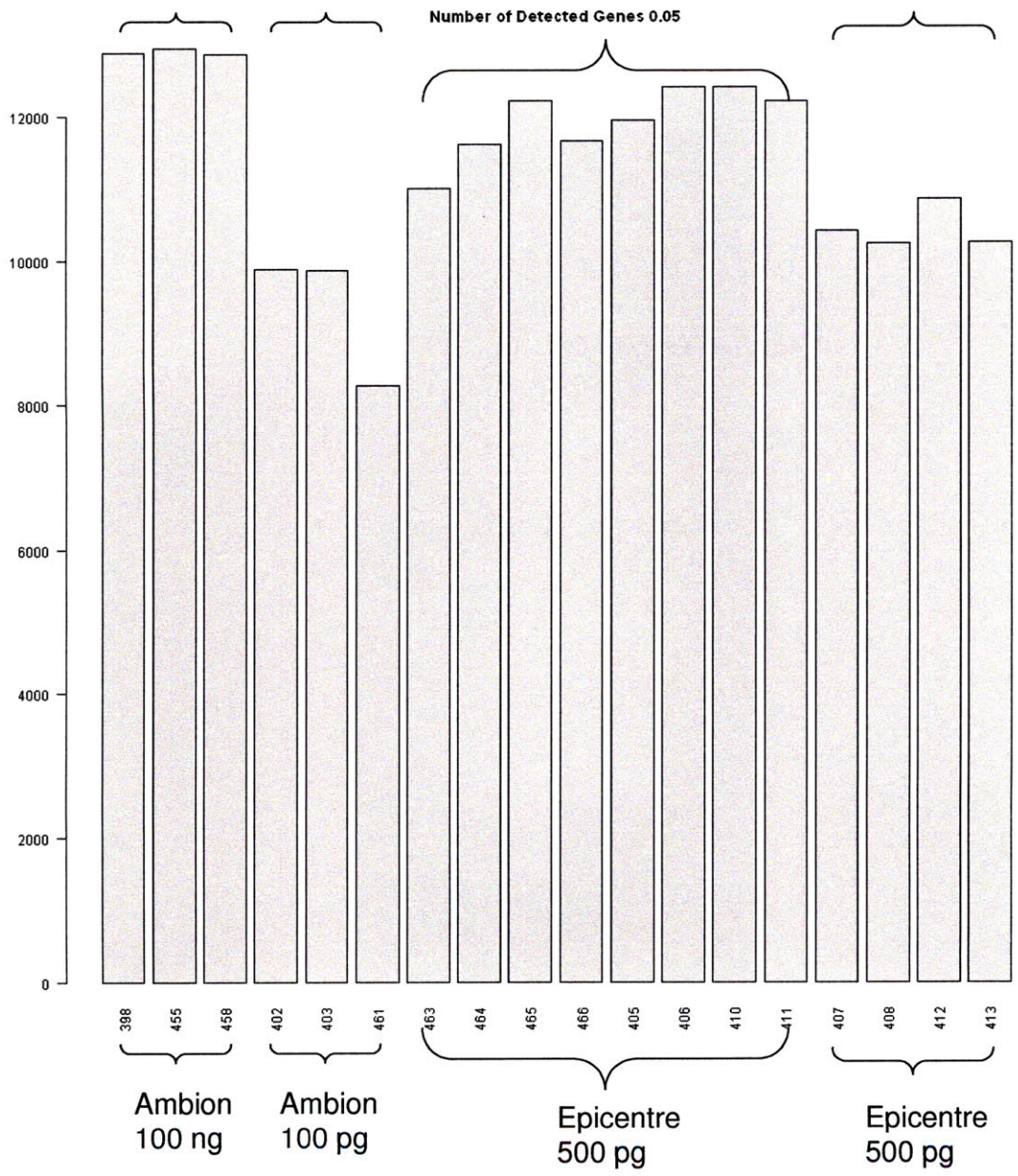

Figure 3.4. Number of genes expressed in the Ambion or Epicentre amplified aRNA.

From the above analysis, it is apparent that the two amplification methods provide equivalent data. There is, however, a time advantage to using the Epicentre Kit, since it takes one day less to process the samples. Therefore, the decision was made to use the Epicentre TargetAmp 2-Round Biotin-aRNA Amplification Kit 3.0 for amplifying future RNA samples.

Purified RNA versus cell lysates for amplification

Obtaining high quality purified RNA from limited cell numbers (less than 1,000 cells) remains a challenge. Measurable high quality RNA cannot be obtained from less than 1,000 cells consistently. Therefore, the possibility of using cell lysates without RNA purification in the amplification process is being investigated. A preliminary experiment to check the feasibility of using cell lysates was conducted.

One thousand monkey peripheral blood mononuclear cells (PBMCs) were frozen at -80°C in 20 ul of phosphate buffered saline (PBS) and then lysed by quick thaw at room temperature with an addition of 1 ul of RNase Inhibitor. One microliter of the thawed cell lysate was then input into the Epicentre 2-round amplification procedure. At the end of two rounds of amplification, 10.3 ug of aRNA was obtained. The aRNA had good Nanodrop ratios (A260/A280 between 1.8 and 2), and good Agilent Bioanalyzer readouts (product lengths corresponding to between 250 nt and 5000 nt) (Fig. 3.5 and 3.6). A purified RNA sample (Hela control) was amplified for comparison.

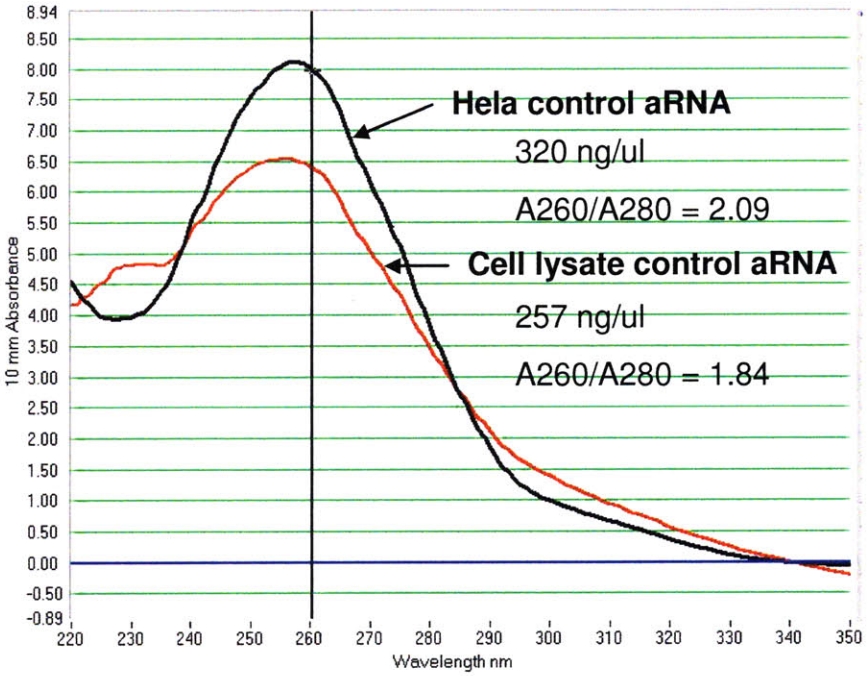

Figure 3.5. Nanodrop reading for amplified aRNA from Hela control and 1 ul of lysate from 1,000 normal monkey peripheral blood mononuclear cells (PBMCs). The aRNA samples were resuspended in 40 ul of Rnase-free water.

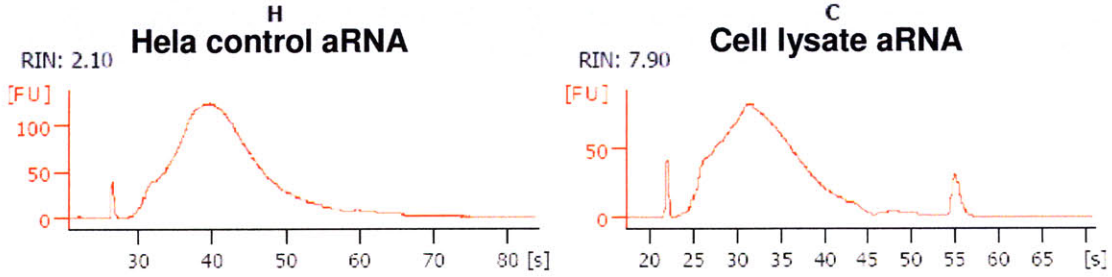

Figure 3.6. Agilent Bioanalyzer readouts for amplified aRNA for Hela control and 1 ul of cell lysate from 1,000 monkey PBMCs.

A SYBR Green-based real time quantification of GAPDH was then performed on the aRNA from both the cell lysate and the Hela control and showed successful detection of GAPDH after

17 cycles for the cell lysate derived aRNA and after 21 cycles for the Hela control aRNA (Fig. 3.7).

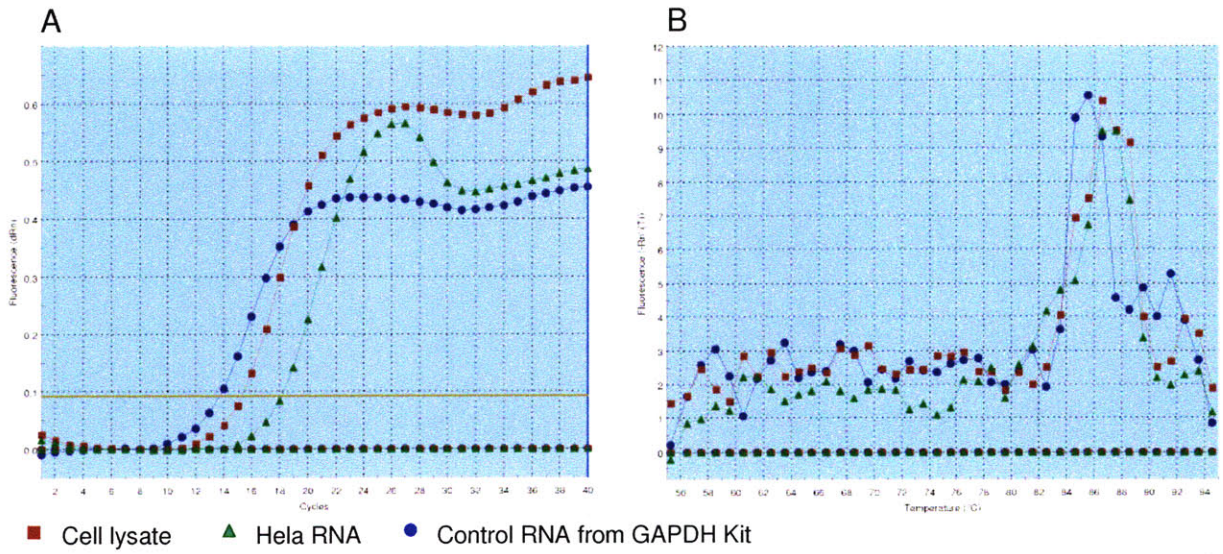

Figure 3.7. SYBR Green QPCR of GAPDH on amplified cell lysate from monkey PBMCs as well as Hela and control RNAs. **(A)** Amplification curves for GAPDH gene. **(B)** Dissociation curves for GAPDH gene.

Given these initial positive results, the feasibility of amplifying lysates from sorted cells was assessed. Epitope-specific (p11C+) CD8+ T cells from monkey peripheral blood and mucosal biopsies were collected by FACS sorting and the cells were either lysed directly or the RNA was extracted from them using Trizol. From mucosal cells, only lysates of p11C+ CD8+ T cells were tested due to limiting cell numbers. Adequate yields of aRNA were obtained from both the purified RNA and the cell lysates (Table 3.3 and Fig. 3.8), with lysates giving higher yields than purified RNA at higher cell numbers and purified RNA giving higher yields than lysates at lower cell numbers.

Table 3.3. Comparison of aRNA yield from purified RNA and cell lysate from mucosal and blood p11C+ CD8+ T lymphocytes. (P) = Purified RNA. (L) = Cell lysate.

ID	Sample Description	aRNA amount (ug)
1	Hela control	77
4	Duodenum (L)	18
8	Colon (L)	13
6	1000 Blood cells (P)	15
2	1000 Blood cells (L)	32
7	800 Blood cells (P)	15
9	800 Blood cells (L)	10
3	600 Blood cells (P)	24
5	600 Blood cells (L)	17
10	No RNA Control	0.2

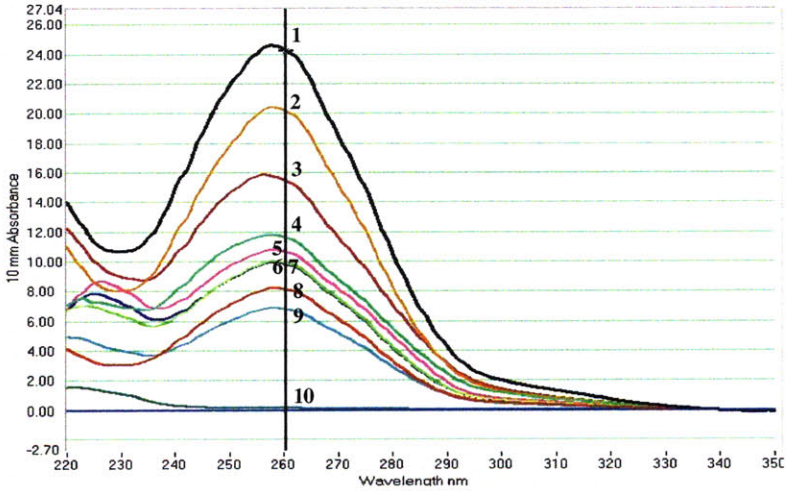

Figure 3.8. Comparison of aRNA yield from purified RNA and cell lysate from mucosal and blood p11C+ CD8+ T lymphocytes. The numbers along the curves correspond to the ID numbers in Table 3.3.

However, simply looking at yield is not sufficient. The most important consideration is how well the samples perform on the Illumina Human BeadChip. To create enough statistical power,

to make this evaluation useful, two biological replicates (PBMCs from 2 chronically SIV-infected rhesus monkeys), and triplicates of purified RNA or cell lysates at limiting cell number dilutions were generated. All samples were amplified using the Epicentre TargetAmp 2-Round Biotin-aRNA Amplification Kit 3.0 and hybridized to the Illumina Human BeadChip. Once a reproducibility and repeatability analysis can be conducted, the feasibility of using cell lysates for amplification and gene expression analysis will be assessed. The experimental results are pending. Once the decision is made, the entire gene expression assay will be complete (Fig. 3.9).

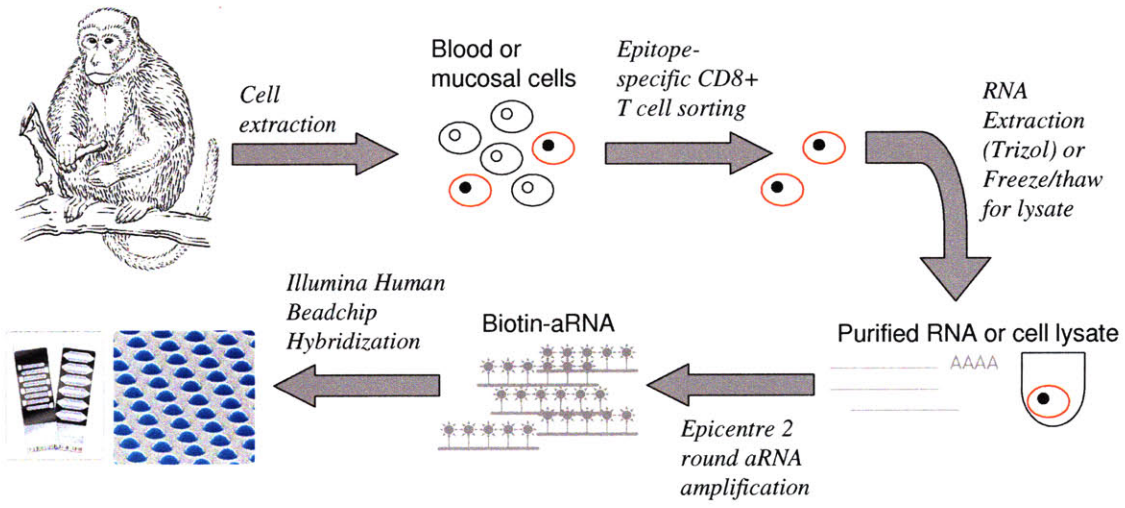

Figure 3.9. Schematic of gene expression profiling assay for epitope-specific CD8+ T lymphocytes.

Discussion

The Trizol method gave higher yields of purified RNA from limiting numbers of cells than the RNeasy Micro Kit, or the Arcturus PicoPure Kit. Trizol extracted RNA was also of high integrity (Fig 3.1) and can be amplified successfully using the Epicentre TargetAmp 2-Round Biotin-aRNA Amplification Kit 3.0 (Fig. 3.8). The Trizol method does not employ a column, which enhances the final RNA yield. This method may lead to contamination with organics that can be detrimental to the assays that will be employed to analyze the RNA. Therefore, this method requires careful attention to avoid contaminants in the isolated RNA.

The Epicentre TargetAmp 2-Round Biotin-aRNA Amplification Kit 3.0 and the Ambion MessageAmp II aRNA Amplification Kit yielded comparable quantities of high quality aRNA. These kits had comparable reproducibility and generated comparable gene expression analyses (Figs. 3.2 and 3.3). While amplification is necessary to investigate the gene expression profile of rare cell populations, the process of amplification can also bias the profile. The linear amplification methods used by both Epicentre and Ambion minimize bias. Nevertheless, amplified samples can only be compared with other similarly amplified samples and not with unamplified samples.

The direct amplification of cell lysates can be used for gene expression analysis of as few as tens of cells. However, the mRNA in lysates of cells contains contaminants and therefore, the amplification efficiency will not be perfect. An oligo-dT primer must sift through a large quantity of cellular matter to bind the mRNA. Because of this, it is possible that some of the

mRNA in those cells will be 'lost in the mix' and will not be amplified. Therefore, there is a chance that the gene expression profile generated will be limited. In addition, there are proteases in the cellular matter, including RNases. It is essential that any RNases be eliminated immediately upon thawing the cells. Otherwise, as noted previously, some of the mRNA will be degraded and therefore not available for amplification.

The Illumina Human BeadChip platform is precise, reproducible, and cost effective, and can run many samples in parallel. However, the BeadChip is a human chip and therefore, will not have identical homology to the rhesus monkey genome. While homology is great enough for our uses, looking forward, it may be worthwhile to custom design an Illumina BeadChip to match the rhesus monkey genome.

CHAPTER 4: Gene expression profile of peripheral blood SIV Gag epitope-specific CD8+ T lymphocytes during primary SIV infection in Mamu-A*01+ and Mamu-A*02+ rhesus monkeys

Introduction

Emerging data suggest that CD8+ cytotoxic T cells can contribute substantially to early virus control. Kuroda et al. showed that the emergence of SIV-specific CD8+ cytotoxic T cells coincides with a decrease in viral loads.[24] Schmitz et al. showed that upon depletion of CD8+ cytotoxic T cells, early control of SIV fails.[25] Viral loads also increase in chronic SIV infection upon CD8+ T cell depletion.[26,27] In addition, the evolution of viral mutants in vivo is characterized by mutations that cause the virus to evade recognition by CD8+ cytotoxic T cells.[3]

Previous studies have indicated an association between the expression of the MHC class I allele Mamu-A*01 and a reduction in plasma virus RNA levels in monkeys infected with SIVmac239[158,159] and SIVmac251,[160,161] and lower lymph node-associated virus concentrations in SHIV-89.6P infections.[162] SIV-infected A*01+ rhesus monkeys have one or more logs lower plasma virus RNA levels than A*01- monkeys. Because A*01 is a class I MHC molecule, CD8+ T cells likely play a role in the control of viremia in these monkeys.To test this hypothesis, blood-derived SIV-specific CD8+ T cells from A*01+ (A*02-) and A*02+ (A*01-) monkeys can be studied temporally using different functional and genomic assays.

Previous studies have also shown that Mamu-B*17 and Mamu-B*08 are associated with superior SIV viral control.[159,163,164] To abrogate the possible confounding effects of these two alleles,

monkeys will be chosen based on their B*08$^-$ B*17$^-$ status. Several virus epitope-specific CD8+ T lymphocyte populations can be sorted and analyzed specifically, including the dominant Gag-p11C and Tat-TL8 specific CD8+ T cells and the subdominant Env p54AS (or Env TL9) specific CD8+ T cells from A*01+ monkeys and the dominant Nef-p199RY specific CD8+ T cells from A*02+ monkeys.[2,156,165-170]

While virus-specific CD8+ memory T lymphocyte differentiation in the setting of viral infections has been intensively studied in murine models,[171-174] limited work has been done in this area in non-human primate/SIV models. HIV-1 and its non-human primate counterpart SIV are different from other chronic infections because of the persistence of viremia and loss of CD4+ T cell help. Therefore, we might expect the evolution of CD8+ T lymphocytes to differ in the setting of SIV infections from that of other chronic persistent viral infections.

Gene expression studies of T cells have evaluated naïve, effector, and memory T cells, resting versus activated T cells, and T cells undergoing homeostatic proliferation.[44,46,174-178] Results suggest a coordinated progression of lymphocyte gene expression changes following activation and suggest that trafficking of T cells is inhibited early during T cell activation.[44] The genetic program of naïve, effector, and memory T cell specific for LCMV in mice was studied by several groups.[172-174] Looking primarily at genes involved in effector and regulatory functions, in cell cycle control, and in susceptibility to apoptosis, naïve CD8+ T cells had a gene signature of high levels of lung Kruppel-like factor (LKLF) and the cyclin-dependent kinase inhibitor (CDKi) p27, moderate levels of the anti-apoptotic *Bcl-2* and pro-apoptotic *Bax,* and low levels of perforin, IFN-γ, FasL, pro-apototic *Bad,* anti-apoptotic *Bcl-x_L,* and the CDKi p21.[173,175] Following

infection with LCMV, the cells changed to an effector phenotype and their genetic signature evolved as well, exhibiting high levels of IFN-γ, perforin, FasL, granzymes A,B, D, and K, and RANTES, moderate levels of *Bcl-2*, and low levels of *Bad*, *Bax*, and *Bcl-x_L*. LKLF, p27, and p21 levels decreased initially but increased again by day 8 following infection.[173,174] Genes encoding chemotactic proteins, cell adhesion proteins, and P-selectin ligand were increased in effector CD8+ T cells while lymph node homing proteins were reduced.[174] Signal transduction genes involved in TCR signaling, intracellular Ca^{2+} signaling, and cytokine signaling were expressed at higher levels. To counteract that with negative regulations of TCR and cytokine signaling, PEP phosphatase and SOCS-5 expression was increased and IL-4, IL-7, and IFN-γ receptor α chain expression was decreased.[174] Genes regulating actin polymerization showed increased expression, which can lead to increased cell motility and signaling, while genes involved in protein translation showed decreased expression, which can contribute to effector cell apoptosis.[174] After viral clearance, the antigen-specific CD8+ T cells entered the memory phase and the genotype changed to one of high levels of IFN-γ, *Bcl-2, Bax*, RANTES, MIP-1β, granzymes B, K, M, and LKLF, and decreased levels of *Bcl-x_L,* p27 and p21.[173] There were mixed results on perforin and FasL, where one study showed lower expression[173] in memory T cells, while another study showed higher levels.[174] This discrepancy may be due to differences in the experimental conditions and differences between total CD8+ T cell populations[174] versus the focused antigen-specific CD8+ T cell population.[173] In addition, CXCR4 was selectively up-regulated in memory CD8+ T cell, as were the GPI-linked proteins Ly-6C and Ly-6A/E, members of the p38 and JNK signaling pathways, cyclin E1, E2, and B1, and the IL-16Rα chain.[174] In summary, approximately 350 genes were differentially expressed at least 1.7-fold in either effector or memory CD8+ T cells as compared to naïve cells, of which 30% were up-

regulated in both effector and memory CD8+ T cells.[174] This suggests that many of the regulatory gene changes that occurred during the transition from naïve to effector CD8+ T cell were maintained in memory cells.[174] However, there were subsets of genes that were differentially expressed between effector and memory CD8+ T cells, suggesting that they are two distinct cell populations.[174] Temporal gene expression studies showed memory cell qualities were acquired between days 8 and 22 post-infection. [174]

The development of gene microarrays have provided investigators with a tool to measure subtle changes in mRNA levels.[177] Affymetric gene array analysis of superantigen-activated T cells showed expression of many genes associated with cycling cells such as those of the cyclins, cyclin dependent kinases, and DNA polymerases, while resting T cells expressed a number of cytokine receptor genes and genes thought to suppress cell division.[175] Results also suggested that the MAP kinase signaling pathway may be significantly dampened in activated T cells.[175] Activation, while changing the spectrum of genes expressed, did not change the diversity of genes expressed.[175] Shortly after T cell activation, genes for interferon receptors and for Stat1 are repressed.[177]

Several studies have shown that cytotoxic T cells are impaired in function in the setting of persistent viral infection,[179-181] while others have countered this by describing the preservation of CTL function in chronic persistent viral infections, including HIV.[179,182,183] Gene expression analysis of the virus-specific CD8+ T lymphocytes will shed new light on this question and uncover mechanisms to explain the functional and phenotypic observations.

During chronic viral infections, CD8+ T cell responses often become dysfunctional and sometimes virus-specific CD8+ T cells fail to differentiate into memory CD8+ T cell.[184,185] During chronic LCMV infection, virus-specific CD8+ T cells gradually lose effector functions, whereby IL-2, cytotoxity, and proliferation function are lost early and IFN-γ persists longer.[186] If the virus load is high and CD4+ T cell help is absent, virus-specific CD8+ T cells can lose all effector functions.[186,187] An important microarray study looking at gene expression profile differences between CD8+ T cells in chronic viral infection versus acute viral infection in a mouse LCMV model showed that exhausted CD8+ T cells over-expressed a number of inhibitory receptors such as PD-1, LAG-3, and 2B4, down-regulated genes associated with TCR signaling and cytokine receptors such as IL-7 and IL-15, and displayed altered expression of genes involved in chemotaxis, adhesion, and migration.[180,185] There appeared to be perturbations in the signaling apparatus available to communicate extracellular information via both the TCR and cytokine receptors to the nucleus.[185] Exhausted CD8 T cells had many translational, metabolic and bioenergetic deficiencies and also expressed a distinct set of transcription factors.[185] There appeared to be perturbations in the signaling apparatus available to communicate extracellular information via both the TCR and cytokine receptors to the nucleus.[185] This model of exhaustion may well apply to HIV-1 and SIV infections where the virus persists and CD8+ T cell dysfunction develops.[30-32,188]

Materials and Methods

Animals

Six Mamu-A*01^{+} Mamu-A*02^{-} Indian-origin rhesus monkeys (*Macaca mulatta*) and 6 Mamu-A*02^{+}Mamu-A*01^{-} rhesus monkeys, all B*08^{-} and B*17^{-}, were selected for the study after PCR-based MHC typing. They were challenged intra-rectally with 4.65 log RNA copies of SIVmac251. These animals were maintained in accordance with the guidelines of the Committee on Animals for the Harvard Medical School and the Guide for the Care and Use of Laboratory Animals.

Antibodies, tetramers, and peptides

Mamu-A*01/p11C,C-M/B2m (SIVmac Gag), Mamu-A*01/TL8/B2m (SIVmac Tat), Mamu-A*01/p54AS/B2m (SIVmac Env), Mamu-A*02/p199RY/B2m (SIVmac Nef) tetramer complexes were prepared as previously described.[156,157,165] Streptavidin-PE (ProZyme), streptavidin-APC (ProZyme), and streptavidin-QDot655 (Invitrogen) were mixed stepwise with biotinylated Mamu-A*01/peptide or Mamu-A*02/peptide complexes at a molar ratio of 1:4 to produce the tetrameric complexes. Conjugated antibodies used in this study included anti-CD247 Alexa488 (Clone K25-407.69; BD Product No. 558486), anti-phosphotyrosine PE (Clone PY20; BD Product No. 558008), anti-CD3 APC (Clone SP34.2; BD-Pharmingen). The rest of the antibodies used in this study were directly coupled to phycoerythrin (PE), allophycocyanin (APC), fluorescein isothiocyanate (FITC), peridinin chlorophyll protein-Cy5.5 (PerCpCy5.5), allophycocyanin-Cy7, ECD, and PECy7. The following monoclonal antibodies were used: anti-CD8α (clone SK1; BD-Pharmingen), anti-CD3 (Clones SP34; BD-Pharmingen), anti-CD4

(Clone 19Thy5D7; in house production), anti-CD4 (Clone L200; BD-Pharmingen), anti-CD28 (Clone CD28.2; eBioscience), and anti-CD95 (Clone DX2; BD-Pharmingen).

Blood processing and cell staining

Peripheral blood was collected from the 12 rhesus monkeys at weekly intervals post-SIVmac251 challenge. In addition, blood was collected a week prior to infection and on the day of infection (day 0) to establish baseline complete blood count (CBC) using the ADVIA 120 Hematology System (Bayer) and expression profile measurements on total or naïve CD8+ T cells in addition to a baseline tetramer staining. For each timepoint, 10 ml of blood with EDTA was collected and 850 ul of whole blood was saved for CBC analysis. The blood was then layered over 4ml of Ficoll and spun at 3,000 rpm for 20 min. Plasma from the top layer was collected in 5 aliquots of 500 ul each and frozen at -80°C. Viral RNA was routinely isolated from 200 ul or 400 ul of cell-free blood plasma following manufacturer's protocol. Using a qRT-PCR based method, viral load was determined by comparing against a SIV RNA standard harboring the first 731 bp of the SIVmac239-Gag Gene. PBMCs were recovered from the buffy layer and were washed twice with PBS containing 2% FBS. For baseline measurements (pre-infection), cells were stained for 10 min at 4°C with a mixture of anti-CD4, anti-CD3, anti-CD8, anti-CD28, and anti-CD95 antibodies to stain for naïve CD8+ T cells and a mixture of anti-CD4, anti-CD3, and anti-CD8 to stain for total CD8+ T cells. On day 0 and weekly post-infection, cells were stained with Mamu-A*01/p11C,C-M/B2m, Mamu-A*01/TL8/B2m, and Mamu-A*01/p54AS/B2m, or Mamu-A*02/p199RY/B2m tetramers for 15 min at 4°C. Cells were then stained with a mixture of anti-CD3 and anti-CD8 Abs for 10 min at 4°C. The cells were washed with PBS/2%FBS and resuspended in 1 ml of cold PBS per every 10^7 cells. The p11C+ CD8+ T cells were sorted

using the FACS-Vantage Flow Cytometer/Cell Sorter (Becton-Dickinson) and collected in RNAprotect (Qiagen).

RNA Extraction

RNA was extracted from the cell pellet using Trizol (Invitrogen). Briefly, 1 ml of Trizol was added to the cell pellet and incubated for 5 min at room temperature. Two hundred microliters of chloroform was added and shaken vigorously by hand for 15 seconds, and incubated at room temperature for 2-3 min. The samples were then centrifuged at 13,000 rpm for 15 min at 4°C. The colorless upper aqueous phase was carefully transferred to a new tube, and 2ul of linear acrylamide was added and mixed in. An equal volume of isopropyl alcohol was then added and mixed. The mixture was incubated at room temperature for 10min and centrifuged at 13,000 rpm for 10 min at 4°C. The supernatant was removed and the RNA was washed with 1ml of 70% ethanol and centrifuged at 10,500rpm for 5 min at 4°C. The supernatant was completely removed and the RNA pellet was allowed to airdry. The RNA was then resuspended in RNase-free water and stored at -80°C. To check for RNA integrity, 1 ul of the sample was tested using an Agilent Bioanalyer.

RNA Amplification

RNA was amplified from Trizol extracted total RNA using the TargetAmp 2-Round Biotin-aRNA Amplfication Kit 3.0 (Epicentre Biotechnologies). The amplification process provides two rounds of cDNA synthesis and in vitro transcription (IVT). The first strand cDNA synthesis is primed with a T7-Oligo(dT) primer and the first strand cDNA synthesis is catalyzed by either Superscript II or II Reverse Transcriptase (Invitrogen). The double stranded cDNA is

synthesized by a DNA polymerase and the IVT is catalyzed by a T7 polymerase. The first round IVT runs for 4 hours and the 2nd round IVT rounds for 9 hours, with biotin-UTP added in the 2nd IVT. RNA purification is performed using the Zymo RNA Clean and Concentrator (Zymo Research) between the first and second rounds of amplification and the RNeasy MinElute Cleanup Kit (Qiagen) after the second round of amplification. Amplified aRNA is resuspended in RNase-free water and stored at -80°C. Samples that only need to be amplified one round were amplified with the Illumina(R) TotalPrep(TM) RNA Amplification Kit (Ambion). Nanodrop ND-1000 is used to determine RNA concentration and an Agilent Bioanalyzer is used to determine aRNA integrity.

Microarray processing

Amplified RNA was hybridized to Illumina HumanHT-12 Expression BeadChips according to the manufacturer's instructions (Illumina, San Diego, CA, USA). The HumanHT-12 BeadChip has the same panel of probes as the Illumina HumanWG-6 v3.0 BeadChip, which assays 48,000 transcripts, but can process 12 samples in parallel. The BeadChips contain content derived from the National Center for Biotechnology Information Reference Sequence (NCBI RefSeq) database (Build 36.2, Release 22). Arrays were scanned with an Illumina bead array reader confocal scanner, according to the manufacturer's instructions. Array data processing was performed using Illumina BeadStudio software.

Results

Testing early activation after Mamu-A*01/p11C tetramer staining before and after sorting

In order to isolate virus epitope-specific CD8+ T cells, MHC class I tetramers are used to label the cells and identify them for sorting. It is, however, possible that the tetramers may induce TCR activation, which can alter the gene expression profiles of these cells. To test this, cells were stained with antibodies specific for phosphorylation sites on the CD3 molecule (CD3ζ) as well as with Mamu-A*01/p11C (SIVmac Gag) tetramer under various temperature conditions and for varying incubation times. Figure 4.1 shows that long-term incubation on ice does not appear to have any effect on phosphorylation of CD3ζ. However, Figures 4.2 and 4.3 show that sorted cells that had been stained with tetramer exhibited high amounts of CD3 phosphorylation, and thus activation. Simply staining the cells with tetramer on ice or at 37°C did not induce as much phosphorylation. Staining on ice induced the least amount of activation.

Stimulation	Fix	Gate
Unstimulated	37C	CD8
Sorted unstained	37C	CD8 (thick line)
CD3/28 3min 37C	37C	CD8 (Far right histogram)
Ice-10min	37C	p11C-(CD8)
Ice-20min	37C	p11C-(CD8)
Ice-30min	37C	p11C-(CD8)
Ice-40min	37C	p11C-(CD8)
Ice-50min	37C	p11C-(CD8)
Ice-60min	37C	p11C-(CD8)
Ice-70min	37C	p11C-(CD8)
Ice-80min	37C	p11C-(CD8)
Ice-90min	37C	p11C-(CD8)
Ice-100min	37C	p11C-(CD8)
Ice-110min	37C	p11C-(CD8)
Ice-120min	37C	p11C-(CD8)

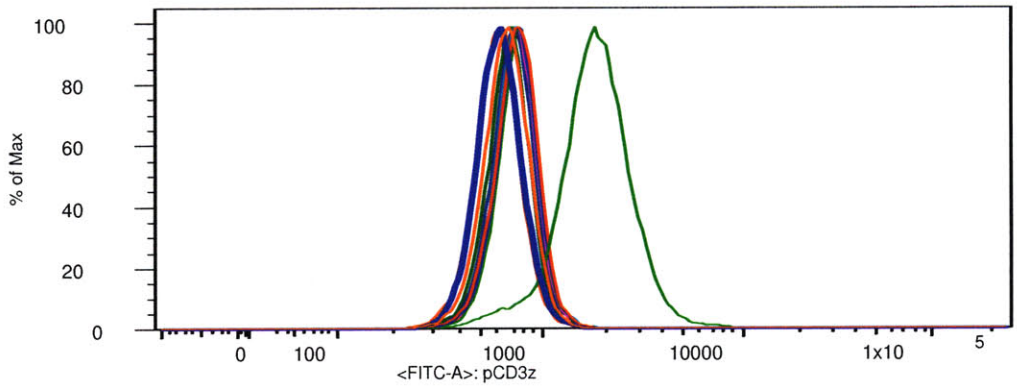

Figure 4.1. Effect of long-term incubation of tetramer-stained cells on ice on phosphorylation of CD3ζ. PBMCs were isolated using Ficoll density gradient. The positive control was stimulated with anti-CD3 and anti-CD28, fixed, and stained for anti-pCD3ζ (light green histogram to the far right). Unstimulated cells that were only stained with anti-pCD3ζ were also used as a negative control (orange histogram). A population of cells were not labeled with tetramer and simply passed through the sorter (thick blue line to the far left). The remainder of the cells were stained with Mamu-A*01/p11C on ice for varying amounts of times ranging from 10 min to 2 hrs before fixing with BD Fix Buffer I and staining with anti-pCD3ζ.

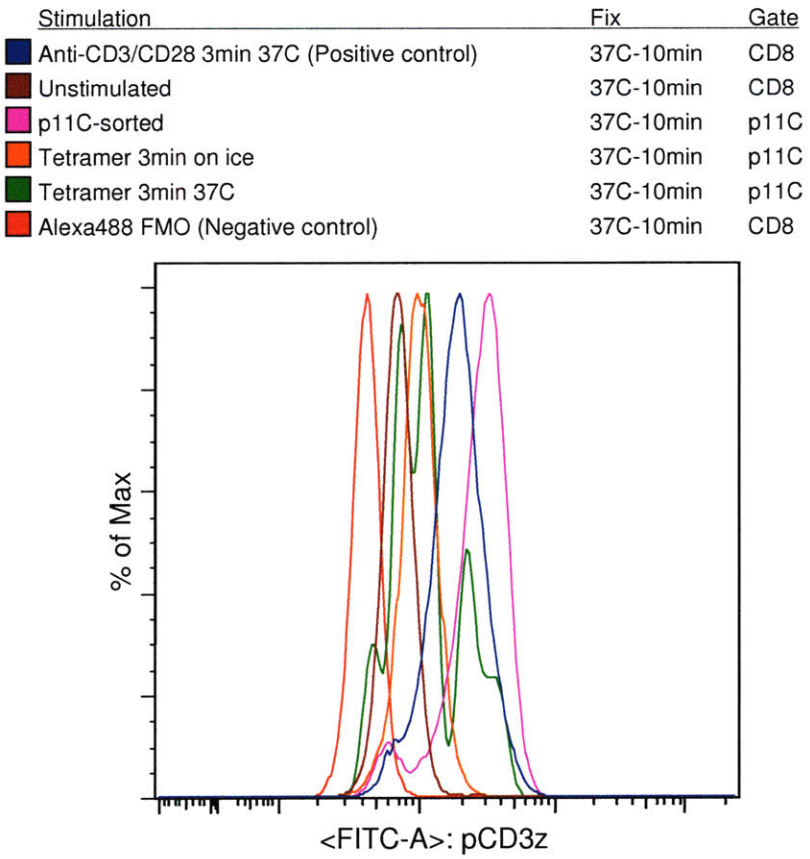

Figure 4.2. Staining with anti-phosporylated CD3ζ and fixing at 37°C. PBMCs from a Mamu-A*01+ rhesus monkey were isolated by Ficoll density gradient. All samples were fixed in BD Fix Buffer I (4% formaldehyde) at 37°C for 10 min. The positive control was stimulated with anti-CD3 and anti-CD28, fixed, and stained for anti-pCD3ζ (Blue histogram). Alexa488 FMO was used as a negative control (Red histogram). Unstimulated cells that were only stained with anti-pCD3ζ were also used as a negative control (Brown histogram). Experimental cells were incubated with Mamu-A*01/p11C for either 3 min on ice (orange histogram) or at 37°C (green histogram) and then fixed and permeabilized with BD Fix Buffer I and stained with anti-pCD3ζ. The p11C-sorted cells were stained with Mamu-A*01/p11C for 15 min at 4°C, sorted by FACS Vantage, and fixed and permeabilized with BD Fix Buffer I and stained with anti-pCD3ζ (Pink histogram).

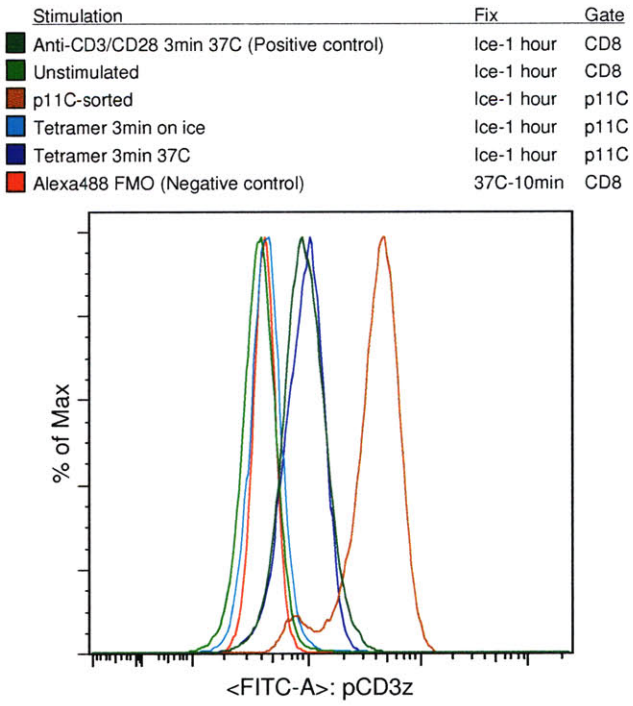

Figure 4.3. Staining with anti-phosporylated CD3ζ and fixing on ice. PBMCs from a Mamu-A*01+ rhesus monkey were isolated by Ficoll density gradient. All samples with the exception of the negative control (Alexa488 FMO) were fixed in BD Fix Buffer I (4% formaldehyde) on ice for 1 hr. The positive control was stimulated with anti-CD3 and anti-CD28, fixed, and stained for anti-pCD3ζ (dark green histogram). Alexa488 FMO was used as a negative control (Red histogram). Unstimulated cells that were only stained with anti-pCD3ζ were also used as a negative control (light green histogram). Experimental cells were incubated with Mamu-A*01/p11C for either 3 min on ice (light blue histogram) or at 37°C (dark blue histogram) and then fixed and permeabilized with BD Fix Buffer I and stained with anti-pCD3ζ. The p11C-sorted cells were stained with Mamu-A*01/p11C for 15 min at 4°C, sorted by FACS Vantage, and fixed and permeabilized with BD Fix Buffer I and stained with anti-pCD3ζ (brown histogram).

CD8+ T cell isolation from peripheral blood and RNA extraction for baseline measurements

For use as baseline comparators, total CD8+ T cells and naïve CD8+ T cells were isolated one week prior to challenge and on the day of challenge pre-infection from peripheral blood using FACS. The sorting schematic is shown in Figure 4.4 using a representative set of Mamu-A*01+ and Mamu-A*02+ monkeys.

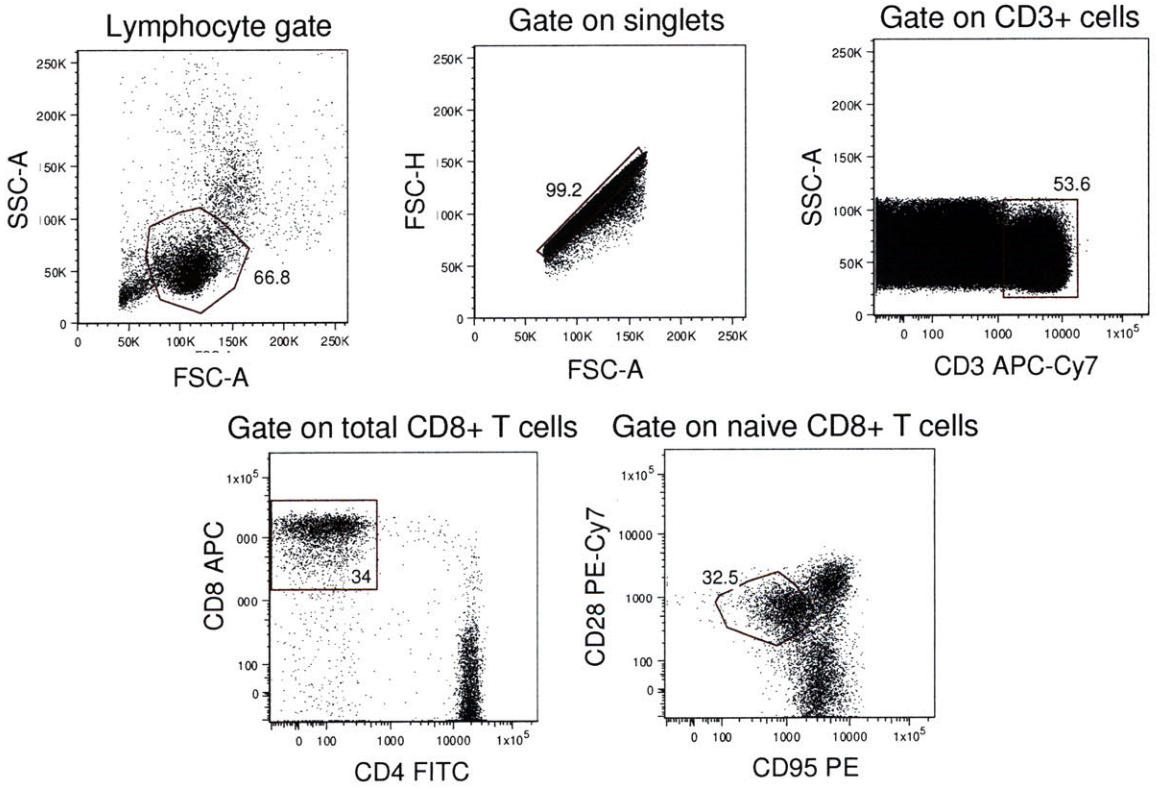

Figure 4.4. Schematic for sorting total and naïve CD8+ T cells for baseline measurements. From A*01+ Mm107-2006, 150,000 naïve CD8+ T cells and 280,000 total CD8+ T cells were collected. From A*02+ Mm337-2008, 900,000 naïve CD8+ T cells and 1,145,000 total CD8+ T cells were collected.

From the FACS isolated total and naïve CD8+ T cells, high quality RNA with RNA Integrity Numbers (RIN) greater than seven as measured by an Agilent Bioanalyzer were extracted using the Trizol method (Fig. 4.5).

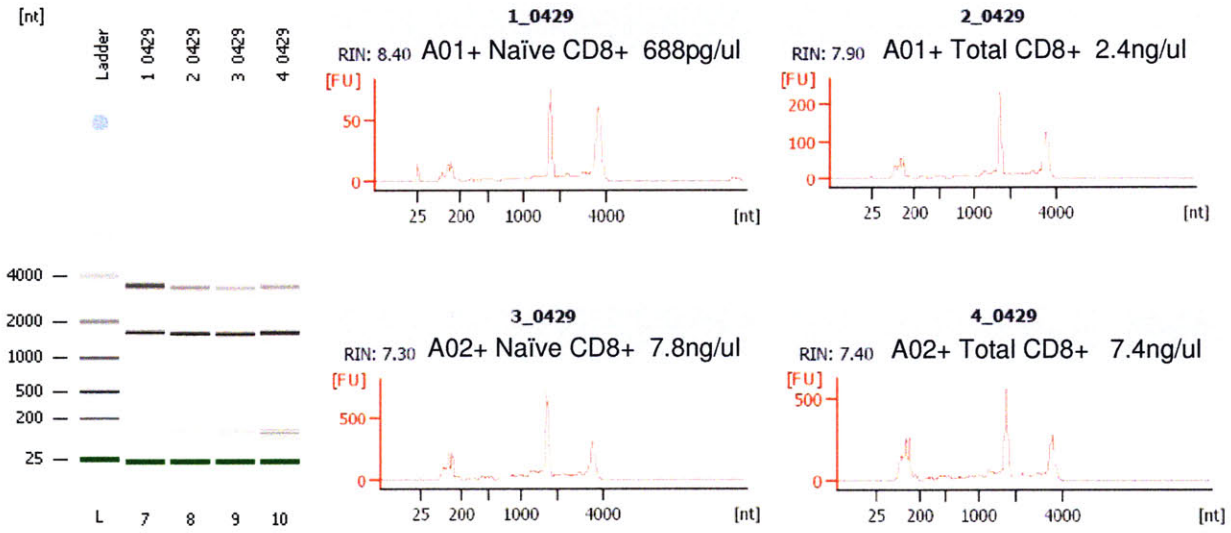

Figure 4.5. RNA integrity and quantity from baseline total and naïve CD8+ T cells for Mm107-20076 (A*01+) and Mm337-2008 (A*02+) pre-challenge on Day 0. RNA was extracted using the Trizol method. Analysis was done by Agilent Bioanalyzer and all samples were resuspended in 10 ul RNase-free water.

Isolation of SIV Gag epitope-specific CD8+ T cells from peripheral blood and RNA extraction

Weekly following SIVmac251 intra-rectal challenge, 10 ml of blood was obtained from each monkey and virus epitope-specific CD8+ T cells were isolated using FACS. From the Mamu-A*01+ monkeys, Mamu-A*01/p11C, Mamu-A*01/TL8, and Mamu-A*01/p54AS were isolated and collected in RNAprotect. From the Mamu-A*02+ monkeys, Mamu-A*02/p199RY tetramer positive cells were collected. The sorting schematic used is shown in Figures 4.6 and 4.7.

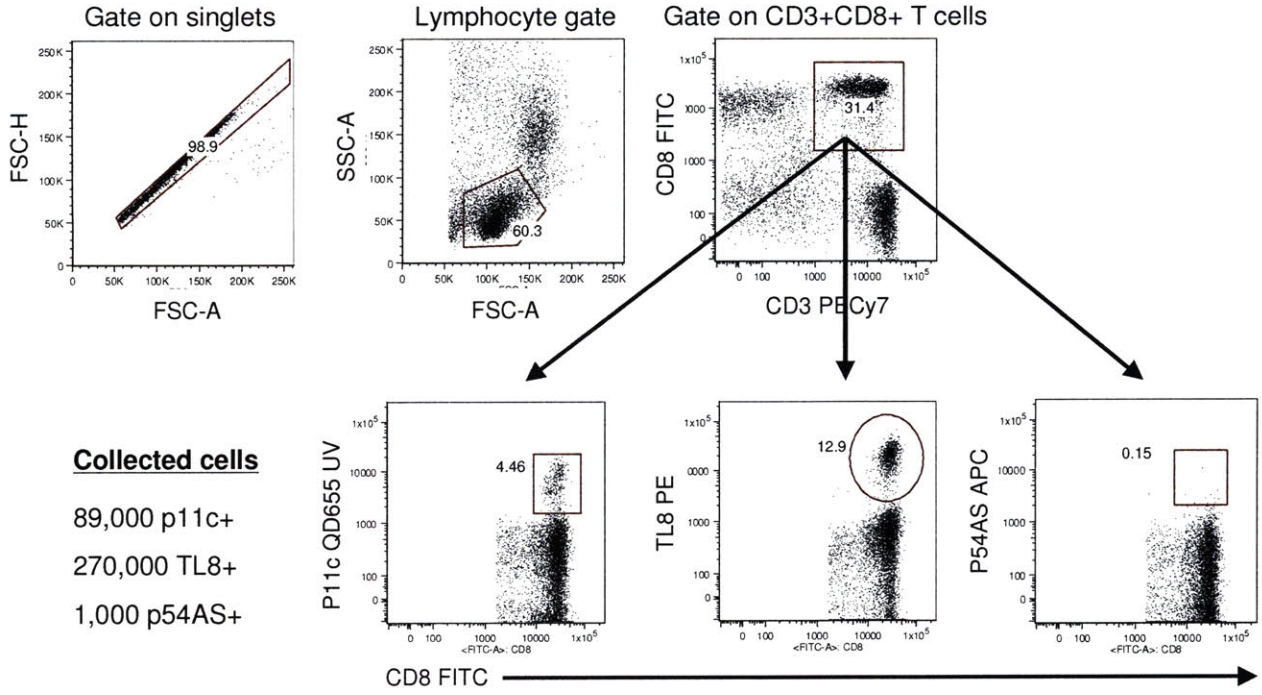

Figure 4.6. Tetramer cell sorting for Mm107-2006 (A*01+) on Day 14 post SIVmac251 intra-rectal challenge. Gating schematic is shown above, selecting for singlets, then lymphocytes, then CD3+CD8+ T cells. Mamu-A*01/p11C, Mamu-A*01/TL8, Mamu-A*01/p54AS, Mamu-A*02/p199RY tetramer positive cells were sorted in parallel into FACS tubes filled with RNAprotect Reagent. A total of 89,000 p11C+ cells, 270,000 TL8+ cells, and 1,000 p54AS+ cells were collected.

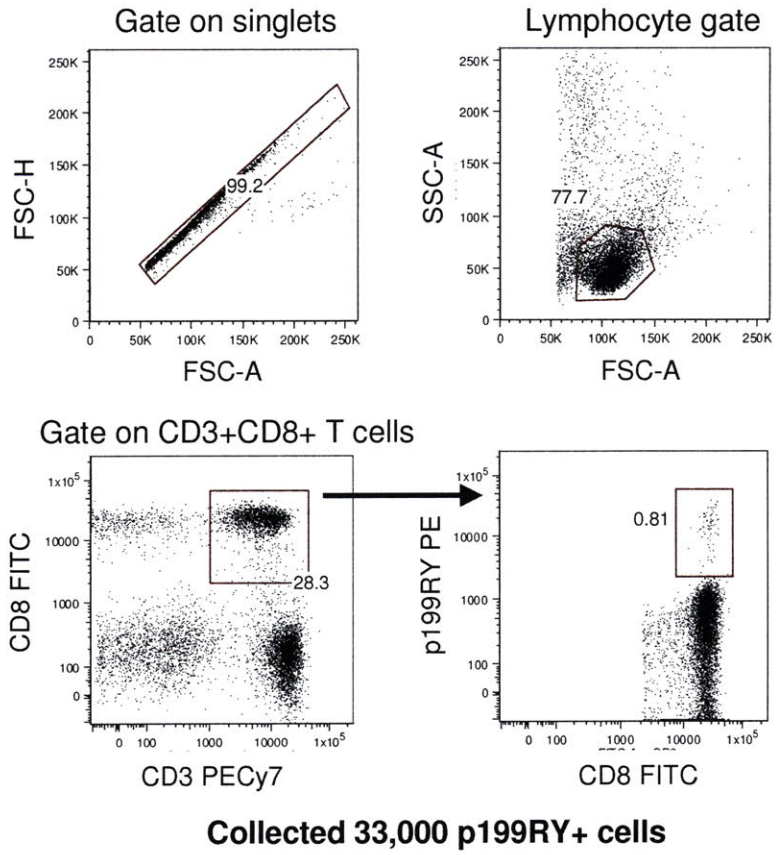

Figure 4.7. Tetramer cell sorting for Mm337-2008 (A*02+) on Day 14 post SIVmac251 intra-rectal challenge. Gating schematic is shown above, selecting for singlets, then lymphocytes, then CD3+CD8+ T cells. Mamu-A*02/p199RY tetramer positive cells were sorted in parallel into FACS tubes filled with RNAprotect Reagent. A total of 33,000 p199RY+ cells were collected.

RNA was extracted from sorted virus epitope-specific CD8+ T cells using the Trizol method and the RNA integrity was measured by an Agilent Bioanalyzer (Fig. 4.8).

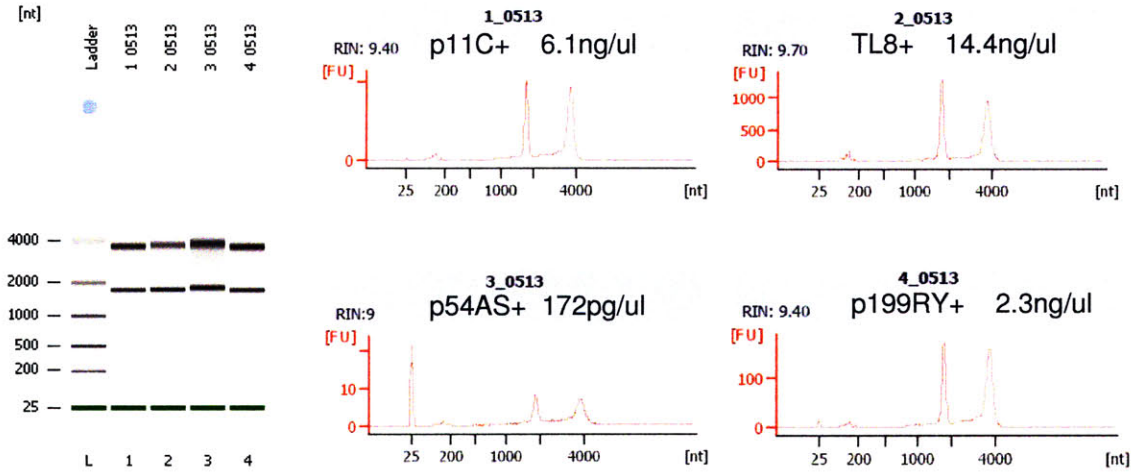

Figure 4.8. RNA integrity and quantity from tetramer positive cells on Day 14 post SIVmac251 challenge for Mm107-2006 (A*01+) and Mm337-2008 (A*02+). The A01 restricted epitopes are p11C, TL8, and p54AS. The A*02 restricted epitope is p199RY. The RNA was extracted using the Trizol method and integrity analysis was performed by Agilent Bioanalyzer and all samples were resuspended in 5 ul RNase-free water.

For each sample that was collected at each timepoint, 500 pg of RNA was taken and amplified using the TargetAmp 2-Round Biotin-aRNA Amplfication Kit 3.0 (Epicentre Biotechnologies) to produce biotin-aRNA to be hybridized to the Illumina HumanHT-12 Expression Beadchip. A total of 1.5 ug of biotin-aRNA is required for hybridization. Table 4.1 and Figure 4.9 show a representative amplification from 500 pg of starting CD8+ T cell total RNA.

Table 4.1 Amplified biotin-aRNA from total CD8+ T cells from Mm107-2006 (A*01+) and Mm337-2008 (A*02+). Total RNA in the amount of 500 pg was amplified using the TargetAmp 2-Round Biotin-aRNA Amplification Kit 3.0 (Epicentre Biotechnologies) and resuspended in 40 ul RNase-free water. These samples were obtained 14 and 21 days before challenge to establish baseline as well as to verify procedure. The No RNA Control was included as a negative control.

	aRNA concentration (ng/ul)	Total aRNA amt (ug)
107-2006 Total CD8 -21DPI	2543	101.72
337-2008 Total CD8 -21DPI	2467	98.68
107-2006 Total CD8 -14DPI	1804	72.16
337-2008 Total CD8 -14DPI	2079	83.16
No RNA control	30	1.2

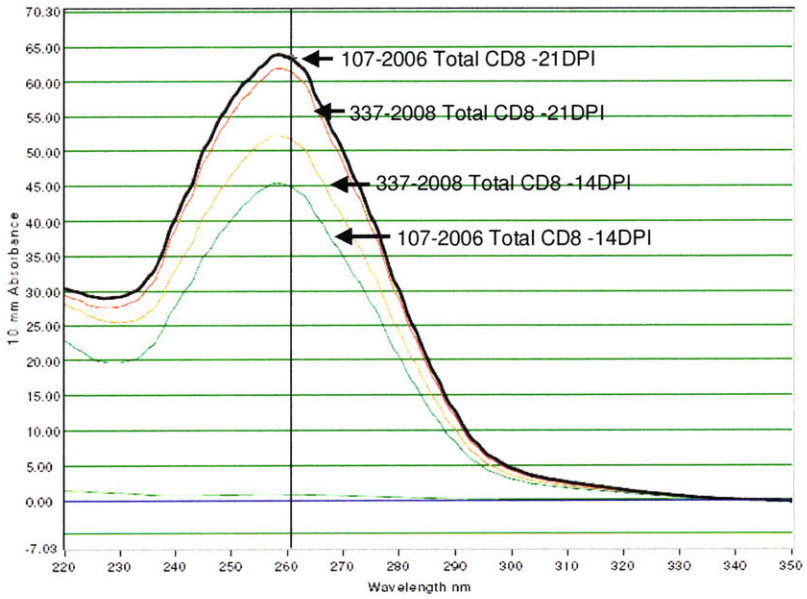

Figure 4.9. Amplified biotin-aRNA from total CD8+ T cells from Mm107-2006 (A*01+) and Mm337-2008 (A*02+). Total RNA in the amount of 500 pg was amplified using the TargetAmp 2-Round Biotin-aRNA Amplification Kit 3.0 (Epicentre Biotechnologies) and resuspended in 40ul RNase-free water and measured on Nanodrop ND-1000. These samples were obtained 14 and 21 days before challenge to establish the baseline as well as to verify the procedure.

For some of the samples, enough total RNA was extracted from the cells to allow for one round of amplification. For these samples, the remaining RNA that was not used for the two-round amplification was amplified one-round with the Illumina(R) TotalPrep(TM) RNA Amplification Kit (Ambion) and hybridized to the Illumina HumanHT-12 Expression Beadchip.

Tetramer responses

Weekly following SIVmac251 intra-rectal challenge, 10 ml of blood was obtained from 6 Mamu-A*01+ and 6 Mamu-A*02+ rhesus monkeys. PBMCs from Mamu-A*01+ rhesus monkeys were stained with Mamu-A*01/p11C, Mamu-A*01/TL8, and Mamu-A*01/p54AS, and PBMCs from Mamu-A*02+ rhesus monkeys were stained with Mamu-A*02/p199RY tetramer. Gating on CD3+CD8+ lymphocytes, tetramer-binding cells were detected by week 2 post-infection (Fig. 4.10), consistent with previous reports.[189] In some animals, the tetramer response was already detectable by week one post-infection. Tat TL8-specific CD8+ T lymphocyte responses peaked by 2 wk, and then rapidly declined. Gag p11C-specific CD8+ T lymphocyte responses developed more slowly, were of lesser magnitude than the Tat TL8-specific responses, and had more gradual increases and decreases. The Gag p11C-specific CD8+ T lymphocyte responses in monkeys 107-2006 and 112-2006 were bimodal. The subdominant Env p54AS-specific CD8+ T lymphocyte response was much lesser than the dominant Gag p11C and Tat TL8 responses and in monkey 125-2008, it was undetectable.

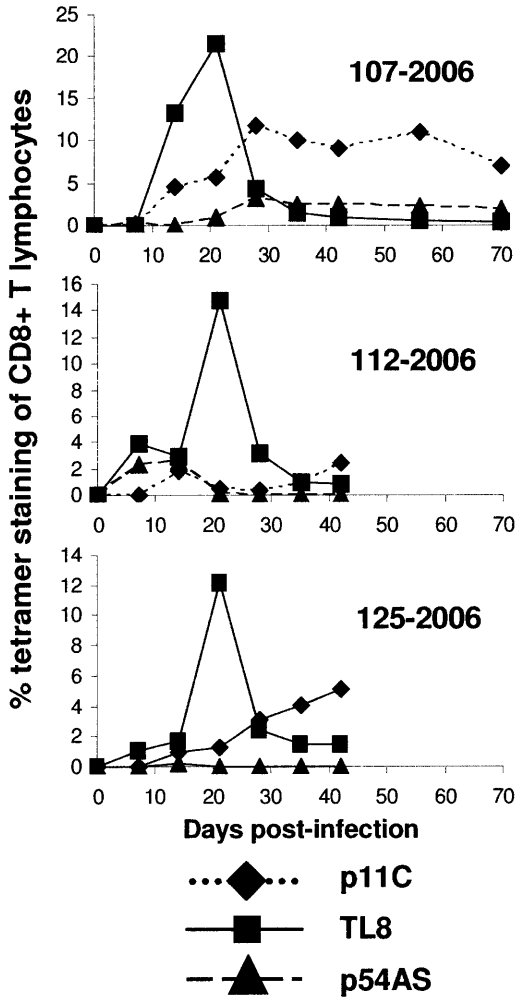

Figure 4.10. Mamu-A*01-restricted, SIV epitope-specific T lymphocyte responses in SIVmac251-infected Mamu-A*01+ rhesus monkeys. Shown are three of six monkeys intra-rectally infected with SIVmac251. The development of T lymphocyte responses specific for the Mamu-A*01-restricted epitope Gag p11C, Tat TL8, and Env p54AS was monitored by tetramer staining of PBMCs. Shown are the percentages of cells gated on the lymphocyte population that stained positively for CD3, CD8α, and a soluble tetramer complex containing Mamu-A*01 and the indicated epitope peptide. For monkeys 112-2006 and 125-2006, tetramer responses for later timepoints are pending.

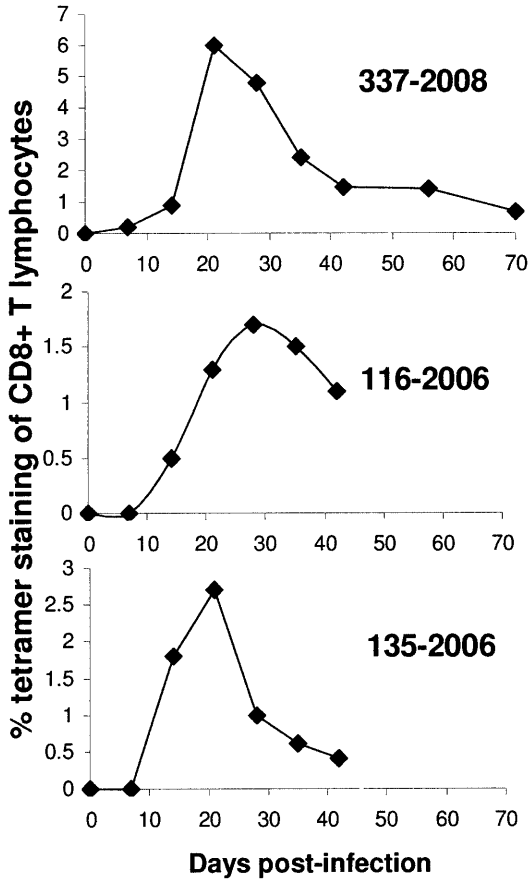

Figure 4.11. Mamu-A*02-restricted, SIV epitope-specific T lymphocyte responses in SIVmac251-infected Mamu-A*02+ rhesus monkeys. Shown are data from 3 or 6 monkeys intra-rectally infected with SIVmac251. The development of T lymphocyte responses specific for the Mamu-A*02-restricted epitope Nef p199RY was monitored by tetramer staining of PBMCs. Shown are the percentages of cells gated on the lymphocyte population that stained positively for CD3, CD8α, and a soluble tetramer complex containing Mamu-A*02 and p199RY. For monkeys 116-2006 and 135-2006, tetramer responses for later timepoints are pending.

In the Mamu-A*02+ monkeys, Nef p199RY tetramer-binding CD8+ T lymphocytes were detected by 2 wk post-infection and peaked by 2 or 3 wk post-infection (Fig. 4.11). The magnitude of the tetramer response differed among animals with peak tetramer percentages of

CD8+ T lymphocytes ranging from 1.7% to 6%. This variability has also been seen in previous studies.[189]

Plasma Viral Loads

Plasma virus RNA levels were assessed over time in all experimental animals. Plasma viral RNA levels are shown for 3 of the 6 pairs of A*01+ and A*02+ animals in Figure 4.12. The time to peak viremia and magnitude of peak viremia was comparable between the groups of monkeys. Virus RNA levels were consistent with tetramer CD8+ T lymphocyte responses (Fig. 4.10 and 4.11), showing the development of tetramer responses shortly after peak viremia.

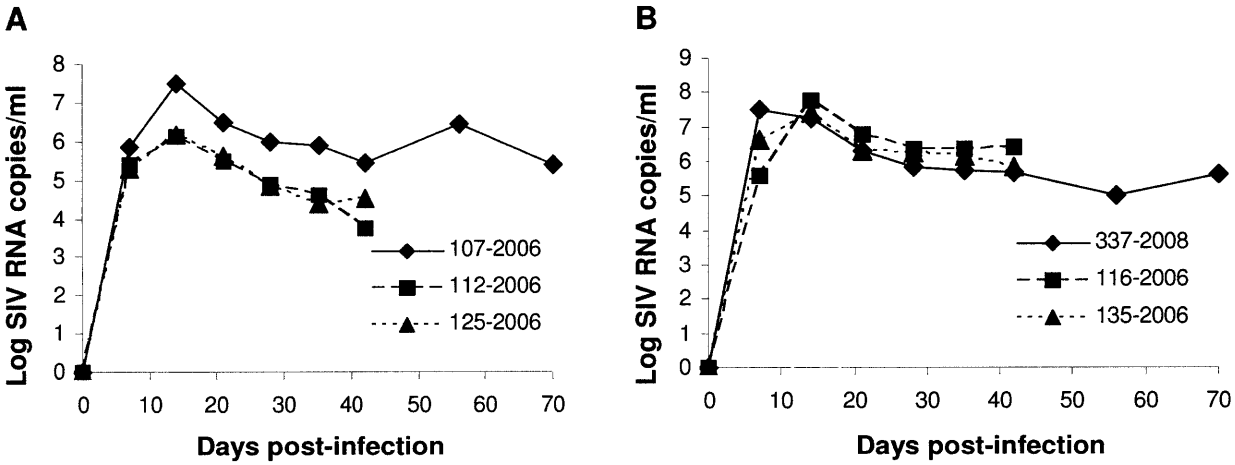

Figure 4.12. SIV viral load kinetics and magnitude for Mamu-A*01+ (A) and Mamu-A*02+ (B) rhesus monkeys. Viral loads are given for 3 of the 6 pairs of A*01+ and A*02+ rhesus monkeys. For monkeys 112-2006, 125-2006, 116-2006, and 135-2006, viral loads for later timepoints are pending.

Discussion

While results from this study are pending, there are two possible expected outcomes. One possibility is that there is a difference between the Mamu-A*01 and Mamu-A*02 positive monkeys that lies within the RNA transcripts of their respective virus epitope-specific CD8+ T cells. Gene expression profiling will uncover any such differences and from there, the particular gene targets can be validated by quantitative PCR, and various pathways can be explored with the hope of elucidating underlying mechanisms of action. The other possible outcome is that there is no difference in biology at the transcript level between the A*01 restricted CTLs and the A*02 restricted CTLs. If that proves to be the case, we must look elsewhere for explanations for the difference in viral control between the Mamu-A*01+ and Mamu-A*02+ monkeys.

There are factors that cannot be explored by gene expression profiling that may contribute to differences in SIV control between Mamu-A*01 and Mamu-A*02 positive monkeys. For example, recent studies in HIV-infected individuals have shown that the functional avidity of HIV-specific CD8+ T cells are consistently higher and the tetramer dissociation rates consistently lower in early infection as compared to chronic infection.[190] Further in vivo studies have suggested that the functional avidity of CD8+ T cells is linked to their antiviral activity. These data suggest that high-avidity HIV-specific CD8+ T cells recruited during early infection might significantly contribute to the dramatic decline of HIV viremia during early infection.[190] In converse, the loss of functional avidity by HIV-specific CD8+ T cells during chronic infection may contribute to viral persistence and disease progression.[190] Extending these findings to our

current study, it is possible that there may be a difference in CTL TCR affinity for viral peptides in association with MHC class I molecules in the Mamu-A*01+ and Mamu-A*02+ monkeys.

Another potential explanation for differences in SIV control between the Mamu-A*01+ and Mamu-A*02+ monkeys is difference in mutation rates in the immunodominant epitopes. Due to both the high replication rate of SIV and HIV and the high error rate of the RT encoded by HIV and SIV, viral mutations are generated rapidly in a setting of significant immune selection pressure conferred by the CTLs. Evidence of viral escape from CTL recognition has been shown in both chronic and acute HIV infection, occurring as early as day 50 post-infection for the HLA-B44-restricted epitope of gp160 or the HLA-B8-restricted epitope of Nef.[191,192] Mutations in CTL epitopes have also been seen in both acute and chronic infection in SIV Nef, Env, Tat, and Gag.[193] However, certain CTL epitopes are more restricted in their ability to tolerate amino acid substitutions while other are more permissive for substitutions.[193] Studies by other groups have shown a rapid emergence of Tat SL8 epitope variants[2] and slow emergence of Gag p11C epitope variants.[3,194-196] In a study of Mamu-A*01+ and Mamu-A*02+ animals infected with SIVmac251, an increase in frequency of mutation in the immunodominant Nef p199RY epitope[165] was shown, where 78-100% of the virus in each monkey had mutations, and 26% of these mutations were in the residues of the peptide that are most important for binding to Mamu-A*02.[189,197,198] Explanations for the variations in frequency of immunodominant epitope mutations include differences in protein expression kinetics, CTL avidity, and structural constraints on the virus.[193] The structural constraints explanation, however, is perhaps the most compelling. Viral escape from CTL epitopes located within constrained regions of viral structural proteins may require multiple compensatory mutations to facilitate assembly of viable virus.[193] The generation of

such compensatory mutations may occur infrequently during infection.[193] Unlike Tat, Nef, and Env proteins, which can retain function with numerous mutations and even large deletions, the structural Gag protein has limited tolerance for mutations.[199] Successful SIV/HIV escape from CTL recognition likely requires a balance between the selection pressures exerted by CTL and the maintenance of viral structural competency. The Gag p11C epitope is located in a highly conserved region of the capsid protein, which has been shown by various groups to play a critical role in SIV/HIV replication.[200,201] Mutations within the Gag p11C epitope are likely to interfere with virus assembly, and therefore compensatory mutations are necessary to maintain a viable virus.[193,202] The fitness costs of mutations in the Gag p11C epitope limit viral escape from CTLs.[203] The limited ability of SIV to escape from CTL at that dominant Gag epitope may contribute to the superior control of SIV in the Mamu-A*01+ monkeys. The requirement for coincident compensatory mutations may also explain why viral mutations in this epitope occur more infrequently than they do in other epitopes.[193]

CHAPTER 5: DISCUSSION

The work presented here paves the way for the study of rare cell populations in both peripheral blood and mucosal tissues. The evolution of virus-specific CD8+ T lymphocytes in mucosal compartments in the setting of primary SIV infection is not well understood. Most studies of CD8+ T cells that have been carried out to date only evaluate peripheral blood or unfractionated lymphocyte populations from mucosal specimens.[24,204-206] While the present study is an analysis of the evolution of virus-specific CD8+ T cells in the blood, one can build on this knowledge by performing a similar study of virus-specific CD8+ T cells from mucosal compartments such as the duodenum, distal colon, and from bronchoalveolar lavage specimens, using peripheral blood virus-specific CD8+ T cells as a comparator. One can then ask the question if the biology or the temporal evolution of virus-specific CD8+ T cells differ at the transcript level between the blood and mucosa and between different mucosal compartments. The strategies presented in Chapters 2 and 3 can also be used to assess the evolution during primary infection of various other cell populations, such as B cells, NK cells, and dendritic cells. While the majority of studies in the HIV and SIV literature have focused on adaptive cellular immunity, the role of the innate immune system has recently been implicated in HIV pathogenesis.[207-213] A study of the evolution of gene expression in innate immune cells in the setting of HIV or SIV infection should be very useful to further our understanding of AIDS pathogenesis.

While immune responses to HIV or SIV depend on the expression of cellular genes, understanding the entire picture of the immune response requires a more integrated approach. While functional genomics strives to identify the role of genes in cellular processes by way of hybridizing mRNA to complementary DNA, functional immunomics aim to identify roles of

chemical/biological targets involved in immunological processes by examining specific cellular and humoral immune responses elicited by antigens presented to the immune system.[101,102,214,215] For example, antibody microarrays might be used to probe post-translational functional genomics, since there has been some evidence of poor correlations between concentrations of mRNAs and their corresponding proteins.[216,217] Other immunomic microarrays include those that focus on peptide, cell, serum, and peptide-MHC.[218] Whereas DNA microarrays can only assay one parameter (the level of transcription of each gene), immunomic microarrays can measure several parameters pertaining to the immune responses against a single epitope.[218] For example, in peptide-MHC arrays, not only can one assay binding to individual peptide-MHC complexes, one can also assay the quantity and quality of the cytokine responses to these complexes.[218] The complexity of statistical analyses for immunomic microarrays is significantly greater than for DNA microarrays. While there are roughly 30,000 genes in humans, the number of different T cell receptors generated by somatic recombination is estimated to be on the order of 10^7 to 10^{15}. In addition, DNA is composed of combinations of four different bases (A, T, C, G), while peptide epitopes are composed of combinations of up to 20 different amino acids. While there are many challenges, immunomics may eventually be an additional tool one can use to study T cell immune responses to SIV or HIV.

Another technology that can be useful for studying immune responses in SIV and HIV infection is the new generation of gene sequencing. Sequencing technologies such as 454 sequencing technology, Illumina/Solexa, and ABI/SoLiD have had a tremendous impact on genomics research.[219] These technologies can perform thousands of reactions in parallel and are more cost-effective than traditional Sanger sequencing, and also replace troublesome in vivo cloning

with in vitro clonal amplification using emulsion PCR or bridge amplification on solid surfaces.[219] The downside to these new sequencing methods is the shorter read lengths (35bp for Solexa and ABI/SOLiD and 300bp for 454).[219] However, there are applications such as sequence census that can benefit from short reads. The sequence census approach uses short reads to establish the site of origin of the read instead of the whole sequence.[219] A novel use of the sequence census approach identifies protein binding sites on the DNA using chromatin immunoprecipitation followed by next-generation sequencing (ChIP-Seq).[219] This has been applied to identification of transcription factor binding sites as well as histone modifications on a genome-wide scale.[219] The use of next generation sequencing technology for transcriptome sequencing can provide insight into the level of gene expression, the structure of the genomic loci, sequence variation present at loci, and profiling of noncoding RNA (e.g. tRNA, rRNA, miRNA, and siRNA).[219-221]

Lastly, single cell PCR, which was first described over a decade ago, has reached new levels of accuracy and efficiency. Single cell PCR was first used in the area of fetal diagnostics, researchers have increasingly used this technology for a number of different applications.[222] Single cell PCR has been used in the analysis of TCR repertoires of CD8+ T cells in response to antigenic challenge.[223] Single-cell RT-PCR has enabled gene expression analysis of single cells. This is powerful technology that can potentially allow for a complete analysis of very small subpopulations of cells and even individual cells within a subpopulation. Single cells can be obtained by laser mediated micromanipulation systems (e.g. laser capture microdissection) and then assayed for mRNA expression.[222] Combining single cell PCR with array analysis can

provide a true analysis of the heterogeneity of the immune response in particular cell subpopulations and can lead to new insights into cell-cell interactions and cellular dynamics.

There is much that is still unknown about the immune response following SIV and HIV infection. However, new tools are currently being developed that in the coming years will provide new ways of studying the immune response and lead to an increasingly better understanding of SIV and HIV pathogenesis.

REFERENCES

1. UNAIDS & WHO. AIDS Epidemic Update. (2006).
2. Allen, T.M., *et al.* Tat-specific cytotoxic T lymphocytes select for SIV escape variants during resolution of primary viraemia. *Nature* **407**, 386-390 (2000).
3. Evans, D.T., *et al.* Virus-specific cytotoxic T-lymphocyte responses select for amino-acid variation in simian immunodeficiency virus Env and Nef. *Nat Med* **5**, 1270-1276 (1999).
4. Geels, M.J., *et al.* Identification of Sequential Viral Escape Mutants Associated with Altered T-Cell Responses in a Human Immunodeficiency Virus Type 1-Infected Individual. *J Virol* **77**, 12430-12440 (2003).
5. Lee, H.Y., Perelson, A.S., Park, S.-C. & Leitner, T. Dynamic Correlation between Intrahost HIV-1 Quasispecies Evolution and Disease Progression. *PLoS Comput Biol* **4**, e1000240 (2008).
6. McMichael, A.J. & Phillips, R.E. Escape of Human Immunodeficiency Virus from Immune Control. *Annual Reviews Immunology* **15**, 271-296 (1997).
7. Darlix, J.-L., Lapadat-Tapolsky, M., de Rocquigny, H. & Roques, B.P. First Glimpses at Structure-function Relationships of the Nucleocapsid Protein of Retroviruses. *Journal of Molecular Biology* **254**, 523-537 (1995).
8. Krishnamoorthy, G., Roques, B., Darlix, J.-L. & Mely, Y. DNA condensation by the nucleocapsid protein of HIV-1: a mechanism ensuring DNA protection. *Nucleic Acids Res* **31**, 5425-5432 (2003).
9. Bukrinsky, M.I., *et al.* Association of integrase, matrix, and reverse transcriptase antigens of human immunodeficiency virus type 1 with viral nucleic acids following acute infection. *Proc Natl Acad Sci U S A* **90**, 6125-6129 (1993).
10. Lackner, A.A., Vogel, P., Ramos, R.A., Kluge, J.D. & Marthas, M. Early events in tissues during infection with pathogenic (SIVmac239) and nonpathogenic (SIVmac1A11) molecular clones of simian immunodeficiency virus. *Am J Pathol* **145**, 428-439 (1994).
11. DeVico, A.L. & Gallo, R.C. Control of HIV-1 infection by soluble factors of the immune response. *Nat Rev Micro* **2**, 401-413 (2004).
12. Biron, C.A. & Brossay, L. NK cells and NKT cells in innate defense against viral infections. *Current Opinion in Immunology* **13**, 458-464 (2001).
13. Biron, C.A., Nguyen, K.B., Pien, G.C., Cousens, L.P. & Salazar-Mather, T.P. NATURAL KILLER CELLS IN ANTIVIRAL DEFENSE: Function and Regulation by Innate Cytokines. *Annual Reviews Immunology* **17**, 189-220 (1999).
14. Wallace, M., Malkovsky, M. & Carding, S.R. Gamma/delta T lymphocytes in viral infections. *J Leukoc Biol* **58**, 277-283 (1995).
15. Selin, L.K., Santolucito, P.A., Pinto, A.K., Szomolanyi-Tsuda, E. & Welsh, R.M. Innate Immunity to Viruses: Control of Vaccinia Virus Infection by Gamma Delta T Cells. *J Immunol* **166**, 6784-6794 (2001).
16. Burton, D.R., *et al.* HIV vaccine design and the neutralizing antibody problem. *Nat Immunol* **5**, 233-236 (2004).
17. Karlsson Hedestam, G.B., *et al.* The challenges of eliciting neutralizing antibodies to HIV-1 and to influenza virus. *Nat Rev Micro* **6**, 143-155 (2008).
18. Moore, J.P., *et al.* Primary isolates of human immunodeficiency virus type 1 are relatively resistant to neutralization by monoclonal antibodies to gp120, and their

neutralization is not predicted by studies with monomeric gp120. *J Virol* **69**, 101-109 (1995).
19. Klausner, R.D., *et al.* MEDICINE: Enhanced: The Need for a Global HIV Vaccine Enterprise. *Science* **300**, 2036-2039 (2003).
20. McMichael, A.J. & Rowland-Jones, S.L. Cellular immune responses to HIV. *Nature* **410**, 980-987 (2001).
21. Walker, C.M., Moody, D.J., Stites, D.P. & Levy, J.A. CD8+ Lymphocytes Can Control HIV Infection in vitro by Suppressing Virus Replication. *Science* **234**, 1563-1566 (1986).
22. Geiben-Lynn, R., *et al.* Noncytolytic Inhibition of X4 Virus by Bulk CD8+ Cells from Human Immunodeficiency Virus Type 1 (HIV-1)-Infected Persons and HIV-1-Specific Cytotoxic T Lymphocytes Is Not Mediated by {beta}-Chemokines. *J Virol* **75**, 8306-8316 (2001).
23. Koup, R.A., *et al.* Temporal association of cellular immune responses with the initial control of viremia in primary human immunodeficiency virus type 1 syndrome. *J Virol* **68**, 4650-4655 (1994).
24. Kuroda, M.J., *et al.* Emergence of CTL coincides with clearance of virus during primary simian immunodeficiency virus infection in rhesus monkeys. *J Immunol* **162**, 5127-5133 (1999).
25. Schmitz, J.E., *et al.* Control of viremia in simian immunodeficiency virus infection by CD8+ lymphocytes. *Science* **283**, 857-860 (1999).
26. Jin, X., *et al.* Dramatic Rise in Plasma Viremia after CD8+ T Cell Depletion in Simian Immunodeficiency Virus-infected Macaques. *J Exp Med* **189**, 991-998 (1999).
27. Lifson, J.D., *et al.* Role of CD8+ Lymphocytes in Control of Simian Immunodeficiency Virus Infection and Resistance to Rechallenge after Transient Early Antiretroviral Treatment. *J Virol* **75**, 10187-10199 (2001).
28. McNeil, A.C., *et al.* High-level HIV-1 viremia suppresses viral antigen-specific CD4+ T cell proliferation. *Proc Natl Acad Sci U S A* **98**, 13878-13883 (2001).
29. Douek, D.C., *et al.* HIV preferentially infects HIV-specific CD4+ T cells. *Nature* **417**, 95-98 (2002).
30. Day, C.L., *et al.* PD-1 expression on HIV-specific T cells is associated with T-cell exhaustion and disease progression. *Nature* **443**, 350-354 (2006).
31. Petrovas, C., *et al.* PD-1 is a regulator of virus-specific CD8+ T cell survival in HIV infection. *J Exp Med* **203**, 2281-2292 (2006).
32. Trautmann, L., *et al.* Upregulation of PD-1 expression on HIV-specific CD8+ T cells leads to reversible immune dysfunction. *Nat Med* **12**, 1198-1202 (2006).
33. Hiroyuki Yamamoto, T.M. Anti-HIV adaptive immunity: determinants for viral persistence. *Reviews in Medical Virology* **18**, 293-303 (2008).
34. B. L. Shacklett, J.W.C.A.L.F.T.L.H. Mucosal T-cell responses to HIV: responding at the front lines. *J Intern Med* **265**, 58-66 (2009).
35. Neutra, M.R. & Kozlowski, P.A. Mucosal vaccines: the promise and the challenge. *Nat Rev Immunol* **6**, 148-158 (2006).
36. Veazey, R.S., *et al.* Gastrointestinal Tract as a Major Site of CD4+ T Cell Depletion and Viral Replication in SIV Infection. *Science* **280**, 427-431 (1998).
37. Belyakov, I.M., *et al.* Mucosal AIDS vaccine reduces disease and viral load in gut reservoir and blood after mucosal infection of macaques. *Nat Med* **7**, 1320-1326 (2001).

38. Berzofsky, J.A., *et al.* Approaches to improve engineered vaccines for human immunodeficiency virus and other viruses that cause chronic infections. *Immunol Rev* **170**, 151-172 (1999).
39. Czerkinsky, C., *et al.* Mucosal immunity and tolerance: relevance to vaccine development. *Immunol Rev* **170**, 197-222 (1999).
40. Lehner, T., Bergmeier, L., Wang, Y., Tao, L. & Mitchell, E. A rational basis for mucosal vaccination against HIV infection. *Immunol Rev* **170**, 183-196 (1999).
41. McMichael, A. & Hanke, T. The quest for an AIDS vaccine: is the CD8+ T-cell approach feasible? *Nat Rev Immunol* **2**, 283-291 (2002).
42. Streeck, H., Frahm, N. & Walker, B.D. The role of IFN-[gamma] Elispot assay in HIV vaccine research. *Nat. Protocols* **4**, 461-469 (2009).
43. Gauduin, M.-C. Intracellular cytokine staining for the characterization and quantitation of antigen-specific T lymphocyte responses. *Methods* **38**, 263-273 (2006).
44. Alizadeh, A., Eisen, M., Botstein, D., Brown, P.O. & Staudt, L.M. Probing Lymphocyte Biology by Genomic-Scale Gene Expression Analysis. *Journal of Clinical Immunology* **18**, 373-379 (1998).
45. Schena, M., Shalon, D., Davis, R.W. & Brown, P.O. Quantitative Monitoring of Gene Expression Patterns with a Complementary DNA Microarray. *Science* **270**, 467-470 (1995).
46. Hyatt, G., *et al.* Gene expression microarrays: glimpses of the immunological genome. *Nat Immunol* **7**, 686-691 (2006).
47. Bennett, L., *et al.* Interferon and Granulopoiesis Signatures in Systemic Lupus Erythematosus Blood. *J Exp Med* **197**, 711-723 (2003).
48. Adarichev, V., *et al.* Gene expression profiling in murine autoimmune arthritis during the initiation and progression of joint inflammation. *Arthritis Res Ther* **7**, R196 - R207 (2005).
49. Poirot, L., Benoist, C. & Mathis, D. Natural killer cells distinguish innocuous and destructive forms of pancreatic islet autoimmunity. *Proc Natl Acad Sci U S A* **101**, 8102-8107 (2004).
50. Matos, M., Park, R., Mathis, D. & Benoist, C. Progression to Islet Destruction in a Cyclophosphamide-Induced Transgenic Model. *Diabetes* **53**, 2310-2321 (2004).
51. Kluger, Y., *et al.* Lineage specificity of gene expression patterns. *Proc Natl Acad Sci U S A* **101**, 6508-6513 (2004).
52. Hashimoto, S.-i., *et al.* Gene expression profile in human leukocytes. *Blood* **101**, 3509-3513 (2003).
53. Hutton, J., *et al.* Microarray and comparative genomics-based identification of genes and gene regulatory regions of the mouse immune system. *BMC Genomics* **5**, 82 (2004).
54. Su, A.I., *et al.* A gene atlas of the mouse and human protein-encoding transcriptomes. *Proc Natl Acad Sci U S A* **101**, 6062-6067 (2004).
55. Abbas, A.R., *et al.* Immune response in silico (IRIS): immune-specific genes identified from a compendium of microarray expression data. *Genes Immun* **6**, 319-331 (2005).
56. Geiss, G.K., *et al.* Large-Scale Monitoring of Host Cell Gene Expression during HIV-1 Infection Using cDNA Microarrays. *Virology* **266**, 8-16 (2000).
57. Giri, M.S., Nebozhyn, M., Showe, L. & Montaner, L.J. Microarray data on gene modulation by HIV-1 in immune cells: 2000-2006. *J Leukoc Biol* **80**, 1031-1043 (2006).

58. Cicala, C., *et al.* HIV envelope induces a cascade of cell signals in non-proliferating target cells that favor virus replication. *Proc Natl Acad Sci U S A* **99**, 9380-9385 (2002).
59. Cicala, C., *et al.* R5 and X4 HIV envelopes induce distinct gene expression profiles in primary peripheral blood mononuclear cells. *Proc Natl Acad Sci U S A* **103**, 3746-3751 (2006).
60. Shapiro, L., Heidenreich, K.A., Meintzer, M.K. & Dinarello, C.A. Role of p38 mitogen-activated protein kinase in HIV type 1 production in vitro. *Proc Natl Acad Sci U S A* **95**, 7422-7426 (1998).
61. Yang, Z. & Engel, J.D. Human T cell transcription factor GATA-3 stimulates HIV-1 expression. *Nucleic Acids Res* **21**, 2831-2836 (1993).
62. Muthumani, K., *et al.* HIV-1 Vpr inhibits the maturation and activation of macrophages and dendritic cells in vitro. *International Immunology* **17**, 103-116 (2005).
63. Janket, M.L., *et al.* Differential regulation of host cellular genes by HIV-1 viral protein R (Vpr): cDNA microarray analysis using isogenic virus. *Biochemical and Biophysical Research Communications* **314**, 1126-1132 (2004).
64. Vanitharani, R., *et al.* HIV-1 Vpr Transactivates LTR-Directed Expression through Sequences Present within -278 to -176 and Increases Virus Replication in Vitro. *Virology* **289**, 334-342 (2001).
65. Boutboul, F., *et al.* Modulation of interleukin-7 receptor expression characterizes differentiation of CD8 T cells specific for HIV, EBV and CMV. *Aids* **19**, 1981-1986 (2005).
66. Motomura, K., *et al.* Identification of a host gene subset related to disease prognosis of HIV-1 infected individuals. *International Immunopharmacology* **4**, 1829-1836 (2004).
67. Corbeil, J., *et al.* Temporal gene regulation during HIV-1 infection of human CD4+ T cells. *Genome Res* **11**, 1198-1204 (2001).
68. van 't Wout, A.B., *et al.* Nef Induces Multiple Genes Involved in Cholesterol Synthesis and Uptake in Human Immunodeficiency Virus Type 1-Infected T Cells. *J Virol* **79**, 10053-10058 (2005).
69. Giacca, M. HIV-1 Tat, apoptosis and the mitochondria: a tubulin link? *Retrovirology* **2**, 7 (2005).
70. Gougeon, M.-L. Apoptosis as an HIV strategy to escape immune attack. *Nat Rev Immunol* **3**, 392-404 (2003).
71. Ahr, B., Robert-Hebmann, V., Devaux, C. & Biard-Piechaczyk, M. Apoptosis of uninfected cells induced by HIV envelope glycoproteins. *Retrovirology* **1**, 12 (2004).
72. Chun, T.-W., *et al.* Gene expression and viral prodution in latently infected, resting CD4+ T cells in viremic versus aviremic HIV-infected individuals. *Proc Natl Acad Sci U S A* **100**, 1908-1913 (2003).
73. Woelk, C.H., *et al.* Interferon Gene Expression following HIV Type 1 Infection of Monocyte-Derived Macrophages. *AIDS Res Hum Retroviruses* **20**, 1210-1222 (2004).
74. Robert T. Bailer, B.L.L.J.M. IL-13 and TNF-a; inhibit dual-tropic HIV-1 in primary macrophages by reduction of surface expression of CD4, chemokine receptors CCR5, CXCR4 and post-entry viral gene expression. *Eur J Immunol* **30**, 1340-1349 (2000).
75. Giri, M.S., *et al.* Circulating Monocytes in HIV-1-Infected Viremic Subjects Exhibit an Antiapoptosis Gene Signature and Virus- and Host-Mediated Apoptosis Resistance. *J Immunol* **182**, 4459-4470 (2009).

76. Figueroa-Tentori, D., Querol, S., Dodi, I.A., Madrigal, A. & Duggleby, R. High purity and yield of natural Tregs from cord blood using a single step selection method. *Journal of Immunological Methods* **339**, 228-235 (2008).
77. Mariappan, D., *et al.* Transcriptional profiling of CD31(+) cells isolated from murine embryonic stem cells. *Genes Cells* **14**, 243-260 (2009).
78. Talasaz, A.H., *et al.* Isolating highly enriched populations of circulating epithelial cells and other rare cells from blood using a magnetic sweeper device. *Proc Natl Acad Sci U S A* **106**, 3970-3975 (2009).
79. Neurauter, A., *et al.* Cell Isolation and Expansion Using Dynabeads ®. in *Cell Separation* 41-73 (2007).
80. Horgan, K., Shaw, S. & Boirivant, M. Immunomagnetic purification of T cell subpopulations. *Curr Protoc Immunol* **Chapter 7**, Unit7 4 (2009).
81. Furdui, V.I. & Harrison, D.J. Immunomagnetic T cell capture from blood for PCR analysis using microfluidic systems. *Lab Chip* **4**, 614-618 (2004).
82. Irimia, D. & Toner, M. Cell handling using microstructured membranes. *Lab Chip* **6**, 345-352 (2006).
83. Toner, M. & Irimia, D. Blood-on-a-chip. *Annu Rev Biomed Eng* **7**, 77-103 (2005).
84. Wolff, A., *et al.* Integrating advanced functionality in a microfabricated high-throughput fluorescent-activated cell sorter. *Lab Chip* **3**, 22-27 (2003).
85. Hou, C.S., Godin, M., Payer, K., Chakrabarti, R. & Manalis, S.R. Integrated microelectronic device for label-free nucleic acid amplification and detection. *Lab Chip* **7**, 347-354 (2007).
86. Liao, C.S., Lee, G.B., Liu, H.S., Hsieh, T.M. & Luo, C.H. Miniature RT-PCR system for diagnosis of RNA-based viruses. *Nucleic Acids Res* **33**, e156 (2005).
87. Liu, C.N., Toriello, N.M. & Mathies, R.A. Multichannel PCR-CE microdevice for genetic analysis. *Anal Chem* **78**, 5474-5479 (2006).
88. Marcus, J.S., Anderson, W.F. & Quake, S.R. Parallel picoliter rt-PCR assays using microfluidics. *Anal Chem* **78**, 956-958 (2006).
89. Toriello, N.M., Liu, C.N. & Mathies, R.A. Multichannel reverse transcription-polymerase chain reaction microdevice for rapid gene expression and biomarker analysis. *Anal Chem* **78**, 7997-8003 (2006).
90. Xiang, Q., Xu, B., Fu, R. & Li, D. Real time PCR on disposable PDMS chip with a miniaturized thermal cycler. *Biomed Microdevices* **7**, 273-279 (2005).
91. Xiang, Q., Xu, B. & Li, D. Miniature real time PCR on chip with multi-channel fiber optical fluorescence detection module. *Biomed Microdevices* (2007).
92. Wu, H., Wheeler, A. & Zare, R.N. Chemical cytometry on a picoliter-scale integrated microfluidic chip. *Proc Natl Acad Sci U S A* **101**, 12809-12813 (2004).
93. Liu, R.H., *et al.* Fully integrated miniature device for automated gene expression DNA microarray processing. *Anal Chem* **78**, 1980-1986 (2006).
94. Lenigk, R., *et al.* Plastic biochannel hybridization devices: a new concept for microfluidic DNA arrays. *Anal Biochem* **311**, 40-49 (2002).
95. King, K.R., *et al.* A high-throughput microfluidic real-time gene expression living cell array. *Lab Chip* **7**, 77-85 (2007).
96. Huang, B., Wu, H., Kim, S., Kobilka, B.K. & Zare, R.N. Phospholipid biotinylation of polydimethylsiloxane (PDMS) for protein immobilization. *Lab Chip* **6**, 369-373 (2006).

97. Liu, D., Perdue, R.K., Sun, L. & Crooks, R.M. Immobilization of DNA onto poly(dimethylsiloxane) surfaces and application to a microelectrochemical enzyme-amplified DNA hybridization assay. *Langmuir* **20**, 5905-5910 (2004).
98. Makamba, H., Kim, J.H., Lim, K., Park, N. & Hahn, J.H. Surface modification of poly(dimethylsiloxane) microchannels. *Electrophoresis* **24**, 3607-3619 (2003).
99. Rogers, Y.H., *et al.* Immobilization of oligonucleotides onto a glass support via disulfide bonds: A method for preparation of DNA microarrays. *Anal Biochem* **266**, 23-30 (1999).
100. Chen, D.S. & Davis, M.M. Molecular and functional analysis using live cell microarrays. *Curr Opin Chem Biol* **10**, 28-34 (2006).
101. Soen, Y., Chen, D.S., Kraft, D.L., Davis, M.M. & Brown, P.O. Detection and characterization of cellular immune responses using peptide-MHC microarrays. *PLoS Biol* **1**, E65 (2003).
102. Stone, J.D., Demkowicz, W.E., Jr. & Stern, L.J. HLA-restricted epitope identification and detection of functional T cell responses by using MHC-peptide and costimulatory microarrays. *Proc Natl Acad Sci U S A* **102**, 3744-3749 (2005).
103. Chen, D.S., *et al.* Marked differences in human melanoma antigen-specific T cell responsiveness after vaccination using a functional microarray. *PLoS Med* **2**, e265 (2005).
104. Sin, A., Murthy, S.K., Revzin, A., Tompkins, R.G. & Toner, M. Enrichment using antibody-coated microfluidic chambers in shear flow: model mixtures of human lymphocytes. *Biotechnol Bioeng* **91**, 816-826 (2005).
105. Revzin, A., Sekine, K., Sin, A., Tompkins, R.G. & Toner, M. Development of a microfabricated cytometry platform for characterization and sorting of individual leukocytes. *Lab Chip* **5**, 30-37 (2005).
106. Sethu, P., Sin, A. & Toner, M. Microfluidic diffusive filter for apheresis (leukapheresis). *Lab Chip* **6**, 83-89 (2006).
107. Samuel K. Sia, G.M.W. Microfluidic devices fabricated in Poly(dimethylsiloxane) for biological studies. *Electrophoresis* **24**, 3563-3576 (2003).
108. Situma, C., Hashimoto, M. & Soper, S.A. Merging microfluidics with microarray-based bioassays. *Biomol Eng* **23**, 213-231 (2006).
109. Liu, A.Y., *et al.* Cell-cell interaction in prostate gene regulation and cytodifferentiation. *Proc Natl Acad Sci U S A* **94**, 10705-10710 (1997).
110. Stanley Tamaki, K.E.D.H.R.S.M.D.G.J.R.T.M.R.B.H.A.T.F.G.I.W.N.U. Engraftment of sorted/expanded human central nervous system stem cells from fetal brain. *J Neurosci Res* **69**, 976-986 (2002).
111. Huntly, B.J.P. & Gilliland, D.G. Leukaemia stem cells and the evolution of cancer-stem-cell research. *Nat Rev Cancer* **5**, 311-321 (2005).
112. Wognum, A.W., Eaves, A.C. & Thomas, T.E. Identification and isolation of hematopoietic stem cells. *Arch Med Res* **34**, 461-475 (2003).
113. Li, J., Greco, V., Guasch, G.r., Fuchs, E. & Mombaerts, P. Mice cloned from skin cells. *Proc Natl Acad Sci U S A* **104**, 2738-2743 (2007).
114. Daugherty, P.S., Iverson, B.L. & Georgiou, G. Flow cytometric screening of cell-based libraries. *Journal of Immunological Methods* **243**, 211-227 (2000).
115. Galbraith, D.W., Elumalai, R. & Gong, F.C. Integrative Flow Cytometric and Microarray Approaches for Use in Transcriptional Profiling. in *Flow Cytometry Protocols* 259-279 (2004).

116. Ibrahim, S. & van den Engh, G. Flow Cytometry and Cell Sorting. in *Cell Separation* 19-39 (2007).
117. Mattanovich, D. & Borth, N. Applications of cell sorting in biotechnology. *Microbial Cell Factories* **5**, 12 (2006).
118. Hovav, A.-H., *et al.* The Impact of a Boosting Immunogen on the Differentiation of Secondary Memory CD8+ T Cells. *J Virol* **81**, 12793-12802 (2007).
119. Staats, H.F., *et al.* Cytokine Requirements for Induction of Systemic and Mucosal CTL After Nasal Immunization. *J Immunol* **167**, 5386-5394 (2001).
120. Marcus, J.S., Anderson, W.F. & Quake, S.R. Microfluidic single-cell mRNA isolation and analysis. *Anal Chem* **78**, 3084-3089 (2006).
121. Studer, V., *et al.* Scaling properties of a low-actuation pressure microfluidic valve. *J Appl Phys* **95**, 393-398 (2004).
122. Schroeder, A., *et al.* The RIN: an RNA integrity number for assigning integrity values to RNA measurements. *BMC Molecular Biology* **7**, 3 (2006).
123. Mueller, O., *et al.* A microfluidic system for high-speed reproducible DNA sizing and quantitation. *Electrophoresis* **21**, 128-134 (2000).
124. Mack, E., Neubauer, A. & Brendel, C. Comparison of RNA yield from small cell populations sorted by flow cytometry applying different isolation procedures. *Cytometry A* **71**, 404-409 (2007).
125. Chirgwin, J.M., Przybyla, A.E., MacDonald, R.J. & Rutter, W.J. Isolation of biologically active ribonucleic acid from sources enriched in ribonuclease. *Biochemistry* **18**, 5294-5299 (1979).
126. Culley, D.E., Kovacik, W.P., Jr., Brockman, F.J. & Zhang, W. Optimization of RNA isolation from the archaebacterium Methanosarcina barkeri and validation for oligonucleotide microarray analysis. *J Microbiol Methods* **67**, 36-43 (2006).
127. Hartshorn, C., Anshelevich, A. & Wangh, L.J. Rapid, single-tube method for quantitative preparation and analysis of RNA and DNA in samples as small as one cell. *BMC Biotechnol* **5**, 2 (2005).
128. Roos-van Groningen, M.C., Eikmans, M., Baelde, H.J., Heer, E.d. & Bruijn, J.A. Improvement of extraction and processing of RNA from renal biopsies. *Kidney Int* **65**, 97-105 (2004).
129. Tattoli, I., *et al.* Optimisation of isolation of richly pure and homogeneous primary human colonic smooth muscle cells. *Dig Liver Dis* **36**, 735-743 (2004).
130. Chomczynski, P. & Sacchi, N. Single-step method of RNA isolation by acid guanidinium thiocyanate-phenol-chloroform extraction. *Analytical Biochemistry* **162**, 156-159 (1987).
131. Chomczynski, P. & Sacchi, N. The single-step method of RNA isolation by acid guanidinium thiocyanate-phenol-chloroform extraction: twenty-something years on. *Nat. Protocols* **1**, 581-585 (2006).
132. Van Gelder, R.N., *et al.* Amplified RNA synthesized from limited quantities of heterogeneous cDNA. *Proc Natl Acad Sci U S A* **87**, 1663-1667 (1990).
133. Gubler, U. & Hoffman, B.J. A simple and very efficient method for generating cDNA libraries. *Gene* **25**, 263-269 (1983).
134. Ginsberg, S.D. RNA amplification strategies for small sample populations. *Methods* **37**, 229-237 (2005).
135. Wang, E., Miller, L.D., Ohnmacht, G.A., Liu, E.T. & Marincola, F.M. High-fidelity mRNA amplification for gene profiling. *Nat Biotech* **18**, 457-459 (2000).

136. Baugh, L.R., Hill, A.A., Brown, E.L. & Hunter, C.P. Quantitative analysis of mRNA amplification by in vitro transcription. *Nucleic Acids Res* **29**, e29- (2001).
137. Zhao, H., Hastie, T., Whitfield, M., Borresen-Dale, A.-L. & Jeffrey, S. Optimization and evaluation of T7 based RNA linear amplification protocols for cDNA microarray analysis. *BMC Genomics* **3**, 31 (2002).
138. Luzzi, V., Mahadevappa, M., Raja, R., Warrington, J.A. & Watson, M.A. Accurate and Reproducible Gene Expression Profiles from Laser Capture Microdissection, Transcript Amplification, and High Density Oligonucleotide Microarray Analysis. *Journal of Molecular Diagnostics* **5**, 9-14 (2003).
139. Xiang, C.C., *et al.* A new strategy to amplify degraded RNA from small tissue samples for microarray studies. *Biomed Microdevices* **31**, e53- (2003).
140. Iiizumi, M., *et al.* EphA4 receptor, overexpressed in pancreatic ductal adenocarcinoma, promotes cancer cell growth. *Cancer Sci* **97**, 1211-1216 (2006).
141. Gebert, M., Dresselhaus, T. & Sprunck, S. F-Actin Organization and Pollen Tube Tip Growth in Arabidopsis Are Dependent on the Gametophyte-Specific Armadillo Repeat Protein ARO1. *Plant Cell* **20**, 2798-2814 (2008).
142. Yang, F., *et al.* Laser microdissection and microarray analysis of breast tumors reveal ER-[alpha] related genes and pathways. *Oncogene* **25**, 1413-1419 (2005).
143. Sung, L.-Y., *et al.* Differentiated cells are more efficient than adult stem cells for cloning by somatic cell nuclear transfer. *Nat Genet* **38**, 1323-1328 (2006).
144. Kaler, G., *et al.* Olfactory mucosa-expressed organic anion transporter, Oat6, manifests high affinity interactions with odorant organic anions. *Biochem Biophys Res Commun* **351**, 872-876 (2006).
145. Negri, L., *et al.* Impaired Nociception and Inflammatory Pain Sensation in Mice Lacking the Prokineticin Receptor PKR1: Focus on Interaction between PKR1 and the Capsaicin Receptor TRPV1 in Pain Behavior. *Journal of Neuroscience* **26**, 6716-6727 (2006).
146. Iscove, N.N., *et al.* Representation is faithfully preserved in global cDNA amplified exponentially from sub-picogram quantities of mRNA. *Nat Biotech* **20**, 940-943 (2002).
147. Brandt, S., Kloska, S., Altmann, T. & Kehr, J. Using array hybridization to monitor gene expression at the single cell level. *Journal of Experimental Botany* **53**, 2315-2323 (2002).
148. Ginsberg, S.D. & Che, S. RNA Amplification in Brain Tissues. *Neurochemical Research* **27**, 981-992 (2002).
149. Aoyagi, K., *et al.* A faithful method for PCR-mediated global mRNA amplification and its integration into microarray analysis on laser-captured cells. *Biochemical and Biophysical Research Communications* **300**, 915-920 (2003).
150. Chiang, M.-K. & Melton, D.A. Single-Cell Transcript Analysis of Pancreas Development. *Developmental Cell* **4**, 383-393 (2003).
151. Seth, D., *et al.* SMART amplification maintains representation of relative gene expression: quantitative validation by real time PCR and application to studies of alcoholic liver disease in primates. *Journal of Biochemical and Biophysical Methods* **55**, 53-66 (2003).
152. Smith, L., *et al.* Single primer amplification (SPA) of cDNA for microarray expression analysis. *Nucleic Acids Res* **31**, e9- (2003).
153. Choesmel, V., Foucault, F., Thiery, J.P. & Blin, N. Design of a real time quantitative PCR assay to assess global mRNA amplification of small size specimens for microarray hybridisation. *J Clin Pathol* **57**, 1278-1287 (2004).

154. Bak, M., *et al.* Evaluation of two methods for generating cRNA for microarray experiments from nanogram amounts of total RNA. *Anal Biochem* **358**, 111-119 (2006).
155. Grunenwald, H., Khanna, A. & Pease, J. Sensitive qRT-PCR Obtained from the Lysates of 1-10 Cells Using the MessageBOOSTER cDNA Synthesis Kit for qPCR. *Epicentre Biotechnologies Forum* **13**, 22-23 (2006).
156. Allen, T.M., *et al.* Characterization of the Peptide Binding Motif of a Rhesus MHC Class I Molecule (Mamu-A*01) That Binds an Immunodominant CTL Epitope from Simian Immunodeficiency Virus. *J Immunol* **160**, 6062-6071 (1998).
157. Kuroda, M.J., *et al.* Analysis of Gag-specific Cytotoxic T Lymphocytes in Simian Immunodeficiency Virus-infected Rhesus Monkeys by Cell Staining with a Tetrameric Major Histocompatibility Complex Class I-Peptide Complex. *J Exp Med* **187**, 1373-1381 (1998).
158. Mothe, B.R., *et al.* Expression of the Major Histocompatibility Complex Class I Molecule Mamu-A*01 Is Associated with Control of Simian Immunodeficiency Virus SIVmac239 Replication. *J Virol* **77**, 2736-2740 (2003).
159. O'Connor, D.H., *et al.* Major Histocompatibility Complex Class I Alleles Associated with Slow Simian Immunodeficiency Virus Disease Progression Bind Epitopes Recognized by Dominant Acute-Phase Cytotoxic-T-Lymphocyte Responses. *J Virol* **77**, 9029-9040 (2003).
160. Muhl, T., Krawczak, M., ten Haaft, P., Hunsmann, G. & Sauermann, U. MHC Class I Alleles Influence Set-Point Viral Load and Survival Time in Simian Immunodeficiency Virus-Infected Rhesus Monkeys. *J. Immunol.* **169**, 3438-3446 (2002).
161. Pal, R., *et al.* ALVAC-SIV-gag-pol-env-Based Vaccination and Macaque Major Histocompatibility Complex Class I (A*01) Delay Simian Immunodeficiency Virus SIVmac-Induced Immunodeficiency. *J Virol* **76**, 292-302 (2002).
162. Zhang, Z.-Q., *et al.* Mamu-A*01 Allele-Mediated Attenuation of Disease Progression in Simian-Human Immunodeficiency Virus Infection. *J Virol* **76**, 12845-12854 (2002).
163. Yant, L.J., *et al.* The High-Frequency Major Histocompatibility Complex Class I Allele Mamu-B*17 Is Associated with Control of Simian Immunodeficiency Virus SIVmac239 Replication. *J Virol* **80**, 5074-5077 (2006).
164. Loffredo, J.T., *et al.* CD8+ T Cells from SIV Elite Controller Macaques Recognize Mamu-B*08-Bound Epitopes and Select for Widespread Viral Variation. *PLoS ONE* **2**, e1152 (2007).
165. Newberg, M.H., *et al.* A Simian Immunodeficiency Virus Nef Peptide Is a Dominant Cytotoxic T Lymphocyte Epitope in Indian-Origin Rhesus Monkeys Expressing the Common MHC Class I Allele Mamu-A*02. *Virology* **301**, 365-373 (2002).
166. Allen, T.M., *et al.* CD8+ Lymphocytes from Simian Immunodeficiency Virus-Infected Rhesus Macaques Recognize 14 Different Epitopes Bound by the Major Histocompatibility Complex Class I Molecule Mamu-A*01: Implications for Vaccine Design and Testing. *J Virol* **75**, 738-749 (2001).
167. Furchner, M., *et al.* The Simian Immunodeficiency Virus Envelope Glycoprotein Contains Two Epitopes Presented by the Mamu-A*01 Class I Molecule. *J Virol* **73**, 8035-8039 (1999).
168. Egan, M.A., *et al.* Use of Major Histocompatibility Complex Class I/Peptide/beta 2M Tetramers To Quantitate CD8+ Cytotoxic T Lymphocytes Specific for Dominant and

Nondominant Viral Epitopes in Simian-Human Immunodeficiency Virus-Infected Rhesus Monkeys. *J Virol* **73**, 5466-5472 (1999).
169. Mothe, B.R., *et al.* Dominance of CD8 Responses Specific for Epitopes Bound by a Single Major Histocompatibility Complex Class I Molecule during the Acute Phase of Viral Infection. *J Virol* **76**, 875-884 (2002).
170. Miller, M.D., Yamamoto, H., Hughes, A.L., Watkins, D.I. & Letvin, N.L. Definition of an epitope and MHC class I molecule recognized by gag- specific cytotoxic T lymphocytes in SIVmac-infected rhesus monkeys. *J Immunol* **147**, 320-329 (1991).
171. Wherry, E.J., *et al.* Lineage relationship and protective immunity of memory CD8 T cell subsets. *Nat Immunol* **4**, 225-234 (2003).
172. Wherry, E.J. & Ahmed, R. Memory CD8 T-cell differentiation during viral infection. *J Virol* **78**, 5535-5545 (2004).
173. Grayson, J.M., Murali-Krishna, K., Altman, J.D. & Ahmed, R. Gene Expression in Antigen-Specific CD8+ T Cells During Viral Infection. *J Immunol* **166**, 795-799 (2001).
174. Kaech, S.M., Hemby, S., Kersh, E. & Ahmed, R. Molecular and Functional Profiling of Memory CD8 T Cell Differentiation. *Cell* **111**, 837-851 (2002).
175. Teague, T.K., *et al.* Activation changes the spectrum but not the diversity of genes expressed by T cells. *Proc Natl Acad Sci U S A* **96**, 12691-12696 (1999).
176. Goldrath, A.W., Luckey, C.J., Park, R., Benoist, C. & Mathis, D. The molecular program induced in T cells undergoing homeostatic proliferation. *Proc Natl Acad Sci U S A* **101**, 16885-16890 (2004).
177. Marrack, P., *et al.* Genomic-scale analysis of gene expression in resting and activated T cells. *Current Opinion in Immunology* **12**, 206-209 (2000).
178. Peixoto, A., *et al.* CD8 single-cell gene coexpression reveals three different effector types present at distinct phases of the immune response. *J Exp Med* **204**, 1193-1205 (2007).
179. Appay, V., *et al.* HIV-specific CD8(+) T cells produce antiviral cytokines but are impaired in cytolytic function. *J Exp Med* **192**, 63-75 (2000).
180. Barber, D.L., *et al.* Restoring function in exhausted CD8 T cells during chronic viral infection. *Nature* **439**, 682-687 (2006).
181. George, M.D., Sankaran, S., Reay, E., Gelli, A.C. & Dandekar, S. High-throughput gene expression profiling indicates dysregulation of intestinal cell cycle mediators and growth factors during primary simian immunodeficiency virus infection. *Virology* **312**, 84-94 (2003).
182. Migueles, S.A., *et al.* HIV-specific CD8+ T cell proliferation is coupled to perforin expression and is maintained in nonprogressors. *Nat Immunol* **3**, 1061-1068 (2002).
183. Lichterfeld, M., *et al.* HIV-1-specific cytotoxicity is preferentially mediated by a subset of CD8(+) T cells producing both interferon-gamma and tumor necrosis factor-alpha. *Blood* **104**, 487-494 (2004).
184. Shin, H. & Wherry, E.J. CD8 T cell dysfunction during chronic viral infection. *Current Opinion in Immunology* **19**, 408-415 (2007).
185. Wherry, E.J., *et al.* Molecular Signature of CD8+ T Cell Exhaustion during Chronic Viral Infection. *Immunity* **27**, 670-684 (2007).
186. Wherry, E.J., Blattman, J.N., Murali-Krishna, K., van der Most, R. & Ahmed, R. Viral Persistence Alters CD8 T-Cell Immunodominance and Tissue Distribution and Results in Distinct Stages of Functional Impairment. *J Virol* **77**, 4911-4927 (2003).

187. Fuller, M.J. & Zajac, A.J. Ablation of CD8 and CD4 T Cell Responses by High Viral Loads. *J Immunol* **170**, 477-486 (2003).
188. Petrovas, C., *et al.* SIV-specific CD8+ T cells express high levels of PD1 and cytokines but have impaired proliferative capacity in acute and chronic SIVmac251 infection. *Blood* **110**, 928-936 (2007).
189. Newberg, M.H., *et al.* Immunodomination in the Evolution of Dominant Epitope-Specific CD8+ T Lymphocyte Responses in Simian Immunodeficiency Virus-Infected Rhesus Monkeys. *J Immunol* **176**, 319-328 (2006).
190. Lichterfeld, M., *et al.* Selective Depletion of High-Avidity Human Immunodeficiency Virus Type 1 (HIV-1)-Specific CD8+ T Cells after Early HIV-1 Infection. *J Virol* **81**, 4199-4214 (2007).
191. Price, D.A., *et al.* Positive selection of HIV-1 cytotoxic T lymphocyte escape variants during primary infection. *Proc Natl Acad Sci U S A* **94**, 1890-1895 (1997).
192. Borrow, P., *et al.* Antiviral pressure exerted by HIV-l-specific cytotoxic T lymphocytes (CTLs) during primary infection demonstrated by rapid selection of CTL escape virus. *Nat Med* **3**, 205-211 (1997).
193. Peyerl, F.W., Barouch, D.H. & Letvin, N.L. Structural constraints on viral escape from HIV- and SIV-specific cytotoxic T-lymphocytes. *Viral Immunol* **17**, 144-151 (2004).
194. Barouch, D.H., *et al.* Eventual AIDS vaccine failure in a rhesus monkey by viral escape from cytotoxic T lymphocytes. *Nature* **415**, 335-339 (2002).
195. Chen, Z.W., *et al.* Simian Immunodeficiency Virus Evades a Dominant Epitope-Specific Cytotoxic T Lymphocyte Response Through a Mutation Resulting in the Accelerated Dissociation of Viral Peptide and MHC Class I. *J Immunol* **164**, 6474-6479 (2000).
196. Barouch, D.H., *et al.* Viral Escape from Dominant Simian Immunodeficiency Virus Epitope-Specific Cytotoxic T Lymphocytes in DNA-Vaccinated Rhesus Monkeys. *J Virol* **77**, 7367-7375 (2003).
197. Loffredo, J.T., *et al.* Identification of Seventeen New Simian Immunodeficiency Virus-Derived CD8+ T Cell Epitopes Restricted by the High Frequency Molecule, Mamu-A*02, and Potential Escape from CTL Recognition. *J Immunol* **173**, 5064-5076 (2004).
198. Vogel, T.U., *et al.* Escape in One of Two Cytotoxic T-Lymphocyte Epitopes Bound by a High-Frequency Major Histocompatibility Complex Class I Molecule, Mamu-A*02: a Paradigm for Virus Evolution and Persistence? *J Virol* **76**, 11623-11636 (2002).
199. von Schwedler, U.K., Stray, K.M., Garrus, J.E. & Sundquist, W.I. Functional Surfaces of the Human Immunodeficiency Virus Type 1 Capsid Protein. *J Virol* **77**, 5439-5450 (2003).
200. von Schwedler, U.K., *et al.* Proteolytic refolding of the HIV-1 capsid protein amino-terminus facilitates viral core assembly. *Embo J* **17**, 1555-1568 (1998).
201. Rue, S.M., Roos, J.W., Amzel, L.M., Clements, J.E. & Barber, S.A. Hydrogen Bonding at a Conserved Threonine in Lentivirus Capsid Is Required for Virus Replication. *J Virol* **77**, 8009-8018 (2003).
202. Peyerl, F.W., *et al.* Simian-Human Immunodeficiency Virus Escape from Cytotoxic T-Lymphocyte Recognition at a Structurally Constrained Epitope. *J Virol* **77**, 12572-12578 (2003).
203. Peyerl, F.W., *et al.* Fitness Costs Limit Viral Escape from Cytotoxic T Lymphocytes at a Structurally Constrained Epitope. *J Virol* **78**, 13901-13910 (2004).

204. George, M.D., Verhoeven, D., McBride, Z. & Dandekar, S. Gene expression profiling of gut mucosa and mesenteric lymph nodes in simian immunodeficiency virus-infected macaques with divergent disease course. *J Med Primatol* **35**, 261-269 (2006).
205. Champagne, P., *et al.* Skewed maturation of memory HIV-specific CD8 T lymphocytes. *Nature* **410**, 106-111 (2001).
206. Thomas, M.J., *et al.* Functional gene analysis of individual response to challenge of SIVmac239 in M. mulatta PBMC culture. *Virology* **348**, 242-252 (2006).
207. Alter, G. & Altfeld, M. NK cells in HIV-1 infection: evidence for their role in the control of HIV-1 infection. *J Intern Med* **265**, 29-42 (2009).
208. Hong, H.S., *et al.* Exogenous HIV-1 Vpr disrupts IFN-alpha response by plasmacytoid dendritic cells (pDCs) and subsequent pDC/NK interplay. *Immunol Lett* (2009).
209. Ahlers, J.D. & Belyakov, I.M. Strategies for recruiting and targeting dendritic cells for optimizing HIV vaccines. *Trends Mol Med* **15**, 263-274 (2009).
210. Brown, K.N., Wijewardana, V., Liu, X. & Barratt-Boyes, S.M. Rapid Influx and Death of Plasmacytoid Dendritic Cells in Lymph Nodes Mediate Depletion in Acute Simian Immunodeficiency Virus Infection. *PLoS Pathog* **5**, e1000413 (2009).
211. Williams Kc Fau - Burdo, T.H. & Burdo, T.H. HIV and SIV infection: the role of cellular restriction and immune responses in viral replication and pathogenesis.
212. Hasegawa, A., *et al.* The level of monocyte turnover predicts disease progression in the macaque model of AIDS. *Blood* **114**(2009).
213. Levy, J.A. The importance of the innate immune system in controlling HIV infection and disease. *Trends in Immunology* **22**, 312-316 (2001).
214. Brusic, V. FROM IMMUNOINFORMATICS TO IMMUNOMICS. *Journal of Bioinformatics & Computational Biology* **1**, 179 (2003).
215. Quintana, F.J., *et al.* Functional immunomics: Microarray analysis of IgG autoantibody repertoires predicts the future response of mice to induced diabetes. *Proc Natl Acad Sci U S A* **101**, 14615-14621 (2004).
216. Klysik, J. Concept of Immunomics: A New Frontier in the Battle for Gene Function? *Acta Biotheoretica* **49**, 191-202 (2001).
217. Leigh Anderson, J.S. A comparison of selected mRNA and protein abundances in human liver. *Electrophoresis* **18**, 533-537 (1997).
218. Braga-Neto, U.M. & Marques, E.T.A., Jr. From Functional Genomics to Functional Immunomics: New Challenges, Old Problems, Big Rewards. *PLoS Comput Biol* **2**, e81 (2006).
219. Morozova, O. & Marra, M.A. Applications of next-generation sequencing technologies in functional genomics. *Genomics* **92**, 255-264 (2008).
220. Wang, E.T., *et al.* Alternative isoform regulation in human tissue transcriptomes. *Nature* **456**, 470-476 (2008).
221. Chi, S.W., Zang, J.B., Mele, A. & Darnell, R.B. Argonaute HITS-CLIP decodes microRNA-mRNA interaction maps. *Nature* (2009).
222. Hahn, S., Zhong, X.Y., Troeger, C. & R. Burgemeister, K.G.W.H. Current applications of single-cell PCR. *Cellular and Molecular Life Sciences* **57**, 96-105 (2000).
223. Maryanski, J.L., Jongeneel, C.V., Bucher, P., Casanova, J.-L. & Walker, P.R. Single-Cell PCR Analysis of TCR Repertoires Selected by Antigen In Vivo: A High Magnitude CD8 Response Is Comprised of Very Few Clones. *Immunity* **4**, 47-55 (1996).